# Comparative analyses of tumorigenic mechanisms of Merkel cell polyomavirus T antigens

by

**Justin A. Wendzicki**

Bachelors of Science, Duquesne University, 2013

Submitted to the Graduate Faculty of the

School of Medicine in partial fulfillment

of the requirements for the degree of

Doctor of Philosophy

University of Pittsburgh

2019

UNIVERSITY OF PITTSBURGH

SCHOOL OF MEDICINE

This dissertation was presented

by

**Justin A. Wendzicki**

It was defended on

December 6, 2019

and approved by

Neal A. DeLuca, Professor, Department of Microbiology and Molecular Genetics

Saleem A. Khan, Professor, Department of Microbiology and Molecular Genetics

Paul R. Kinchington, Professor, Department of Microbiology and Molecular Genetics

Roderick J. O'Sullivan, Assistant Professor, Department of Pharmacology and Chemical Biology

Dissertation Director: Yuan Chang, Professor, Department of Pathology

**Comparative analyses of tumorigenic mechanisms of Merkel cell polyomavirus T antigens**

Justin A. Wendzicki, PhD

University of Pittsburgh, 2019

The work described in this dissertation began in 2013 and is focused on characterizing the mechanisms by which Merkel cell polyomavirus (MCV) Large T (LT) and small T (sT) antigens induce tumorigenesis through comparative analyses with oncoproteins from other tumor viruses. A peptide motif in the C-terminal region of MCV LT that bears little sequence homology with other human polyomavirus LT proteins is shown to be critical for maintaining stability of the full-length LT protein (Chapter 3). Comparison between LT antigens of MCV and SV40 demonstrate that MCV LT in direct contrast to SV40 LT is incapable of avidly binding tumor suppressor p53 and inhibiting its transactivation capabilities (Chapter 4). Lastly, promiscuous E3 ligase targeting by MCV sT through its LT-stabilization domain (LSD) results in the formation of a genomically unstable phenotype, a known hallmark of cancer (Chapter 5). Many of the features of genomic instability induced by MCV sT such as centrosome overduplication parallel what has been observed previously for human papillomavirus 16 E7 oncoprotein. Overall, these comparative analyses have not only provided greater insight into MCV biology and how its T antigens function in causing an aggressive cancer like Merkel cell carcinoma (MCC), but they have also revealed new avenues for continued study involving MCV T antigens that will continue to move the field of tumor virology forward.

## Table of Contents

## List of Tables

## List of Figures

## Acknowledgments

I was never under the impression that pursuing a PhD would be an easy process, but I will admit that when I entered this graduate program I was naively unaware of how truly challenging it would be and how much growing up I would do along the way. I know full well I would never have made it this far without an incredible support system around me, and so I would like to take this space to recognize several of those individuals who have made this entire journey possible.

First and foremost, I have to thank my mentors Drs. Yuan Chang and Patrick Moore for all of their support over these past few years, including many helpful discussions, solid career advice, and various general life lessons. I came into their laboratory a fledgling student with little molecular biology experience, and I am closing out this chapter of my life with a much greater level of skill, a wider breadth of knowledge, and a more realized sense of maturity. I also want to take the space to acknowledge all CM Lab members both past and present, without whom I could not have accomplished much of the work contained in this dissertation. I want to specifically highlight Dr. Masahiro Shuda, Dr. Hyun Jin Kwun, Dr. Tuna Toptan, Dr. Kathleen Richards, and Dr. Jennifer Alvarez-Orellana for their consistent assistance, advice, instruction, and humor over the years. I also have to acknowledge Celestino Velasquez, the Thing 1 to my Thing 2 of CM Lab graduate students, who was my compatriot for most of this wild journey.

Working at the UPMC Hillman Cancer Center has been a truly enlightening experience, for the building itself is designed to constantly remind patients, clinicians, and researchers that we are all working side by side to advance scientific knowledge and

medicine. I have to thank other faculty members in the institute for facilitating such a collaborative research environment and constantly sharing equipment and reagents at a moment's notice, specifically Dr. Kathy Shair, Dr. Saumen Sarkar, Dr. Shou-Jiang Gao, Dr. Chris Bakkenist, and Dr. Jian Yu. I also want to thank everyone whose work is more 'behind the scenes' but equally important to ensure our research runs smoothly, from the café staff, to the loading dock, to the glassware facility, to veterinary technicians, to housekeeping staff, and of course our incredible administrative staff. I want to specifically highlight Felicia Steele, who aside from being an organizational wizard for the CVP has also been a consistent source of levity, positivity, serenity, and Netflix recommendations for me personally throughout the years.

Moving outwards to the University of Pittsburgh at large, I want to thank all of my committee members for supporting me, assisting in my graduate training, and helping me to become a more well-rounded young scientist. Thank you, Dr. Neal DeLuca, Dr. Saleem Khan, Dr. Paul Kinchington, and Dr. Roderick O'Sullivan for helping to get me to this point. I also want to thank current and past directors of the MVM program, Dr. Carolyn Coyne and Dr. Fred Homa. I have to recognize the work of our program coordinator Kristin DiGiacomo, who has helped make sure my life as a graduate student has progressed with as few hurdles as possible.

In keeping with CM Lab tradition, I would be remiss in not acknowledging the many musicians and podcasters who have kept me company and helped to alleviate stress during late hours spent in the lab over the years and in the composition of this document. While I cannot possibly thank them all I would like to highlight Elliott Smith, Amanda F. Palmer, Karin Dreijer, Jonna Lee, Anthony Gonzalez, Kelsey Byrne, Emily Haines, Colin

Meloy, Marina Diamandis, Florence Welch, Lights Poxleitner-Bokan, Alice Glass, Megan James, Corin Roddick, Karen Kilgariff, Georgia Hardstark, Chris Fairbanks, Phoebe Judge, the McElroy bothers, Alaska, and Willam Belli.

Lastly, and perhaps most importantly, I have to acknowledge the unending support from my family and friends throughout my graduate career and throughout my life in general. I want to thank my parents and my sisters, who have always been there for me, even at the most difficult times, and have always encouraged me to never give up on my goals. I also want to thank some of the incredible friends I have made during my time at Pitt, who have been a true source of inspiration and all-around fun. Thank you very much, Dr. Eileen Wong, Dr. Mondraya Howard, Dr. James Eles, Dr. Gregory Logan-Graf, Drew Logan-Graf, Dr. Aliyah Weinstein, Dr. Rebecca Eells, Dr. Coyne Drummond, Dr. Stephanie Mutchler, and Anastasia Gorelova, for you all have made the time fly by. Last, but by no means least, I have to thank some of my oldest friends, Rose Bona, Rachel Halle, Joseph Hayek, Mike Balogh, Holly Orosz, and Kristen Haupt, who have always been part of an incredible support system that I cherish constantly, even if we do not see each other often.

Thank you all so very, very much.

# 1.0 Introduction

## 1.1 Viruses and cancer

### 1.1.1 Origins of tumor virology

Viruses represent the cause for numerous human diseases due to their potent ability to replicate within, disseminate throughout, and devastate host tissues. Although many viral infections are acute and short-lived, several viruses have been identified that, through persistent infections, drive tumor formation in their hosts. Once the causative link between infectious agents and cancer became more widely accepted in the latter half of the 20th century, many were hopeful that all human cancers could eventually be linked to microbial pathogenesis (1). While continued research revealed that environmental and chemical carcinogens were instead responsible for the genetic alterations that cause the majority of human cancers, it has been estimated that between 15-20% of human cancers have an infectious origin (2, 3). This translates to infectious agents representing the third leading cause for cancer worldwide, making them a significant public health burden and fruitful area for continued research.

The field of tumor virology dates back to the early 20th century and the experiments of Peyton Rous. He was successful in isolating a filterable agent from a chicken sarcoma specimen that, when injected into young chickens, consistently resulted in sarcoma formation after a regular length of time. This agent that could be serially passed from chicken to chicken was eventually classified as Rous sarcoma virus (RSV) and represents

the first tumor virus to be discovered (4, 5). Unfortunately, Rous's work was initially discounted as implausible, scientifically-flawed, and lacking in any relevance to human disease (6). This challenge of proving causality between viruses and cancer has since become a common thread that runs throughout the history of tumor virology.

Despite initial skepticism over the work of Rous, the field moved forward in 1933 when Shope and Hurst successfully isolated a transmissible, filterable agent from warts on cottontail rabbits that was capable of producing warts in naïve rabbits (7). Rous and Beard then showed that this agent, now known as cottontail rabbit papillomavirus (CRPV), could lead to the formation of carcinomas in domestic rabbits, which are non-permissive for CRPV infection (8). Concurrently, work in mice led to the discovery of mouse mammary tumor virus (9), murine leukemia virus (10), and murine polyomavirus (11). This wave of tumor virus discovery continued again in 1960 when Sweet and Hilleman identified simian vacuolating virus 40 (SV40) as a contaminant in Salk poliovirus vaccines (12). Since its discovery, research involving SV40 has been invaluable for informing our understanding of tumor virology, cancer biology, and molecular biology in general.

### 1.1.2 Human tumor viruses

The continuum of tumor virus discovery in the animal kingdom resulted in a shift in scientific opinion regarding the potential for viruses to cause cancer. This led to concerted efforts to identify viruses responsible for causing cancer in humans, of which seven have been discovered to date (**Table 1**). Epstein, Achong, and Barr identified the first human tumor virus Epstein-Barr virus (EBV) in 1964 through work on Burkitt's lymphoma (13).

**Table 1. Human tumor viruses**

| Virus | Taxonomy | Year of Discovery | Method of Discovery | Associated Cancers | References |
|---|---|---|---|---|---|
| Epstein-Barr virus (EBV) | Herpesvirus (dsDNA) | 1964 | Electron microscopy | Burkitt's lymphoma, nasopharyngeal carcinoma, and other lymphomas | Epstein *et al.*, *Lancet*, 1964 |
| Hepatitis B virus (HBV) | Hepadnavirus (ssDNA /dsDNA) | 1965 | Serology | Some hepatocellular carcinoma | Blumberg *et al.*, *JAMA*, 1965 |
| Human T-cell lymphotropic virus-I (HTLV-I) | Retrovirus (ssRNA+) | 1980 | Tissue culture | Adult T-cell leukemia | Poiesz *et al.*, *PNAS*, 1980 |
| High-risk human papillomaviruses (HPV) 16 and 18 | Papillomavirus (dsDNA) | 1983-84 | DNA cloning | Most cervical and penile cancers and some anogenital and head and neck cancers | Durst *et al.*, *PNAS*, 1983; Boshart *et al.*, *EMBO J*, 1983 |
| Hepatitis C virus (HCV) | Flavivirus (ssRNA+) | 1989 | cDNA cloning | Some hepatocellular carcinoma | Choo *et al.*, *Science*, 1989 |
| Kaposi sarcoma herpesvirus (KSHV) | Herpesvirus (dsDNA) | 1994 | Representational difference analysis (RDA) | Kaposi sarcoma, primary effusion lymphoma, and some multicentric Castleman disease | Chang *et al.*, *Science*, 1994 |
| Merkel cell polyomavirus (MCV) | Polyomavirus (dsDNA) | 2008 | Digital transcriptome subtraction (DTS) | Most Merkel cell carcinoma | Feng *et al.*, *Science*, 2008 |

They were able to visualize virus particles by electron microscopy in cell lines derived from equatorial African Burkitt's lymphoma patients. The classification of EBV as a tumor virus was met with criticism for decades following its initial characterization. Despite mounting evidence of its transforming capabilities (14), scientists wrestled with the seeming contradiction that a ubiquitous and asymptomatic viral infection in the global population could be the primary cause of a rare cancer endemic to a small region in Africa (15, 16). Finally, this controversy was laid to rest in 1997 when the International Agency for Research on Cancer (IARC) officially designated EBV a human carcinogen (17), but overall this saga underscores the complicated nature of defining causality in tumor virology (18). Unlike acute disease, where infection and pathology tend to directly coincide, infection with tumor viruses does not directly guarantee subsequent tumor development in every host. Rather, many other environmental and genetic factors can dictate whether or not a tumor virus infection progresses to oncogenesis. This concept

has shaped our understanding of the multifactorial nature of cancer development and has become dogma within the field.

The identification of the next human tumor virus hepatitis B virus (HBV) was preceded by serological studies conducted by Blumberg, beginning in 1965. He found that an antigen from blood of an Aboriginal Australian (Au antigen) was highly cross-reactive with a serum antibody from an American hemophilia patient (19). Further studies showed that this antigen was present in blood samples of individuals suffering from serum hepatitis, and that the identity of this antigen was the surface antigen of HBV (20). While HBV infection is normally asymptomatic or acute, a small percent of infected adults develop chronic infections, which are highly associated with the development of hepatocellular carcinoma (HCC) (21, 22). Identification of HBV and hepatitis A virus (HAV) led to the realization that a subset of transfusion-associated hepatitis cases was caused by neither virus, which suggested an unknown pathogen might be the cause (6). Using a chimpanzee model for this unknown pathogen, Choo *et. al* succeeded at constructing a cDNA library from nucleic acids present in plasma of infected chimpanzees. One of these clones expressed an antigen from an undiscovered flavivirus, which was subsequently named hepatitis C virus (HCV) and characterized as the causative agent of this subset of serum hepatitis (23, 24). Much like HBV, HCV is associated with the development of cirrhosis and chronic inflammation in the liver, both of which are major risk factors for the development of HCC (25–27).

Harkening back to the foundational works of Shope, Rous, and Beard on CRPV, those studies and subsequent identification of other animal papillomaviruses suggested a potential role for this virus family in human cancers (8, 28, 29). This was confirmed

when work led by zur Hausen showed that papillomavirus sequences hybridized with DNA from cervical cancer specimens (30, 31). These two unique viral sequences were from human papillomaviruses (HPVs) 16 and 18, now classified as high-risk HPVs and represent the causative agent of the vast majority of cervical cancers and a significant proportion of anogenital and head and neck cancers (32–34).

Much like the work of Rous prompted the search for papillomaviruses that caused human cancer, it was also assumed that one or more retroviruses like RSV must be responsible for causing cancer in humans. This led Gallo and colleagues to search for retroviruses in leukemia cells, which resulted in the detection of canonical reverse transcriptase activity associated with these viruses as well as virus particles in T-cell lymphoma cells (35). This first human retrovirus was named human T-cell lymphotropic virus-I (HTLV-I), and its causal role in adult T-cell leukemia (ATL) was later confirmed by Hinuma *et al.* and others (36, 37). Similar to the way that EBV plays a causative role in the rare cancer Burkitt's lymphoma in Africa, ATL was initially described as occurring in localized pockets throughout Japan (38), underscoring that research on endemic diseases like these may be a viable route for the identification of new tumor viruses.

Kaposi sarcoma (KS), first described in 1872 (39), is one such endemic disease, with higher prevalence in the Mediterranean basin and Africa; however, it was the explosive outbreak of KS as an AIDS-associated malignancy during the AIDS crisis that prompted the search for its underlying cause (40). Determined not to be caused by HIV itself, statistics hinted at an undefined sexually-transmitted infection as the etiological agent of KS (41). Using the newly-developed technique representational difference analysis (RDA), Chang *et al.* compared DNA fragments from KS tumor tissue with normal

tissue, which revealed the presence of a new herpesvirus sequence: Kaposi sarcoma herpesvirus (KSHV) (42). Subsequent sequence analysis, biochemical testing, and serological testing definitively showed that KSHV was present in both AIDS-associated and non-AIDS forms of KS (43–45). A causative role for KSHV in primary effusion lymphoma (PEL) and a subset of multicentric Castleman disease has also been established (46, 47).

Chang and Moore succeeded once again in identifying the newest addition to the list of human tumor viruses, Merkel cell polyomavirus (MCV). In that study, Feng *et al.* used a bioinformatic-based approach called digital transcriptome subtraction (DTS) to identify viral transcripts present in Merkel cell carcinoma (MCC) tumor specimens (48). As MCV is the main focus of this dissertation, more detailed descriptions of MCV discovery and biology are presented in Section 1.4 (page 29).

In looking back on the history of tumor virology it becomes clear that researchers throughout the past century have relied on the discoveries of their predecessors as a continued source of inspiration in the quest to identify new tumor viruses and drive the field forward. Apart from the discovery of new tumor viruses, key advancements in the field include the development of highly-effective vaccines for HBV and nine HPV family members that are the most prevalent in human disease, helping to reduce transmission of these viruses and incidence of their associated cancers (49, 50). As science and technology continue to develop at lightning speed, it is highly likely that we will see new developments in virus discovery and cancer treatment soon, especially if we continue to let the first century of tumor virology inform the next.

## 1.2 Polyomavirus biology

### 1.2.1 History and discovery

Polyomaviruses are small, circular, non-enveloped, double-stranded DNA viruses with genomes approximately 5.0-5.4 kilobases in length. This virus family contains an ever-growing number of members that infect many species throughout the animal kingdom, from arthropods, to fish, to mammals. Within their natural hosts, polyomavirus infections are generally asymptomatic and controlled by the immune system, but under circumstances they can go on to cause pathology and even tumors within their hosts.

The first discovered member of the polyomavirus family, murine polyomavirus (MuPyV), was identified in 1953 by Ludwik Gross through his studies on leukemia in mice, who, much like Rous decades before, isolated a filterable agent from mouse leukemia cells that was capable of producing tumors upon injection into mice (11). Further characterization of this agent and its ability to cause “many tumors” in hosts led to the name “*polyoma*” to describe this virus (51). Less than a decade later, work by Eddy, Sweet, Hilleman, and others identified a second polyomavirus as a contaminant in poliovirus vaccine preparations which was called simian vacuolating virus 40 (SV40), due to its ability to induce the formation of large vacuoles in infected monkey cells (12, 52, 53). Shortly after its identification, continued work with SV40 showed that it was capable of inducing tumors in both immunocompromised mice and newborn hamsters, solidifying its classification as a polyomavirus (52, 54). Over the decades that followed, a plethora of additional polyomaviruses have been identified that infect a wide array of hosts throughout the animal kingdom.

The first human polyomaviruses (HPyVs) were identified in 1971 and were named by the initials of the patients from which they were isolated: B.K. virus (BKV) and J.C. virus (55, 56). Infection with both of these viruses is generally asymptomatic, and neither is directly associated with causing tumors in humans (57, 58); however, in the case of immunosuppression, both viruses can cause severe pathology in infected patients. BKV is associated with the development of nephropathy in renal transplant patients, and JCV is responsible for causing progressive multifocal leukoencephalopathy (PML) (59, 60). Despite lack of a direct casual association with cancer in humans, the oncogenic potential of BKV and JCV has been widely demonstrated in various cell culture and laboratory animal models (61).

Discovery of new HPyVs laid dormant for the following few decades until 2007 when the discovery of two new polyomaviruses occurred. Both were identified through sequence analysis of human respiratory samples and named after the institutes where the discovery took place: Washington University polyomavirus (WUV) and Karolinska Institute polyomavirus (KIV) (62, 63). Although both viruses were identified from patient samples and have a high seroprevalence within the population, neither virus has come to be associated with any particular disease in humans (64, 65).

The advent of more cost-effective deep sequencing approaches was a major factor in the discovery of the remainder of the HPyVs, a list that now contains more than a dozen members. Merkel cell polyomavirus (MCV) was first identified in 2008 (48) through a high-throughput sequencing method called digital transcriptome subtraction (DTS). The clonal integration pattern of MCV in Merkel cell carcinoma (MCC) tumors is strong evidence for causality, and to date MCV remains the only human polyomavirus with a direct causal

relationship with human cancer. HPyV6 and HPyV7 were discovered concurrently through rolling circle amplification (RCA) and PCR-based methodologies on human skin samples (66). Likewise, an RCA approach was used to amplify viral sequences from a trichodysplasia spinulosa (TS) lesion, which led to the discovery of TS polyomavirus (TSV) (67). HPyV9 was also discovered through a similar methodology in 2011 (68). Three groups independently reported the identification of a new polyomavirus from stool samples, which became known as HPyV10 (69–71). Stool sample sequence analysis also led to the discovery of the of the eleventh HPyV (HPyV11), or STLPyV (72). The twelfth (HPyV12) and thirteenth (NJPyV) human polyomaviruses were isolated from gastrointestinal and pancreatic tissues samples, respectively (73, 74). A putative fourteenth HPyV was recently identified by sequence analysis of human skin samples and termed Lyon IARC polyomavirus (LIPyV) (75). Many of these newly identified HPyVs lack a clear causal relationship with human disease (76).

### 1.2.2 Phylogeny

The taxonomic organization of polyomaviruses remains a point of contention in the field. While it is generally accepted that all polyomaviruses fall within the family *Polyomaviridae*, assignment of specific genera within that family has been highly disputed. This is in part due to the massive expansion in the list of known polyomaviruses, which has prompted multiple attempts at phylogenetic re-clustering. As of 2011, the polyomavirus study group of the International Committee on Taxonomy of Viruses (ICTV) recommended the designation of three polyomavirus genera: *Orthopolyomavirus, Wukipolyomavirus,* and *Avipolyomavirus* (77). This classification system was amended

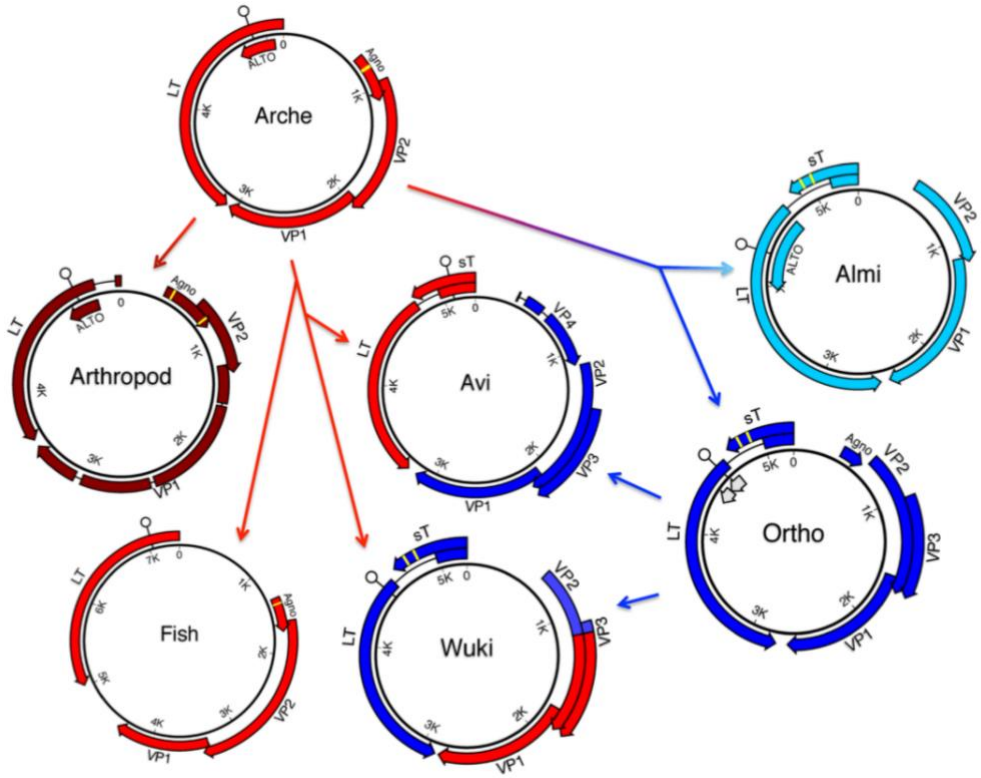


**Figure 1. A framework for ancient recombination events in major polyomavirus clades.**

In the model, a hypothetical ancient polyomavirus, designated Arche gave rise to separate polyomavirus lineages found in arthropods and fish, as well as the mammalian Ortho/Almi lineages. The figure depicts Avi and Wuki clades arising after recombination events involving an unknown vertebrate-Arche lineage and Ortho-like species. White lollipops represent predicted pRb-binding motifs. Yellow bars represent hypothetical metal-binding motifs (CXCXXC or related sequences). The absence of metal-binding motifs in Avi small T antigen (sT) proteins suggests a different evolutionary origin than the classic metal-binding Ortho/Almi sT. Possible ALTO-like ORFs predicted for some Ortho species are shaded gray. (Adapted from Buck *et al.*, 2016)

again in 2016, when the study group proposed a new approach to classification based on host and sequence information for each virus. This new classification system provides for four genera: *Alpha-, Beta-, Gamma-,* and *Deltapolyomavirus* (78). Advanced sequence analysis and continued polyomavirus discovery has led to criticism of the four genera model. Work by Buck *et al.* demonstrates a complex evolutionary history for the polyomavirus family, in which early and late regions of the genome have evolved

independently and show evidence of recombination, which is inconsistent with the four genera model (79). In their proposed evolutionary framework, they show how six major polyomavirus clades may have diverged from a common ancestor (**Figure 1**). Whether or not this new framework for polyomavirus classification will be adopted by the ICTV remains to be seen.

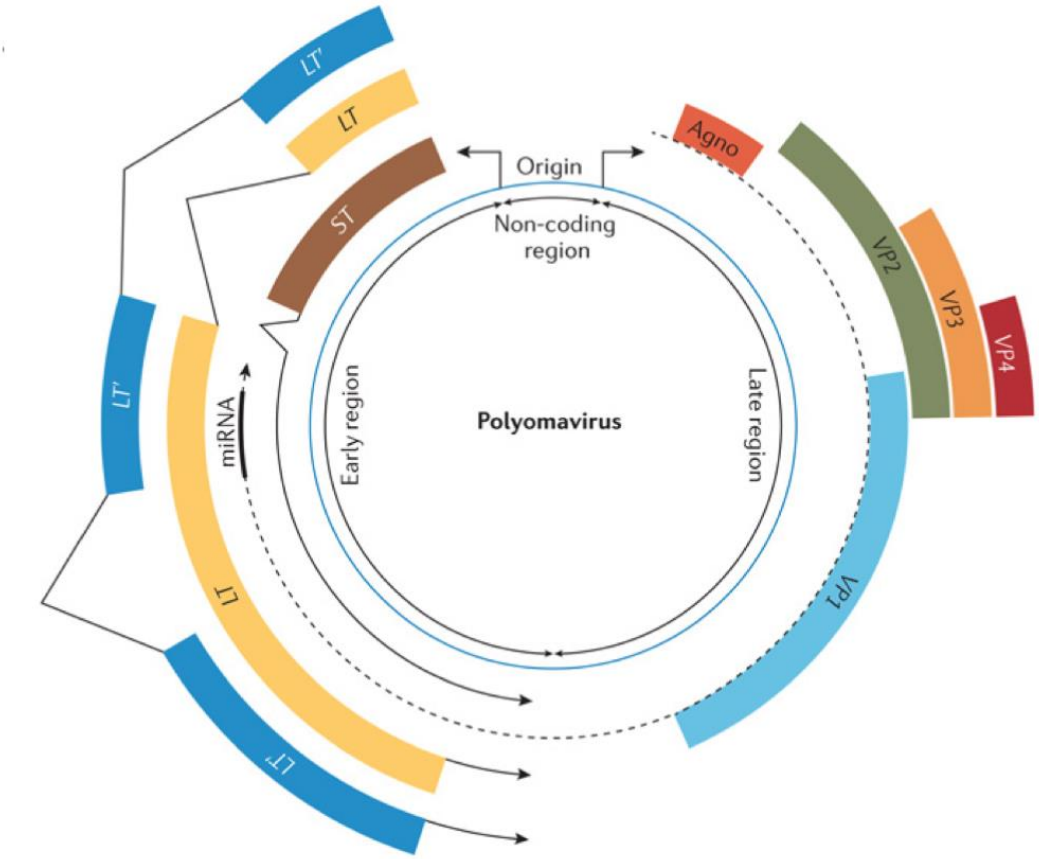


**Figure 2. Polyomavirus genome organization.**

The prototypical circular dsDNA genome has three main regions: a non-coding control region containing the early and late promoters, their transcription start sites and the origin of replication; an early region encoding large LT, sT, and an alternatively spliced LT (LT′); and a late region encoding the viral capsid proteins VP1, VP2, VP3 and VP4. The reading frames for VP2, VP3 and VP4 are identical, but alternative translation start sites generate the different proteins. VP4 has only been confirmed for avian polyomaviruses. Agnoprotein (Agno) is encoded by a late transcript from JCV and BKV, but has yet to be confirmed in the new human polyomaviruses. (Modified from DeCaprio and Garcea, 2013)

### 1.2.3 Genome organization

The polyomavirus genome is composed of circular, chromatinized, double-stranded DNA and is divided into three main parts: the non-coding regulatory region, the early region, and the late region (**Figure 2**). The non-coding regulatory region (NCRR) is the smallest of these three sections and contains the viral origin of replication as well as bidirectional promoter and enhancer elements for the other two transcriptional units of the virus (80).

The early region, so called because it is the first to be transcribed, is responsible for the production of a number of alternatively-spliced transcripts that encode variable tumor (T) antigens (**Figure 3**). This is accomplished using the host cell splicing machinery (81). All polyomaviruses express at least two transcripts from their early region, which based on the size of the corresponding proteins they produce are called Large T (LT) and small T (sT) (82). Many polyomaviruses also produce one or more accessory T antigens that vary in size and apparent function. Some examples include the 57 kT antigen of MCV (83), the 17kT antigen of SV40 (84), the tiny T antigen of TSV (85), and the truncated T (trunc-T) antigen of JCV (86).

The late region of polyomaviruses contains the coding regions for the viral capsid proteins, which are generated through a combination of alternative-splicing of mRNA and internal translation (82). All polyomaviruses encode a major capsid protein VP1 and minor capsid proteins VP2 and VP3, which together compose the viral capsid. Avian polyomaviruses have been shown to also produce a third minor capsid protein VP4 (87). This is not to be confused with the VP4 protein of SV40, which is a viroporin that assists in egress from cells and is not a part of the viral capsid structure (88, 89).

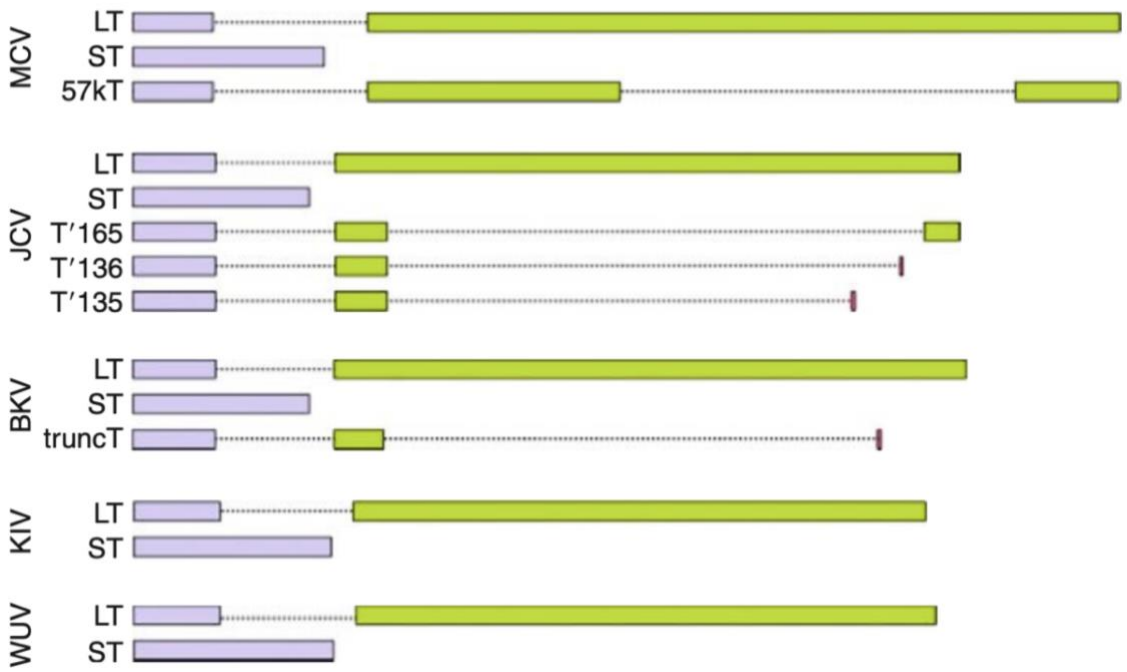


**Figure 3. Early region alternative splicing maps of select human polyomaviruses.**

Colored rectangles indicate coding sequences, whereas dotted lines depicts intronic sequences. Different colored rectangles refer to distinct reading frames after splicing events. All T antigens of each polyomavirus share the sequence encoded within exon 1. The accessory T antigens also share fragments of their respective LT sequences. (Adapted from Gjoerup and Chang, 2010)

In addition to these two main ORFs, there are some unique gene products made by some polyomaviruses that are not common across the entire virus family. For example, only murine and hamster polyomaviruses produce a middle T antigen from their early region, which is necessary for inducing transformation (90). There is also evidence to support that some polyomaviruses code for an alternative T antigen ORF (ALTO) through their early region, but the function of such proteins are unknown (91). The late region of several mammalian polyomaviruses, including BKV and JCV, encodes for an agnoprotein that appears to have variable functions but clearly facilitates a productive life cycle for these viruses (92, 93). There is also evidence to support that many polyomaviruses

encode micro-RNAs (miRNAs) that are important for regulating early region gene expression (94–97).

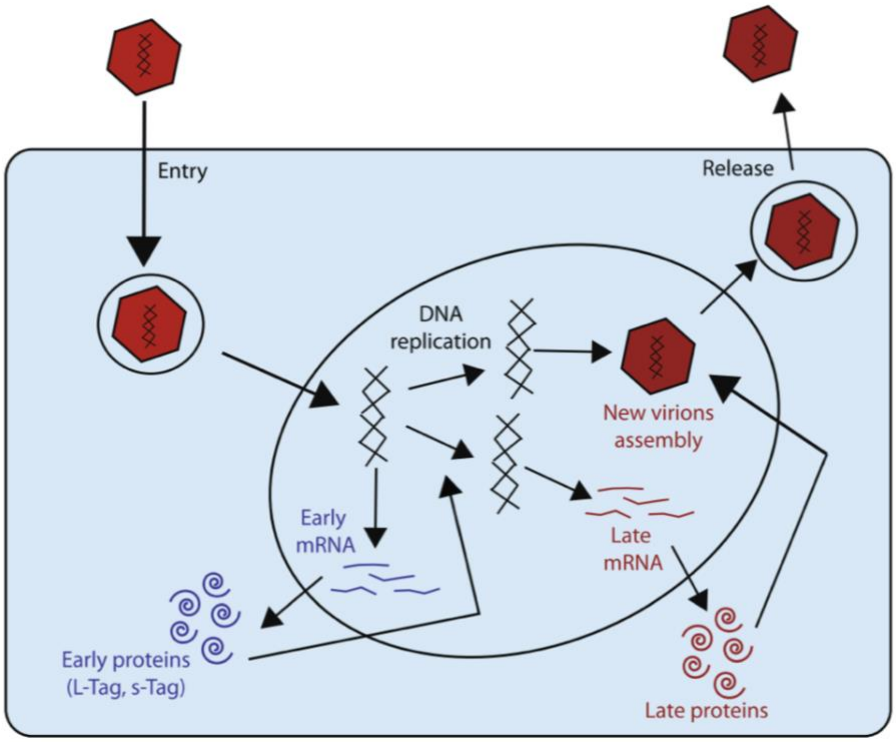


**Figure 4. Polyomavirus life cycle.**

After entry, viral particles pass through the cytoplasm to reach the nucleus, where the main processes of viral replication take place. The first step consists of expression of the early genes (blue), particularly LT, which is necessary for replication of the viral genome. This is followed by production of the viral capsid proteins (red), which prompts assembly of new virions and their release. (Adapted from Topalis *et al.*, 2013)

### 1.2.4 Life cycle

The polyomavirus life cycle is most generally divided into early and late phases based on their gene transcription events, but there are also several additional parts of the complete life cycle (**Figure 4**). The polyomavirus life cycle begins upon attachment of the

outer viral capsid protein VP1 to cell surface gangliosides or sialylated glycoproteins (98, 99). The specific attachment and entry factors differ between polyomavirus species. The majority of polyomaviruses enter cells through caveolin-mediated endocytosis and traffic to the smooth endoplasmic reticulum (ER) by way of microtubule transport (100–102). Traffic between the ER and nucleus is not well understood, but it is believed that uncoating of the viral genome takes place in the nucleus, where early gene transcription takes place. This results in the production of alternatively-spliced transcripts that are translated into the canonical T antigens (80).

The production of the T antigens coincides with the initiation of viral replication. This process is directed by LT, a multi-domain protein that possesses several different functionalities (98). First, LT through its DnaJ domain and LXCXE-motif targets the retinoblastoma (Rb) family of proteins, which creates a transcriptional environment that drives cells into S-phase (103, 104). This is critical because polyomaviruses rely on the host replication machinery to accomplish their own viral replication. LT then binds to the origin of replication on the viral genome through its DNA-binding domain and assembles as a double hexamer (105, 106). The C-terminal helicase domains of LT function to unwind the viral origin so that it can be accessed by the host replication machinery and replication can proceed. These critical functions of LT are discussed in more detail for SV40 in Section 1.3 (page 19) and for MCV in Chapter 2 (page 37).

Following replication of the genome, the late region of the genome is transcribed to produce the viral capsid proteins. Polyomavirus capsids are composed of 72 pentamers of the VP1 protein, with a single VP2 or VP3 monomer per VP1 pentamer that coordinate the chromatinized viral genome inside (107, 108). It is generally believed that

progeny virions are released through host cell lysis, but there is some evidence to support endocytic trafficking to the cell membrane (109).

### 1.2.5 Association with disease in humans

Polyomavirus infections are largely ubiquitous, and it is believed most infections are acquired early in life. After an initial period of viremia, polyomaviruses may enter into a quiescent state that allows them to chronically persist within their hosts. The precise mechanisms governing persistence are not well understood and appear to be specific to each virus and the particular tissues they infect (110). Polyomavirus infection tends to be largely asymptomatic, but a number of virus-associated pathologies have been described, especially in the context of immunosuppression. While many of the human polyomaviruses identified to date were originally isolated from disease samples, only five have been definitely linked with a direct involvement in human disease: BKV in polyomavirus-associated nephropathy (PVAN), JCV in progressive multifocal leukoencephalopathy (PML), MCV in Merkel cell carcinoma (MCC), TSV in trichodysplasia spinulosa (TS), and HPyV7 in transplant-associated pruritic rash (**Figure 5**). There is no evidence that the other human polyomaviruses are causally associated with specific human diseases, and in most cases their presence has been deemed as incidental, passenger infections (65, 105).

PVAN is the most common form of BKV-associated disease seen in renal transplantation patients, and an increase in incidence since its initial description has been observed (111–113). PVAN tends to occur within the first year of transplantation. It is believed that aggressive immunosuppressive drug treatment leads to BKV reactivation

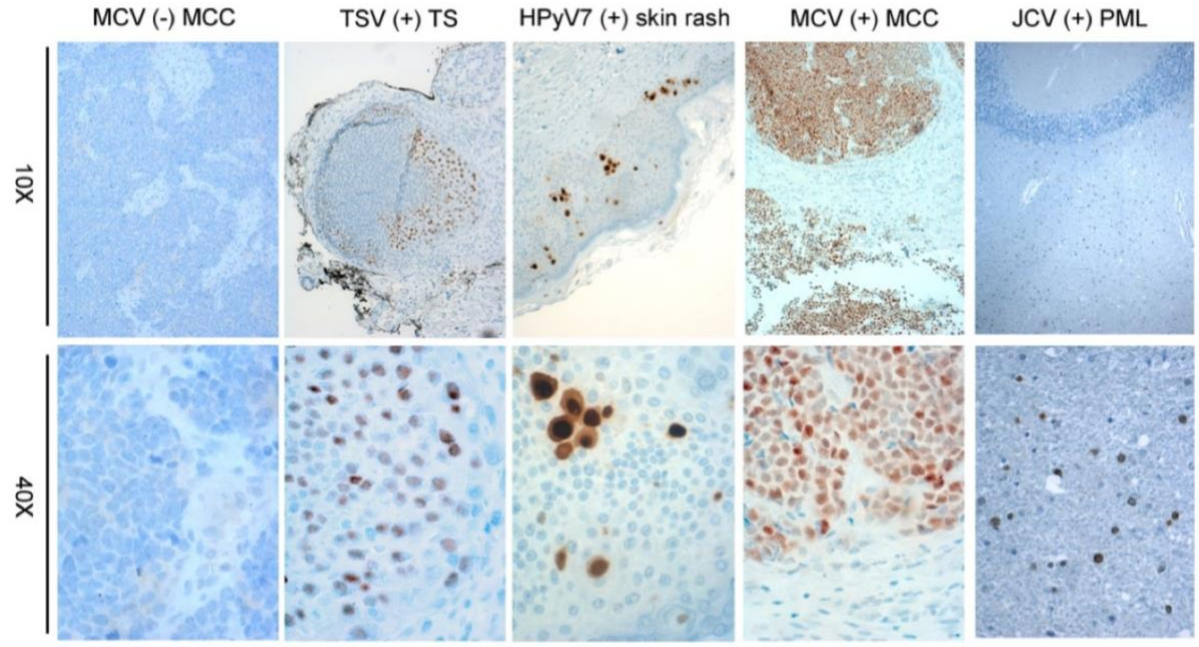


**Figure 5. Immunohistochemical pan-PyV survey on HPyV-associated disease tissues.**

Formalin-fixed paraffin-embedded tissue sections from JCV-related PML, MCV-positive or -negative MCC, HPyV7-related skin rash lesion, and TSV-related trichodysplasia spinulosa (TS) were stained with triple antibody combination for viral T antigens overnight and counterstained with hematoxylin. These results illustrate the presence of each virus in their associated disease tissues, most strikingly with tumor-specific T antigen staining seen in MCV-positive MCC. Results are presented at 10X and 40X magnification. (Republished with permission of ASCI, from Toptan *et al.*, 2016; permission conveyed through Copyright Clearance Center, Inc.)

from a quiescent state in these patients, and progression to PVAN ultimately results in kidney graft failure in many cases (114). There is currently no antiviral treatments for PVAN, and though cessation of immunosuppressive regimens does help to control viremia, it can also lead to graft rejection by the body (115).

PML is a rare disease of the central nervous system that is characterized by demyelination as a result of oligodendrocyte cell death. Oligodendrocytes are responsible for myelination in the central nervous system and are the primary cell type infected by JCV. This devastating disease produces severe symptoms like visual impairment, encephalopathy, and loss of motor function (116). PML is a highly fatal condition, and

many patients die within 4-6 months of diagnosis (117, 118) The disease is caused by JCV reactivation and is most often seen in AIDS patients or other immunocompromised individuals (119). There are currently no effective drug treatments for PML.

MCV as the causative agent of MCC is the only known human polyomavirus that has a causal role in cancer in humans (120). MCV is found to be clonally integrated into ~80% of MCC tumors (48, 121), and tumorigenesis is believed to be driven by expression of the viral T antigens in these cases. The relationship between MCV and MCC is described in more detail in Section 1.4 (page 29).

TS is a dysplastic skin disorder characterized by the presence of spicules and keratin spines that appear on the face of affected individuals (122). TSV was first identified from TS tissue samples (67) and has since been demonstrated to be the causative agent of this disorder (123, 124). TSV like most polyomaviruses has a high seroprevalence among the general population (125), and TS is generally only seen in immunosuppressed individuals. There is currently no specific treatment for TS, but topical antivirals, such as cidofovir, have showed some promise in reducing symptoms (126).

Although, it was first isolated as an incidental skin infection in healthy skin, HPyV7 has since been shown to be associated with pruritic rash and serum viremia in immunosuppressed lung transplant recipients (127). In these cases, HPyV7 was detected in both blood and skin samples from the affected area at high copy numbers, indicating that these were not cases of incidental infection. Continuing to profile diseased tissues for the presence of polyomaviruses especially in the context of immunosuppression may not only lead to the discovery of pathological effects for some of the more newly-identified human polyomaviruses, it may lead to the discovery of even more polyomaviruses (128).

## 1.3 Mechanistic insights from SV40 T antigens

Although there is little evidence to support SV40-induced pathology in humans (82, 129), the vast number of studies that have been conducted with SV40 since its discovery have been invaluable to understanding polyomavirus natural biology, polyomavirus-induced transformation, and cancer biology as a whole. Upon the discovery of new human tumor viruses like MCV, SV40 has proven to be an excellent template for comparison in order to elucidate the complex biology of these viruses and their roles in tumorigenesis. The major focus of this dissertation centers around tumorigenic mechanisms of MCV T antigens, and SV40 T antigens serve as a basis for comparison in future chapters. Therefore, it is only fitting to include information about some of the most important cellular interactors of SV40 T antigens and their roles in tumorigenesis. This remainder of this section focuses on the LT and sT antigens of SV40 and the many cellular proteins they contact (**Figure 6**).

### 1.3.1 Targeting of retinoblastoma family proteins

The retinoblastoma (Rb) family of proteins or pocket proteins pRb, p107, and p130 act as major regulators of transcription in cells and work to control the G1-S phase transition of the cell cycle (130). Under normal conditions, these pocket proteins form tight complexes with the E2F family of transcription factors to repress the transcription of target genes involved in DNA replication, DNA repair, and cell division. At the G1-S phase boundary, these pocket proteins become phosphorylated and dissociate from E2F

members, which then bind to their target promoters to activate or repress transcription. This usually results in progression of the cell cycle (131, 132).

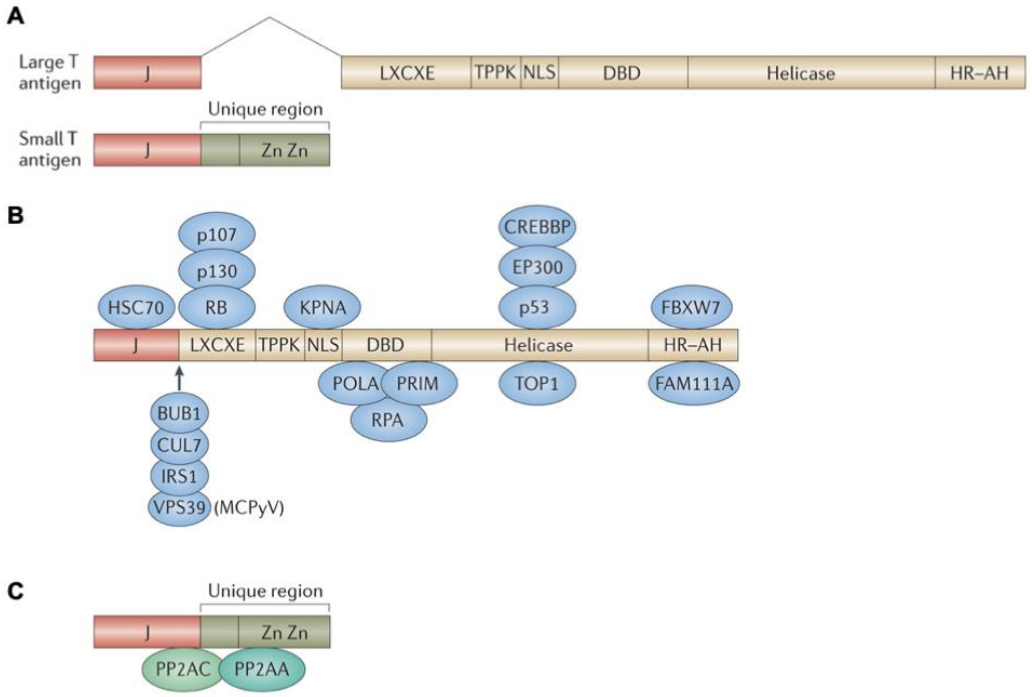


**Figure 6. Functional domains of polyomavirus Large and small T antigens.**

A. The N-terminal DnaJ (J) domain is shared between LT and sT antigens. LT antigen also contains a Rb-binding LXCXE motif, a TPPK motif, a NLS, a DNA-binding domain (DBD), a helicase domain, and a host range domain (HR–AH). sT contains an N-terminal J domain followed by a unique region that contains two zinc-fingers. B. Large T antigen binds many cellular proteins. The J domain recruits Hsc70 homologues. The region between the J domain and LXCXE motif has been shown to bind independently to Cul7, Bub1 and IRS1. The LXCXE domain binds to pocket proteins pRb, p107, and p130. The DBD and helicase domains are required for viral replication and recruit cellular DNA replication factors to the replicating PyV genome. The C-terminus of SV40, JCV, and BKV LTs contain a Thr residue that, when phosphorylated, binds to FBXW7. C. sT binds specifically to the A and C subunits of PP2A. (Modified from DeCaprio and Garcea, 2013)

Tumor viruses that rely on the host replication machinery to accomplish their own viral replication must drive quiescent cells into S-phase in order to complete their life cycles, making the Rb family of proteins a prime target of these viruses, including SV40 (**Figure 7A**). Rb binding by a viral protein was first described for the adenovirus E1A

protein through a conserved LXCXE motif (133). It was subsequently determined that SV40 LT is capable of binding all three pocket proteins through its own LXCXE motif (aa 103-107), the result of which is E2F activation and S-phase transition (134, 135). The interaction between SV40 LT and Rb family members has been shown to be critical for transformation, as LT mutants without a functional LXCXE motif are defective for transformation (136–139).

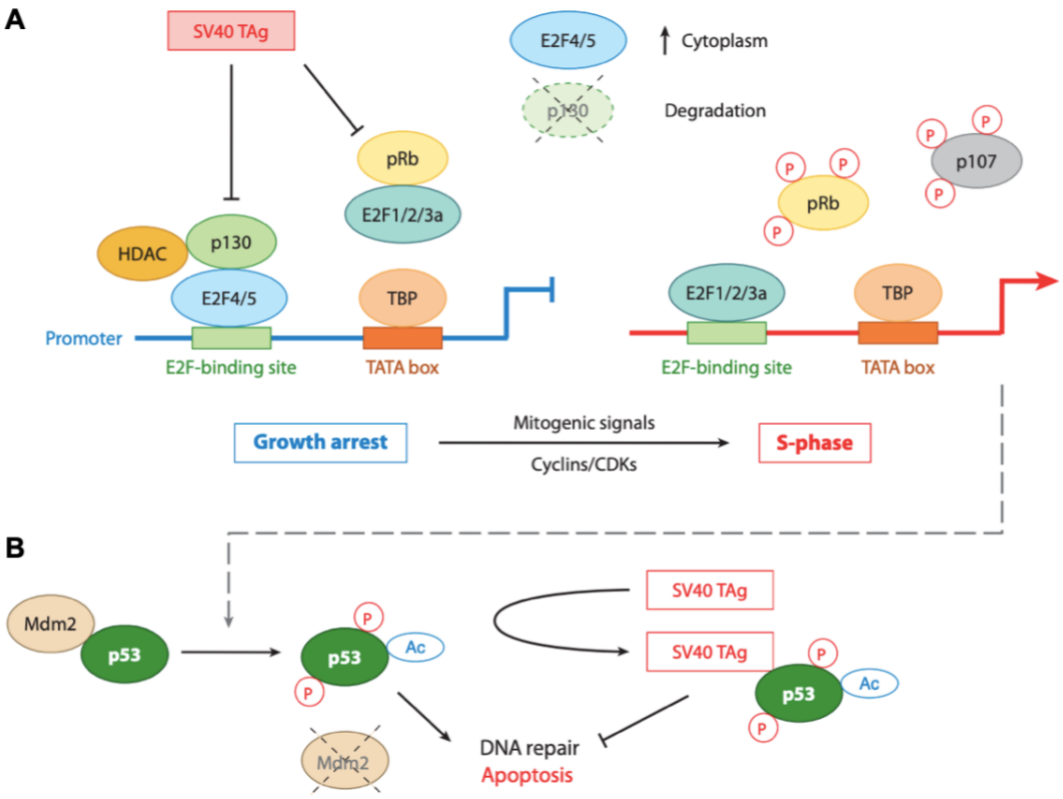


**Figure 7. Manipulation of the host cell machinery by SV40 LT antigen.**

A. Hypophosphorylated pRb blocks G1-S phase transition by binding and inhibiting E2F1/2/3a transcription factors. p130 also complexes with E2F4-5 transcriptional repressors to block transcription. SV40 LT binds Rb family proteins via its LXCXE motif, the transcriptional block is released, and S-phase transition ensues, allowing for replication. B. p53 levels are kept very low in normal cells by the E3 ubiquitin ligase Mdm2, but phosphorylation (P) and acetylation (Ac) allow p53 to become an active transcriptional regulator in response to LT-induced cell cycle dysregulation. LT avoids premature cell death by binding and blocking p53 activity and induction of apoptosis. (Republished with permission of Annual Reviews Inc., from An *et al.*, 2012; permission conveyed through Copyright Clearance Center, Inc.)

### 1.3.2 Targeting of p53

One of the most well-known and well-characterized interactors of SV40 LT is the tumor suppressor p53, which was actually first identified in a complex with LT (140, 141). p53 is a potent transcription factor at the nexus of numerous signaling pathways, including DNA damage, nutrient starvation, and cell cycle dysregulation. Activation of p53 in response to such stimuli generally results in cell cycle arrest or apoptosis (142, 143). As such, functional p53 protein is essential for maintaining genome integrity, which is underscored by the fact that it is the most commonly mutated gene in human cancers (144). Under steady-state conditions, p53 protein levels within cells are kept low, as it is readily targeted for degradation by the E3 ubiquitin ligase Mdm2 (145). Multiple stimuli can trigger the activation of p53, by which a series of post-translational modifications cause it to dissociate from Mdm2, bind to target gene promoters, and activate transcription of multiple genes (146).

The unscheduled transition to S-phase caused by SV40 LT binding to Rb family members is believed to trigger p53 activation, and so p53 inhibition becomes an additional critical step in the polyomavirus life cycle to promote replication and prevent premature cell lysis (**Figure 7B**). The interaction between LT and p53 has been broadly mapped to a bipartite motif in the C-terminal regions of LT (aa 351-450 and 533-626) (103, 147). Crystallographic data regarding this interaction also supports the idea of two large regions of interaction, identifying 23 key residues on SV40 LT that directly contact p53 (148). Whether or not p53 binding by LT is required for SV40-induced transformation remains unclear. While p53 binding by LT is required for immortalization and continued

proliferation in many cellular models (147, 149, 150), others have identified p53-binding mutant LTs that can still induce transformation (139).

Binding between SV40 LT and p53 itself is undisputed, but the downstream consequences of this interaction are not as clear. There are conflicting reports as to whether or not LT through its interactions with p53 prevents its ability to bind DNA and activate target promoters (151–153). Others have suggested that inhibition of p53 by SV40 may occur independently of direct interaction with LT (154). What is clear, however, is that p53 is functionally inhibited in the presence of SV40 LT (155, 156).

Cells that express SV40 LT also curiously show accumulation of p53 protein (157, 158), but the reason for this metabolic stabilization is unclear. Some evidence supports that accumulation of p53 can have an oncogenic gain of function that promotes transformation, as wild-type p53 has been shown to enhance SV40-induced transformation (159, 160). A competing theory is that accumulated p53 could promote SV40 LT binding to p300, leading to modulation of host transcription (161). This interaction is described in more detail below.

### 1.3.3 Targeting of p300 and CBP

CREB-binding protein (CBP) and p300 are scaffold proteins that function as co-activators of transcription through their histone acetyltransferase (HAT) activity and are generally viewed as tumor suppressors (162–164). While histones represent a major target of CBP and p300, they are also capable of interacting with and acetylating a number of cellular proteins, including p53 (165).

Much like pRb, adenovirus E1A was the first viral protein shown to target CBP and p300 through its N-terminal region (166). Soon after, SV40 LT was implicated in binding CBP and p300 (167, 168), but contrastingly this activity was mapped to the C-terminus of LT (169). The binding between LT and CBP/p300 has been shown to also require p53, with the three proteins existing as a ternary complex (161, 170). This complex results in the acetylation of LT by CBP, which is believed to be important for LT stability (171). There are also some reports that LT modulates CBP HAT activity and inhibits CBP/p300 transcriptional activation (168, 172), both of which could contribute to LT-induced transformation. However, due to the indirect nature of these interactions, the precise contributions of CBP/p300 binding to SV40 LT-induced transformation have been difficult to assess directly (173).

### 1.3.4 Additional cellular targets of SV40 LT

The cellular targets of SV40 described above are some of the most well-characterized interactors of SV40 LT and are the most relevant to the interpretation of the studies presented in the rest of this dissertation. The binding partners described in this section are not as integral to the understanding of the data presented in later sections, but are still informative for understanding polyomavirus biology and the tumorigenic potential of these viruses.

#### 1.3.4.1 Heat shock cognate protein 70 (Hsc70)

The N-terminal regions of SV40 T antigens bear sequence homology with the J domain of DnaJ molecular chaperones, including the canonical HPDKGG motif (174,

175). Through this domain SV40 LT binds Hsc70 and stimulates its ATPase activity (176, 177). Several studies have shown that the DnaJ domain is critical both in terms of facilitating viral replication, but also in terms of inhibition of Rb family members (178–180). As such, this domain has been shown to be critical for transformation and the DnaJ domain must be present *in cis* with the Rb-binding motif to elicit transformation (138). There is speculation that SV40 LT may direct Hsc70 to act on multiple cellular targets, such as p300 and cyclin A, but this remains purely speculative (103).

#### 1.3.4.2 Bub1 mitotic checkpoint serine/threonine kinase

Bub1 plays a critical role in the mitotic spindle-assembly checkpoint and as such has a defined role in maintaining genome stability (181). SV40 LT binds to Bub1 through a conserved WExWW motif in its N-terminal region (aa 89-97), which results in mitotic defects (182). LT-Bub1 interaction has thus been associated with the development of aneuploidy and chromosomal instability (183). Not surprising, deletion of this binding motif on LT has been shown to compromise its transformation efficiency (182).

#### 1.3.4.3 Cullin 7

Cullin 7 (Cul7) functions as part of an E3 ubiquitin ligase complex known as the Skp-Cullin-F-box (SCF) complex that targets proteins for degradation (184). Binding of Cul7 by SV40 LT has been mapped to aa 69-83 in the N-terminus of LT, and LT mutants lacking this region are deficient in transformation assays (185, 186). It should be noted that this mutation does not disrupt LT binding to other known partners. Whether LT serves only to inhibit the natural function of this SCF complex or if it redirects it toward other cellular targets remains unknown.

#### 1.3.4.4 Insulin receptor substrate 1 (IRS1)

IRS1 is a key player in the PI3K/Akt pathway of cell cycle regulation, and it is known to be dysregulated and mislocalized in several human cancers (187). SV40 LT has been shown to interact with IRS1, resulting in its nuclear translocation (188). IRS1 binding has also been implicated in SV40-induced transformation (189–191). Binding has been generally mapped to the N-terminal region of LT and may overlap with Rb-binding, as an LXCXE-mutant LT was also deficient in interacting with IRS1 (192).

#### 1.3.4.5 F-box/WD repeat-containing protein 7 (Fbw7)

It has also been reported that SV40 LT is capable of binding to F-box protein Fbw7 through a motif present in its C-terminal host range domain (193). Fbw7 is also a member of the SCF complex, and it recognizes its substrates through specific phosphorylated epitopes known as phosphodegrons to target them for degradation (194). Interestingly, binding of LT to Fbw7 does not result in its degradation, so it has been proposed that it instead acts as a decoy to prevent Fbw7 binding to other cellular targets. Given that the natural targets of Fbw7 are involved in cell cycle control, this interaction may have implications for both viral replication and transformation, but these relationships have not been well studied.

### 1.3.5 PP2A targeting by SV40 sT

In the context of SV40, the sT antigen assists in LT-induced transformation but is not sufficient for transformation in its own right. One of the major cellular targets of sT is the protein phosphatase complex PP2A. This is a heterotrimeric complex consisting of a

scaffold subunit (A), a regulatory subunit (B), and a catalytic subunit (C). PP2A complexes have numerous cellular targets, and the identity of the B subunit, of which there are many, governs the specificity of the complex for a particular substrate (195). SV40 sT acts on PP2A by binding to the A subunit and displacing the B subunit, which leads to a defect in enzyme activity (196). The specific B subunits targeted by sT are still being defined (197, 198), but one known cellular target of sT PP2A targeting is c-myc (199). PP2A targeting by sT has also been shown to activate several cellular kinases, including MAPK, Akt, and PKCζ (200–202). Mutations that disrupt PP2A binding by sT show defects in transformation in human cell lines (203, 204).

### 1.3.6 Permissive vs. non-permissive infections

Much of this section has focused on the properties of SV40 T antigens that allow for cellular transformation, but it is important to note that transformation and tumorigenesis are not the goals of tumor viruses. Transformation is simply a standard for measuring the oncogenic potential of, in this case, T antigens with the notion that such studies will lead to a better understanding of the host proteins and pathways involved in preventing oncogenesis. Tumor formation incidentally serves no purpose in the viral life cycle, because it occludes the ability of these viruses to replicate and disseminate progeny virions (16). Tumorigenesis by these viruses is an unfortunate consequence of an error in their natural life cycle, and it often arises from a non-permissive infection.

In the simplest terms, permissive infections allow for the full completion of the viral life cycle from entry to release of new virions, whereas non-permissive infections result in a roadblock in the viral life cycle at some point (1). Using SV40 as an example, infection

of African green monkey kidney cells with SV40 represents a permissive infection, because the end result is lysis of host cells and release of infectious virions (**Figure 8A**). Infection of rodent cells with SV40, however, represents a non-permissive infection (103). This is because, while the early parts of the SV40 life cycle can be accomplished, there is a block in these cells in terms of viral genome replication, late gene expression, and dissemination. Still, the early events of the SV40 life cycle drive these cells into S-phase, which can result in a temporary "transformation" (**Figure 8B**). As the virus cannot replicate within these cells, the number of genome copies per cell is diluted out through multiple

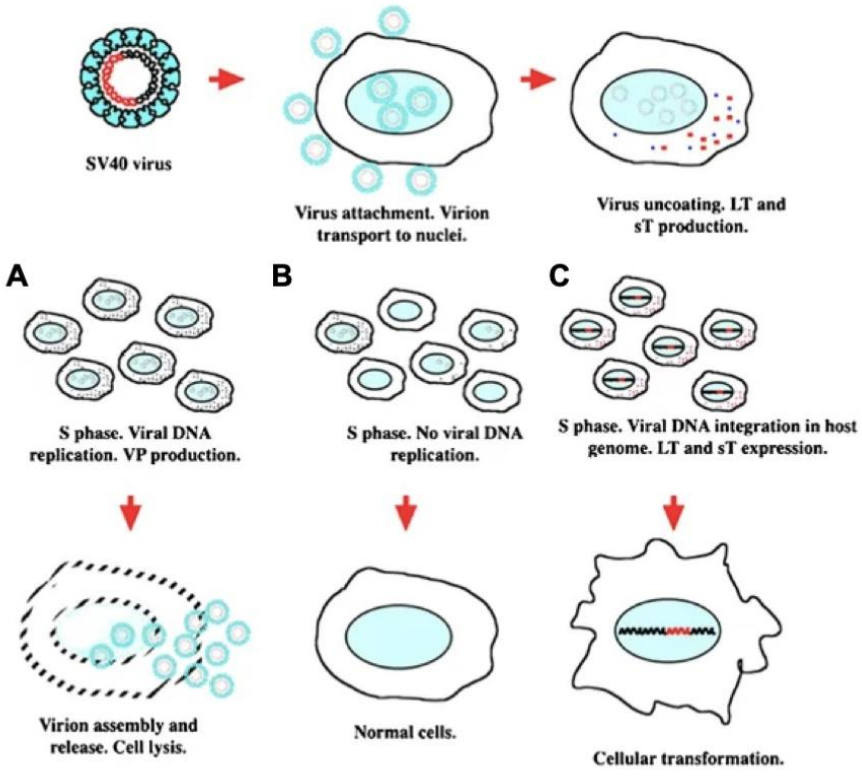


**Figure 8. Results of SV40 infection in different cellular environments.**

A. Infection of permissive cells results in cell death and virion production. B. SV40 infection of rodent cells induces S-phase entry, but does not result in cell death or virus production. C. Integration of viral DNA occurs in a very low percentage of non-permissive cells, which then become stably transformed. (Modified from Ahuja *et al.*, 2005)

rounds of cell division, and the transforming effects of SV40 are lost (103). There is also the possibility for stable transformation of non-permissive cells, but this occurs at a much lower frequency (**Figure 8C**). In this case, after a double-strand DNA break a nonhomologous recombination event results in the integration of the viral genome within the host genome, from which early region transcripts may still be expressed and the T antigens can induce transformation. The infrequency of this entire process serves to explain why transformation itself is quite a rare event (1).

## 1.4 Merkel cell polyomavirus

### 1.4.1 Discovery of MCV

Merkel cell carcinoma (MCC) is a rare but aggressive form of nonmelanoma skin cancer that is believed to originate from mechanoreceptor Merkel cells in the basal layer of the skin (205–207). Although it remains a rare cancer, incidence of MCC has increased sharply in recent decades, with approximately 1,500 new cases diagnosed each year in the United States (120, 208, 209). Despite ongoing research, prognosis for patients with MCC remains poor, and mortality rates remain high (209–211)

Given that MCC has a higher rate of incidence in elderly, immunocompromised individuals, and people with AIDS, it bears striking similarities to other tumors arising from a viral etiology, like Kaposi sarcoma (210, 212, 213). Backed with this knowledge, researchers at the University of Pittsburgh under the direction of Yuan Chang and Patrick Moore developed a bioinformatic approach called digital transcriptome subtraction (DTS)

to search for underlying viral sequences in MCC tumor specimens. This technique relies on deep sequencing of cDNA (>300,000 reads) from tumor specimens, from which human sequences can be computationally subtracted. Using this high-throughput approach, Feng *et al.* were able to identify two critical transcripts that were non-human in nature and matched with a database of viral genes. The first transcript bore high homology to known polyomavirus T antigen sequences and the second was later shown to align with a portion of the viral genome whose full sequence was mapped during the course of the investigation. This newly identified polyomavirus was named Merkel cell polyomavirus due to its association with MCC tumor specimens (48).

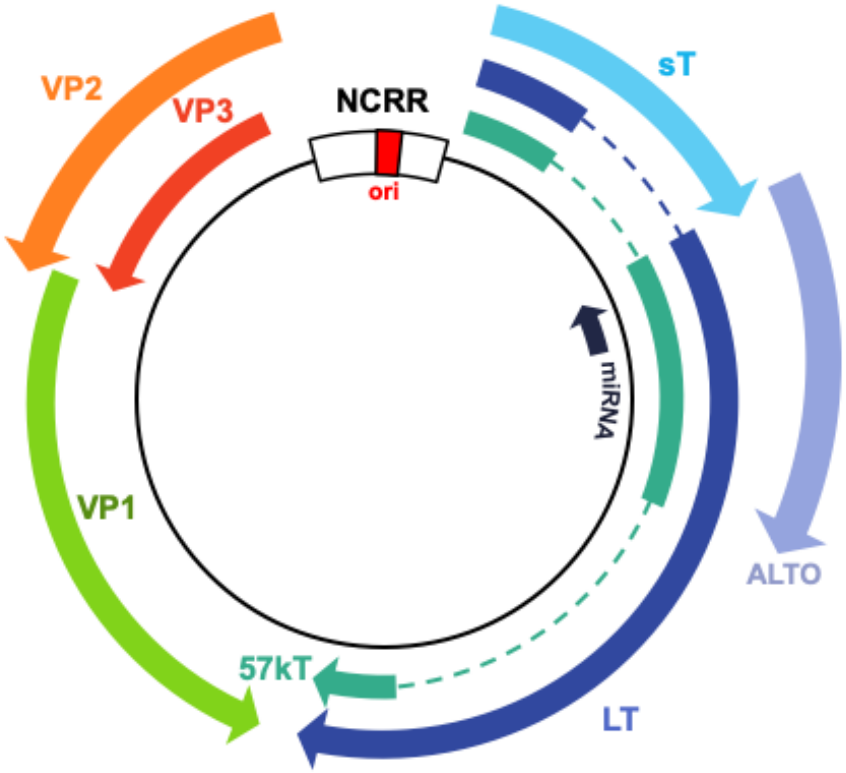


**Figure 9. MCV genome organization.**

Non-coding regulatory region (NCRR): Origin of replication (red) and bidirectional promoter. Early gene region: Splice variants for Large T antigen (LT), small T antigen (sT), 57kT antigen (57kT), alternative T antigen open reading frame (ALTO), MCV microRNA (miRNA). Late gene region: Splice variants for capsid proteins VP1, VP2, and VP3.

### 1.4.2 Genome structure

Like all polyomaviruses, the MCV genome is composed of early and late coding regions, separated by a noncoding regulatory region (**Figure 9**) (82). The early coding region corresponds to the canonical T antigen gene locus of polyomaviruses, from which multiple, alternatively-spliced RNA transcripts are generated and expressed as large T (LT), small T (sT), and 57kT antigens (83). Examination of an MCV-unique region (MUR) in this same stretch led to the identification of an alternative T antigen ORF (ALTO), whose gene product is expressed during replication. While the function of the ALTO protein remains unknown, its discovery links MCV to other polyomaviruses that also show evidence of overprinting in their early coding regions (91).

The late coding region of MCV encodes the viral capsid proteins VP1, VP2, and VP3 (48). Unlike other polyomaviruses, specifically BKV and JCV, MCV does not encode a VP4 or agnoprotein (93). In addition to these three major ORFs, MCV also possesses a region antisense to the early region that codes for the expression of a single microRNA that was first identified through *in silico* prediction and termed MCV-miR-M1 (96). Further *in vitro* and *in vivo* studies have confirmed that this microRNA has a regulatory function in terms of suppressing LT expression, and evidence suggests it may also be involved in immune surveillance by targeting members of the host innate immune response (96, 214).

### 1.4.3 Virus life cycle

The life cycle of MCV during the course of a permissive infection is generally consistent with that of known polyomaviruses. However, the attachment and entry

process for MCV appears to be unique compared to other polyomaviruses in that it requires glycosaminoglycans like heparan sulfate as an initial attachment factor, but subsequent entry requires a sialylated glycan like Gt1b (99, 215–217).

Following entry, the early region of the viral genome is transcribed to produce the T antigens, which drive cells into S-phase and initiates the process of replication (218, 219). MCV LT assembles into a head-to-head double hexamer formation and binds to and unwinds the viral origin of replication to begin this process (220, 221). As MCV T antigens are a major focus of this dissertation, a more comprehensive review of MCV T antigen expression and manipulation of the host cell is presented in Chapter 2 (page 37).

After replication, it is believed that LT may downregulate its own transcription, which causes a switch to late gene transcription and capsid production (222). The miRNA encoded by MCV may also play a role in this process by suppressing LT transcripts (214). Very little is known about the process of MCV capsid assembly and egress from cells. Many polyomaviruses exit cells through direct lysis, but as MCV is known to naturally be present in the skin (66, 223), it may also be naturally shed through the natural differentiation process of the skin.

Overall, the lack of an infectious model system for MCV has made studying its natural biology quite difficult. Trying to identify permissive cells for MCV infection has also proven challenging (224). Only recently was it proposed that human dermal fibroblasts are the natural host cells for MCV (225). While this finding is consistent with reports that MCC often arises in the dermis (226), it has also raised many questions about the origins of MCV-induced MCC. One theory is that Merkel cells represent a non-permissive cell line for MCV that become incidentally infected following virus shedding in the dermis,

leading to malignant transformation (227). Others have suggested that MCV instead reprograms its natural host cells to present Merkel cell markers (228, 229), which is further supported by work by Harold *et al.* that showed that knockdown of T antigen expression in MCC cells results in the loss of expression of Merkel cell marker genes and reversion to a differentiated neuronal cell phenotype that is distinct from Merkel cells (230). Recently, genetic analyses on an MCV-positive MCC derived from a benign trichoblastoma indicate that epithelial skin cells may also serve as a host cell for MCC development (231). Taken together, these reports demonstrate that MCV-induced MCC may arise from multiple cellular lineages (232) and that there are still many questions regarding MCC histogenesis that need to be clarified.

### 1.4.4 Involvement in Merkel cell carcinoma

Much like the other human tumor viruses that preceded it, establishment of the causal relationship between MCV and MCC required a supportive body of evidence before the scientific community at large recognized MCV as a bona fide tumor virus. One of the strongest pieces of evidence came from the discovery report itself, where it was determined that MCV was not just present in MCC tumor specimens, but rather it was clonally integrated into the genome in 8 of 10 specimens that were examined (48). Clonal integration of MCV in MCC tumor specimens and tumor-restricted T antigen expression was further confirmed through follow-up studies (121, 233, 234). These data indicate that the virus was present prior to the outgrowth of the tumor and negates the possibility of MCV being present as a passenger infection. Furthermore, continued proliferation of MCC tumors was also seen to be dependent on the expression of MCV LT and sT

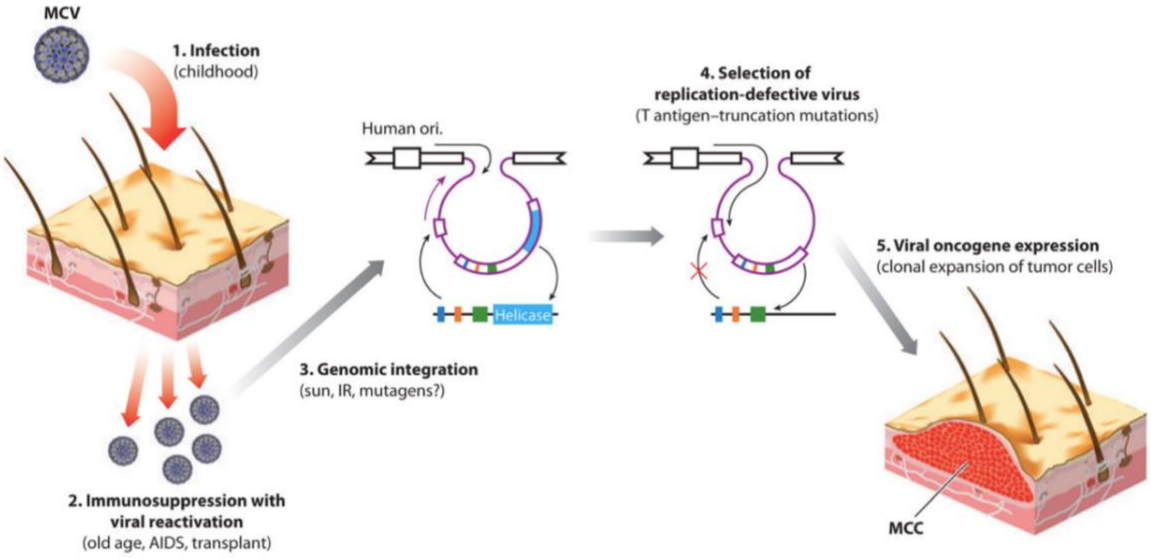


**Figure 10. Hypothetical framework for MCV-induced MCC carcinogenesis.**

MCV infection is acquired in childhood and remains a persistent, asymptomatic infection. Old age and immunosuppression results in reactivation. MCV becomes integrated in the host genome. Selective pressure eliminates replication-competent integrated viruses. T antigen expression drives tumorigenesis leading to MCC development over time. (Republished with permission of Annual Reviews, Inc., from Chang and Moore, 2012; permission conveyed through CCC, Inc.)

antigens (235, 236), and MCV sT has been demonstrated to have *in vitro* and *in vivo* transformative capabilities (237–239). Together, these findings help to solidify the causal relationship between MCV and MCC, while simultaneously providing a diagnostic framework for identifying MCV-positive MCCs.

Having established this causal relationship between MCV and MCC, the question then became how a component of the natural skin flora acquired in childhood manages to induce such an aggressive form of skin cancer (**Figure 10**). It is important to remember that MCC generally arises in elderly and immunosuppressed populations, where it is believed that immune surveillance toward MCV becomes diminished (210, 212). This could stimulate a more productive MCV infection in these populations (240, 241). The next steps in this process are two mutagenic events: first, integration of the viral genome

within the host genome by nonhomologous recombination, and second, nonsense or missense mutations to the viral genome that eliminate the ability of MCV to replicate. Were MCV still able to foster replication following integration, it is believed that this unlicensed replication would trigger host DNA damage sensors resulting in cell death (83). In this way, only cells that undergo both mutagenic events can survive, which results in the clonal expansion from single MCC progenitor tumor cell. Expression of viral T antigens within these cells is also a key factor in promoting tumorigenesis.

### 1.4.5 Mutations in Merkel cell carcinoma

As mentioned in the previous section, one of the defining characteristics of MCV-positive MCCs is the presence of missense or nonsense mutations to the integrated viral genome that result in the production of the C-terminally truncated LT protein in these tumors, leaving the coding sequence for MCV sT intact (83). These C-terminal truncation mutations result in the deletion of the entire the helicase domain and usually most of the origin-binding domain, eliminating the replicative functions of LT (**Figure 11**). Tumor-derived LTs notably retain a functional DnaJ domain and Rb-binding motif, highlighting the importance of each of these regions for tumor outgrowth, which parallels their importance in SV40 LT-induced transformation (203). The preservation of the entire sT coding sequence likewise underscores its role in tumor initiation and tumor maintenance. The functional domains of the MCV T antigens are enumerated in greater detail in the following chapter. Lastly, it should be noted that MCV-positive MCC cases possess a significantly lower frequency of somatic mutations than MCV-negative MCC cases, which are believed to arise from UV-damage (242–245). This is consistent with other virus-

induced cancers, where the viral oncoproteins target tumor suppressors that are frequently mutated in non-infectious cancers.

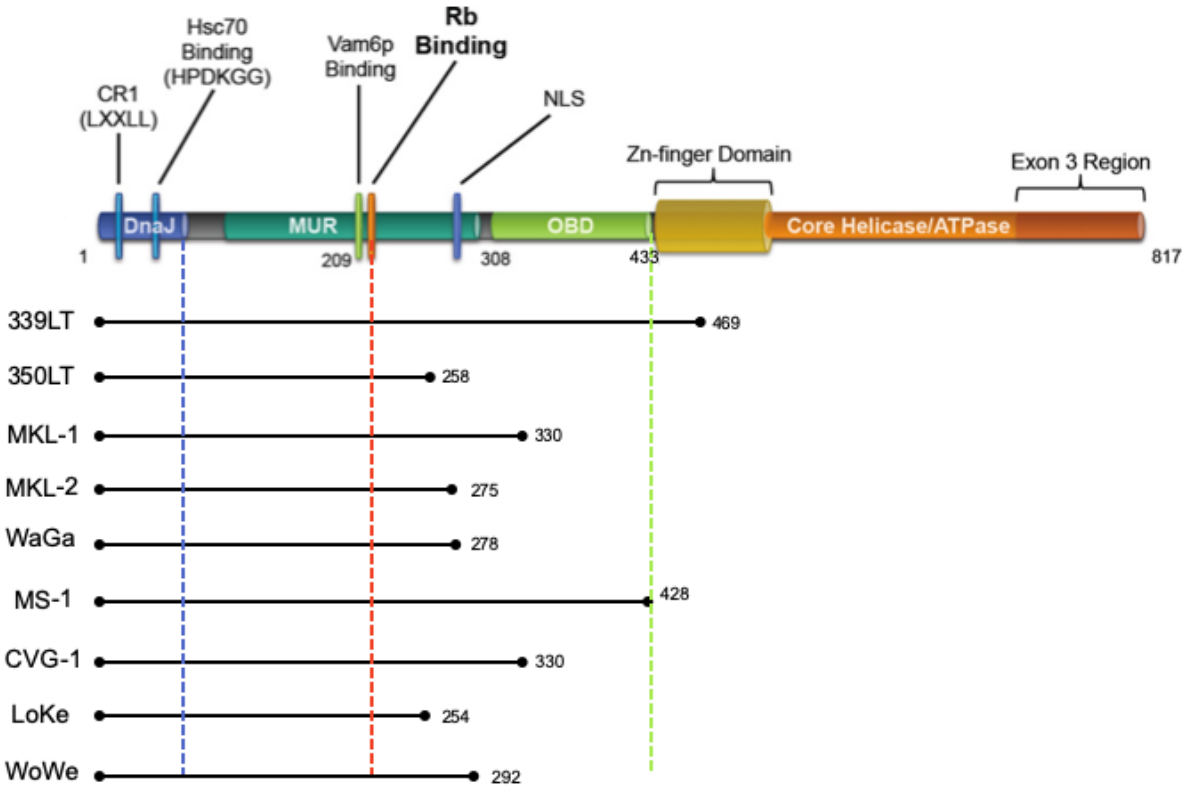


**Figure 11. Schematic of canonical LT truncations in MCC cell lines.**

At the top, a schematic for full-length LT is shown, annotated with amino acid positions for key functional domains and motifs. The lengths in amino acids of truncated LTs present in MCC cell lines are depicted below, showing all that truncated LTs retain the N-terminal DnaJ domain (blue line) and Rb-binding motif (orange line), but lack the C-terminal replicative domains (green line and beyond).

## 2.0 Large T and small T antigens of Merkel cell polyomavirus

The literature review contained in this chapter was published in Current Opinion in Virology

**Curr Opin Virol. 2015 Apr;11:38-43.**

**with authors Wendzicki JA, Moore PS, and Chang Y.**

Minor updates to include new findings have been made since the original date of publication in 2015.

### 2.1 Introduction

Merkel cell polyomavirus (MCV) is the newest member of the short list of human cancer viruses (16, 18), and is the only known human polyomavirus confirmed to be oncogenic (48, 55, 56, 62, 63, 66–74, 246). While MCV was only discovered in 2008, polyomavirus research dates back over a half century, beginning with the isolation of murine polyomavirus (MuPyV) (11) and later simian vacuolating virus 40 (SV40) (12, 52). These polyomaviruses have provided invaluable insights into our mechanistic understanding of tumor and cell biology. Polyomaviruses have small genomes (~5kb) comprised of early and late coding regions, separated by a noncoding regulatory region (NCRR). The early region contains the T (“Tumor”) antigen gene locus (82), from which

multiple, alternatively-spliced RNA transcripts are generated. MCV expresses four unique gene products from this early coding region: the large T (LT), small (sT), and 57kT antigens along with a product from an alternate frame of the LT open reading frame (ALTO) (91) (**Figure 12**). In natural polyomavirus lytic infection, a sequential expression of early antigens followed by late capsid proteins is seen. By contrast, MCV-associated tumorigenesis is characterized and mediated by the sole expression of LT and sT antigens (82, 235). This review will present a biochemical map of the functionally relevant motifs and domains within LT and sT, the two major oncoproteins of MCV.

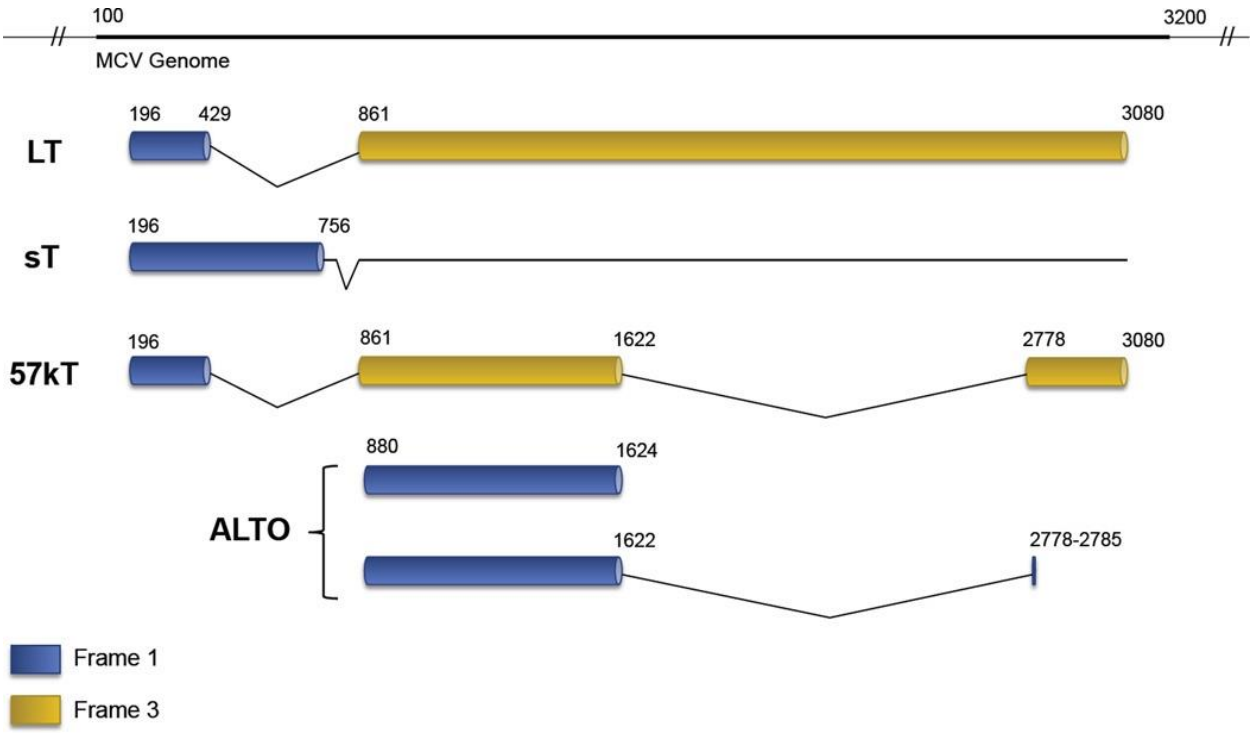


**Figure 12. Gene products of the MCV early coding region.**

Multiple gene products are expressed from the early coding region of the MCV genome as a result of alternative splicing of RNA transcripts. Splicing patterns for each gene product are depicted. LT, sT, and 57kT represent the main T antigens expressed by MCV, which share a common first exon sequence. An alternate frame of the LT open reading frame (ALTO) has also been identified, which is +1-shifted to the second exon of LT. A single microRNA named MCV-miR-M1 is also coded by MCV whose mature sequence is antisense to 1215-1236 nt in the viral genome.

## 2.2 Large T antigen

The LT antigens of polyomaviruses contain a number of common motifs and domains important for facilitating the viral life cycle (247). In the context of oncogenesis, some of these elements also have the effect of disabling tumor suppressor pathways, for example by targeting Rb and p53 (82). The LT antigen of MCV encodes many of these conserved features as well as a few unique ones (**Figure 13**).

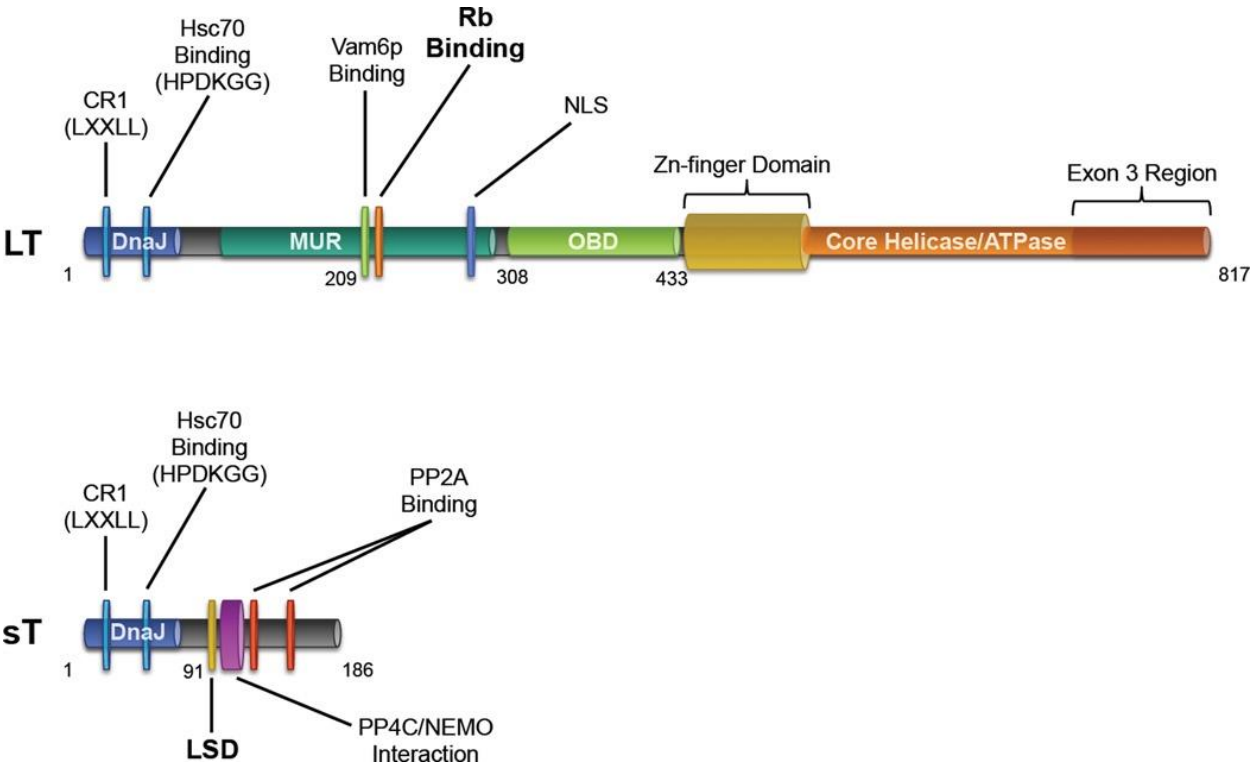


**Figure 13. Schematic of MCV LT and sT functional domains.**

The LT and sT Antigens of MCV are characterized by their multifunctional natures. This schematic representation of these two proteins highlights the location of several motifs and domains that are important in the viral life cycle and tumorigenesis. Regions with a key role in tumorigenesis are bolded. LT contains a DnaJ domain at its N-terminus, followed by the MUR, which contains the binding motifs for Vam6p and Rb family members as well as an NLS. In this region is also the site of complementarity for MCV-miR-M1, the sole microRNA encoded by the MCV genome. The C-terminal portion of LT contains the OBD and the core helicase/ATPase domain, which contains the zinc-finger domain and the region corresponding to Exon 3 of 57 kT. sT contains an identical DnaJ domain, followed by the LSD and sites for PP4C and PP2A interaction.

The N-terminal end of MCV LT (1–70 aa) contains the DnaJ domain (247) comprised of the CR1 (13–17 aa) motif followed by the HPDKGG hexapeptide sequence responsible for Hsc70 binding (42–47 aa) (83, 247). Kwun et al. confirmed that MCV LT interacts with Hsc70, and by disrupting this interaction with a point mutation, they showed the necessity of the DnaJ domain for MCV replication in vitro (248).

Between the first exon and the OBD (~100–300 aa) lies a stretch of sequences that contains a conserved LXCXE motif and nuclear localization signal (249), but otherwise bears little homology to other polyomaviruses. This region, designated the MCV T antigen unique region (MUR) contains a binding motif for the vacuolar sorting protein Vam6p. The LT-Vam6p interaction, which can be ablated by mutation of a single tryptophan residue at position 209, results in the nuclear sequestration of this cytosolic protein and disrupts lysosomal clustering (250). Although Vam6p interaction appears to be unique to MCV, the site of this interaction parallels the site for Bub1 interaction in SV40 LT, which also depends on the presence of tryptophan residues and modulates SV40 LT-mediated transformation by overriding the mitotic spindle checkpoint (82, 182). In an *in vitro* replication assay using an infectious molecular clone of MCV mutated at position 209, Feng *et al.* demonstrated that loss of LT-Vam6p binding leads to enhanced viral replication compared to a wild-type control (219). It is possible that in the natural life cycle of MCV, LT-Vam6p interaction inhibits or minimizes viral reactivation, a potential form of ‘viral latency’. SV40 miRNA has been proposed to serve a similar autoregulatory function by inhibiting SV40 LT expression (94). MCV encodes an miRNA that may have a similar function and may augment Vam6p-related replication silencing (96, 214). Whether or not Vam6p targeting is also important in tumorigenesis is not presently known.

The Rb-binding (LXCXE) motif of LT (212–216 aa) embedded in the MUR lies directly adjacent to the Vamp6-binding site (209 aa). This highly conserved sequence across polyomaviruses allows for dysregulation of E2F-mediated transcription and drives cells into S-phase (82, 251). Rb-binding and subsequent upregulation of E2F target genes such as cyclin E has been confirmed for MCV LT (83, 252). Houben *et al.* showed the importance of the LXCXE motif in the proliferation of MCC tumors cells, since complementation with an Rb-binding mutant of LT after RNAi-mediated T antigen depletion in MCC cell lines was incapable of rescuing cell growth (253). A novel biochemical function was mapped to this region when Arora *et al.* observed that upregulation of the anti-apoptotic protein survivin upon LT expression is dependent on the presence of and intact LXCXE motif (252). Targeting LT-mediated survivin upregulation represents a viable therapeutic option, supported by *in vivo* studies where pharmacologic inhibition of survivin lengthened the survival of mice bearing MCC xenografts (252, 254).

The C-terminal portion of MCV LT contains several critical elements required for viral replication. The OBD of LT (308–433 aa) is responsible for recognition and binding of a minimum 71-bp origin of replication in the MCV NCRR (221, 248). Diaz *et al.* observed that phosphorylation of LT upstream of the OBD at residues T297 and T299 decreases the origin-binding affinity of LT and negatively affects replication initiation (255). Following the OBD is a zinc-finger motif (437–528 aa) that is contained in the core polyomavirus helicase/ATPase domain (441–817 aa), both of which are important for LT oligomerization and initiation of replication (251). In addition to replicase activity, the helicase domain in SV40 contains a bi-partite sequence that can directly bind p53 and

prevent transcription of its target genes, allowing for the evasion of senescence or apoptosis (82, 151, 156, 247, 251, 256). Currently, there is no evidence that either full length or truncated forms of MCV LT directly bind p53 (257, 258). This concept is explored in greater detail in Chapter 4 of this dissertation.

One of the most striking features of the LT antigen of MCV is that the C-terminal domains are consistently truncated by tumor-associated polymorphisms, but the N-terminus up to the Rb-binding motif are always intact (83, 259). The short NLS of MCV LT that lies between these two regions (277–280 aa) was initially believed to also be conserved in tumors (249), but recent evidence indicates that the NLS is not preferentially preserved in MCC (257, 260). In the cases where the NLS is eliminated by tumor-specific mutations to LT (as in cell lines MCC350, MCCL-11, and MCCL-12) nuclear localization is not lost, but rather both nuclear and cytoplasmic distribution are observed (257).

This signature pattern of C-terminal truncation indicates a selective pressure for the elimination of viral replicative elements in tumor development, since a full-length LT could initiate unlicensed replication at the site of integration in the host genome leading to a DNA damage response (DDR) and cell death (83). This is not unlike other polyomaviruses (or other tumor viruses) in which replication competency is lost or suppressed in the setting of tumorigenesis (261–263). This notion is supported by Li *et al.* who observed a DDR induced by MCV infection which was mapped to the core helicase region of LT. The expression of a LT with intact and functional helicase induces ATR and subsequent p53 activation in multiple cell lines (264), leading to cell cycle arrest and decreased proliferation. There exists additional pressure for C-terminal truncation of LT that has been mapped to the very C-terminal end of the protein, corresponding to the

third exon of 57kT, which is shared by LT (717–817 aa). Upon retroviral transduction of an exon 3 construct, Cheng *et al.* noticed retardation of cell growth in an established MCC cell line as well as in human fibroblasts immortalized by SV40. The mechanism underlying this phenotype is presently unknown (258). Altogether, this evidence suggests that the C-terminal portion of LT generally has an antiproliferative effect, necessitating its deletion in tumorigenesis.

## 2.3 Small T antigen

Although MCV LT and sT share exon 1 of the T antigen locus, and the DnaJ domain of LT is required for replication, the functional significance of this domain in sT is unknown. It has been shown that mutating Hsc70 binding on sT does not interfere with its effect on MCV viral replication (248) or the *in vitro* transformative activity of sT (265). This is similar to SV40 in which the DnaJ domain of LT and sT is known to bind Hsc70 (138), but this function also does not impact tumorigenesis (82, 266).

The primary functions of sT antigens in the prototypic polyomaviruses SV40 and MuPyV has been long attributed to modifying Akt-mTOR signaling via their interactions with protein phosphatase 2A (PP2A) (196, 267, 268), a heterotrimeric complex comprised of A, B, and C subunits. sT antigens bind to the A and C subunits of PP2A to displace a variety of modular B subunits (82, 268), but the consequences of these interactions and their requirement in tumorigenesis varies between different polyomavirus species (269). Both SV40 and MuPyV sT antigens have been shown to have broad effects on cell cycle progression, survival, and differentiation that are dependent on PP2A (270, 271). The

primacy of PP2A targeting in other polyomavirus sT antigens contrasts directly with MCV sT, whose PP2A interacting domains (119–124 and 147–152 aa) are dispensable for its *in vitro* and *in vivo* transformative activity (239, 265). MCV sT instead possesses other functionalities in addition to PP2A binding that make it a key oncoprotein for MCC. MCV sT expression alone, independent of LT, is responsible for *in vitro* transformation of rodent fibroblasts in soft agar and focus formation assays (265), and sT is required for continued cell proliferation in MCC (236). Recent work by Verhaegen *et al.* has shown that MCV sT has *in vivo* proliferative activity when expressed in mice (239).

A major feature of MCV sT is a domain spanning 74–98 aa in intron 1 that is predicted to encode for an exposed, unstructured loop remotely located from PP2A binding sites (237). Scanning alanine mutagenesis in this loop has identified a region from 91–95 aa termed the LT-Stabilization Domain (LSD). This domain is responsible for inhibiting the SCFFbw7 E3 ubiquitin ligase (237). Since LT is a target of Fbw7, co-expression of sT prevents LT degradation, increases steady-state LT levels and has been shown to enhance viral replication (237). sT targeting of Fbw7 not only regulates LT levels during natural infections, sT also stabilizes truncated tumor T antigens and other SCFFbw7 substrates, including c-Myc and cyclin E, contributing to carcinogenesis. The importance of the LSD is evidenced by the fact that when mutated, sT loses its *in vitro* transformation activity (237). The promiscuous E3 ligase targeting ability of sT though its LSD and its consequences on genome stability has been recently described (272) and is included as Chapter 5 of this dissertation.

In addition to Fbw7, an intact sT LSD domain is required for targeting 4E-BP1, the major regulator of eukaryotic cap-dependent translation. In its active, hypo-

phosphorylated form, 4E-BP1 directly binds and inhibits eIF4E from interacting with the 5’ cap of mRNA and recruiting 40S ribosomal assembly. Mammalian target of rapamycin complex 1 (mTOR1)-mediated phosphorylation of 4E-BP1 releases eIF4E from 4E-BP1, allowing translation initiation to proceed. sT expression has been shown to result in increased hyperphosphorylated 4E-BP1 that is independent of mTORC1 signaling (265). The mechanism for sT-mediated 4E-BP1 hyperphosphorylation is believed to be mediated through the LSD, which contacts cell division cycle protein 20 (cdc20). This interaction results in the activation of cyclin-dependent kinase 1 (CDK1, which directly hyperphosphorylates 4E-BP1, the effects of which may contribute to sT-induced transformation (273, 274).

Griffiths *et al.* through a mass spectrometric approach have revealed that MCV sT also interacts with protein phosphatase 4C (PP4C) at a region (95–111 aa) directly adjacent to the LSD at 91–95 aa (275). MCV sT binding of PP4C or PP2A Aβ targets the NF-κB essential modulator (NEMO) protein and prevents nuclear translocation of NF-κB, inhibiting NF-κB mediated transcription (275). PP4C binding is also important for the induction of a highly motile cell phenotype that may correspond to the highly metastatic nature of MCC (276).

Most recently, a novel role for MCV sT in modulating host transcription has been described. Cheng *et al.*, show that sT is able to recruit L-myc to the EP400 histone acetyltransferase and chromatin remodeling complex (277). This complex is sufficient to bind to and activate specific gene promoters, namely *MDM2* and *MDM4*. As both of these proteins are involved in p53 regulation, this transcriptional effect of sT may represent an indirect means of targeting the p53 pathway by MCV (278). The formation of this complex

is in part dependent on the LSD of sT, as amino acids E86, E87, K92, and D93 have been identified as critical for binding.

## 2.4 Conclusions

Since its initial discovery in 2008, the map of MCV has transitioned from a simple sketch to a more intricate schematic with detailed characterizations of the viral gene products and how they impact tumorigenesis. Unearthing the functional aspects of the T antigens has aided in identifying novel targets for MCC treatment, spurring the development of MCV-directed vaccines and therapeutics (279–282). Still, there exist uncharted activities associated with MCV infection that warrant additional characterization for a more comprehensive understanding of this virus and its role in MCC. As previous research on polyomaviruses has contributed fundamental concepts in cell and cancer biology, continued efforts in elucidating the mechanisms of MCV pathogenesis may uncover similar discoveries that extend beyond the context of MCC.

## 3.0 The C-terminal domain of MCV Large T antigen is critical for its stability

Work described in this chapter is unpublished.

J.A. Wendzicki performed all experiments described in this chapter. J.A. Wendzicki, P.S. Moore, and Y. Chang conceived the project and analyzed results.

The C-terminal replicative domains of Merkel cell polyomavirus (MCV) Large T (LT) antigen are characteristically truncated in Merkel cell carcinoma (MCC) tumor specimens out of a selective pressure to suppress unlicensed viral replication following integration of the viral into the host genome. Recent work suggests these C-terminal domains may have additional functions aside from replication. In this chapter, we show that a short region within the C-terminus of MCV LT is critical for maintaining the stability of the full-length protein. Mutational analyses revealed that loss of these C-terminal motifs within the terminal 35 amino acids of LT results in poly-ubiquitination and rapid turnover. Attempts to stabilize mutant LTs have been largely unsuccessful. The mechanism of this destabilizing phenotype remains unknown, but these data indicate this region may function in regulating steady-state LT protein levels, which is of importance in the context of a lytic infectious cycle.

## 3.1 Introduction

Merkel cell polyomavirus (MCV) is the causative agent of roughly 80% of all cases of Merkel cell carcinoma (MCC), a rare, aggressive skin cancer. MCV-positive MCCs are characterized by integration of the viral genome within the host genome and the presence of missense or nonsense mutations that result in the expression of a C-terminally truncated Large T (LT) antigen, but an intact small T (sT) antigen (83). As the C-terminal helicase domain of LT is required for viral replication, it has been hypothesized that these truncating mutations arise out of a selective pressure during tumor formation to eliminate this function of the virus. This is because initiation of unlicensed viral replication at sites of integration in the host genome would likely lead to replication fork collisions and double-strand break induction, prompting a cytotoxic DNA damage response by the host cell machinery (83, 283). This elimination of MCV replication in the context of MCC is consistent with other known tumor viruses that are rendered replication incompetent in tumor specimens (261–263, 284, 285)

While a selective pressure to suppress replication following viral integration is evident, it has been suggested that there may be additional reasons for this premature truncation of LT. Recent findings suggest that these signature C-terminal truncation mutations may actually arise prior to viral integration within the host genome (286). Since such mutations effectively eliminate half the amino acid sequence of the protein (83, 287, 288), it is believable that additional functionalities of LT independent of replication exist in this region, which are also selectively lost in tumor populations. Two groups have mapped an anti-proliferative phenotype to the C-terminal region of LT, which further supports the notion that non-replicative functions exist in this region that may be unfavorable for

tumorigenesis (258, 264). Richards *et al.* have additionally showed that a truncated tumor-derived LT protein was expressed at higher levels, resulted in enhanced cellular proliferation, and induced unique transcriptomic changes compared to wild-type, full-length LT protein (289). These results suggest that the absence of C-terminal domains of LT may in part impact its expression levels and ability to modulate cellular pathways.

Changes in protein levels and stability as a result of C-terminal truncation is a common phenomenon that has been reported across numerous species. In many cases these truncations lead to enhanced stability of a protein due to the deletion of sequences that are involved in its targeting for degradation (290–294). The identities of such sequences (known as degrons) have remained elusive, but recent work by Koren *et al.* proposes that the stability of many proteins is regulated by C-terminal degrons (295). In terms of polyomaviruses, it has been identified that removal of C-terminal variable linker and host range region (VHR) from the LT antigen of JCV and SV40 results in lower LT protein levels and has varying impacts on transformation efficiency (296). Although the C-terminal region of MCV LT shows negligible homology to the VHR, these data suggest that this region as a whole may have more nuanced functions in MCV biology than initially believed.

In this study, we initially sought to map and characterize the different functional domains of MCV LT, but it was revealed almost immediately that truncations to the terminal 100 amino acids of the protein drastically altered LT protein levels. Truncation and alanine mutagenesis were used to define hotspots in this C-terminal region that were critical for maintaining stability of the LT protein, which when mutated resulted in increases in LT poly-ubiquitination and degradation. Elucidating the precise mechanism

behind this destabilizing phenotype has remained challenging for several reasons, but identification of these peptide motifs suggests an important role for the C-terminal tail of LT in coordinating the stability of the full-length protein and may function in the course of natural MCV infection to regulate steady-state LT protein levels.

## 3.2 Materials and methods

### 3.2.1 Generation of LT truncation mutants

A PCR-based approach was used to selectively amplify desired genetic regions of a codon-optimized MCV LT, which were restriction cloned into the pCMV-Tag2B vector to allow for uniform N-terminal Flag tags on all LT constructs. The 5' primers for each construct also contained codon sequences for an in-frame nuclear localization signal derived from SV40 LT (PKKKRKV) that would directly precede the desired MCV LT sequence. The 3' primers for each construct included a C-terminal Stop codon directly after the last nucleotides of the desired MCV LT sequence.

### 3.2.2 Alanine mutagenesis

All mutagenesis was carried out using the QuikChange Lightning Site-Directed Mutagenesis Kit (Agilent) according to the manufacturer's instructions. All constructs were then sequenced along the entire MCV LT sequence to confirm the presence of the desired mutation and absence of any extraneous mutations.

### 3.2.3 Cell culture and transfection

293 cells lines were maintained in DMEM (Cellgro, #10-013), supplemented with 10% fetal bovine serum (FBS) (Sigma). Transfections were performed using Lipofectamine 2000 (Invitrogen) following the manufacturer's instructions. In experiments involving MG132 treatment, cells were cultured overnight in the presence of 10 μM MG132 (Selleckchem) or a corresponding amount of DMSO as a negative control.

### 3.2.4 Immunoblotting

At 48 hours post-transfection, cells were washed once in 1x PBS, followed by lysis in RIPA buffer [50 mM Tris-HCl (pH 8.0), 150 mM NaCl, 0.1% SDS, 1% NP-40, 0.5% sodium deoxycholate], supplemented with a protease inhibitor cocktail (Roche). Protein concentration in each lysate was quantitated using the DC Protein Assay (Bio-Rad).
Equal amounts of total protein from each lysate were resolved by SDS-PAGE and transferred to nitrocellulose membranes (GE Healthcare). After blocking in milk, membranes were incubated in primary antibodies for at least 2 hours at RT or overnight at 4°C. IRDye 680CW goat anti-mouse/rat or IRDye 800CW goat anti-rabbit antibodies (LI-COR) were used for secondary detection. Signals were analyzed at 700 or 800 nm wavelengths, using the quantitative Odyssey IR Imaging System (LI-COR). The following primary antibodies were used: anti-MCV LT (CM2B4), anti-Flag (M2 Sigma), anti-α tubulin (11H10 Cell Signaling; 12G10 DSHB), and anti-HA (3F10 Roche).

### 3.2.5 Immunofluorescence

293 cells were seeded on glass slides and transfected with MCV LT constructs. Cells were fixed and permeabilized with cold methanol at -20 °C for 20 minutes. After blocking with 10% fetal bovine serum in PBS, cells were incubated overnight at 4 °C with primary anti-Flag antibody (M2 Sigma), followed by secondary antibody incubation (Alexa Fluor 568-conjugated goat anti-mouse) for 1 hour at room temperature. Stained cells were mounted in aqueous medium containing DAPI (Vector Laboratories). Cells were analyzed by fluorescence imaging using an Olympus AX70 epifluorescence microscope.

### 3.2.6 Ubiquitination assays

293 cells were transfected with expression constructs for wild-type or mutant LTs along with an HA-tagged ubiquitin construct. At 48 hours post-transfection, cells were subjected to a short course of proteasome inhibition by treatment with MG132 (10 μM) for 4 hours. Cells were then lysed in immunoprecipitation (IP) buffer (50 mM Tris-HCl [pH 7.4], 150 mM NaCl, 1% Triton X-100, 5 mM NaF), supplemented freshly with a protease inhibitor cocktail (Roche). Lysates were incubated overnight at 4°C with Flag-antibody (M2 Sigma), followed by incubation with a slurry of Protein A/G Plus Agarose beads (Santa Cruz) for an additional 4 hours. After multiple wash steps, bound proteins were eluted in 2×SDS loading buffer, resolved by SDS-PAGE, and immunoblotted as described above.

### 3.2.7 Structural modeling

Amino acid sequence alignment was performed for all human polyomavirus LT sequences using the Clustal Omega alignment tool (297). The Quick2D feature from the MPI Bioinformatics Toolkit (298) was used to infer secondary structural information about the C-terminal region of MCV LT. Phyre2 (299) was used to gain additional information about secondary structures present in MCV LT and to generate a predicted 3D structure, which was then analyzed in Pymol.

## 3.3 Results

### 3.3.1 C-terminal truncations to MCV LT impact its stability

At the outset of this study, the goal was to create a library of plasmids that could be used to selectively express different functional domains of MCV LT to learn more about their biological function and potential binding partners. The genetic sequences corresponding to functional domains of MCV LT were cloned into a Flag-tagged expression system along with an N-terminal nuclear localization signal (NLS) to ensure uniform localization of all LT truncation mutants (**Figure 14A**). Upon transfection of these LT truncation mutant plasmids into 293 cells and subsequent immunoblotting, it was revealed that only a subset of the mutant LTs showed stable protein expression. Initially owing this finding to an error in transfection, we were surprised to find this phenotype was highly reproducible. Treatment of transfected cells with the proteasome inhibitor MG132

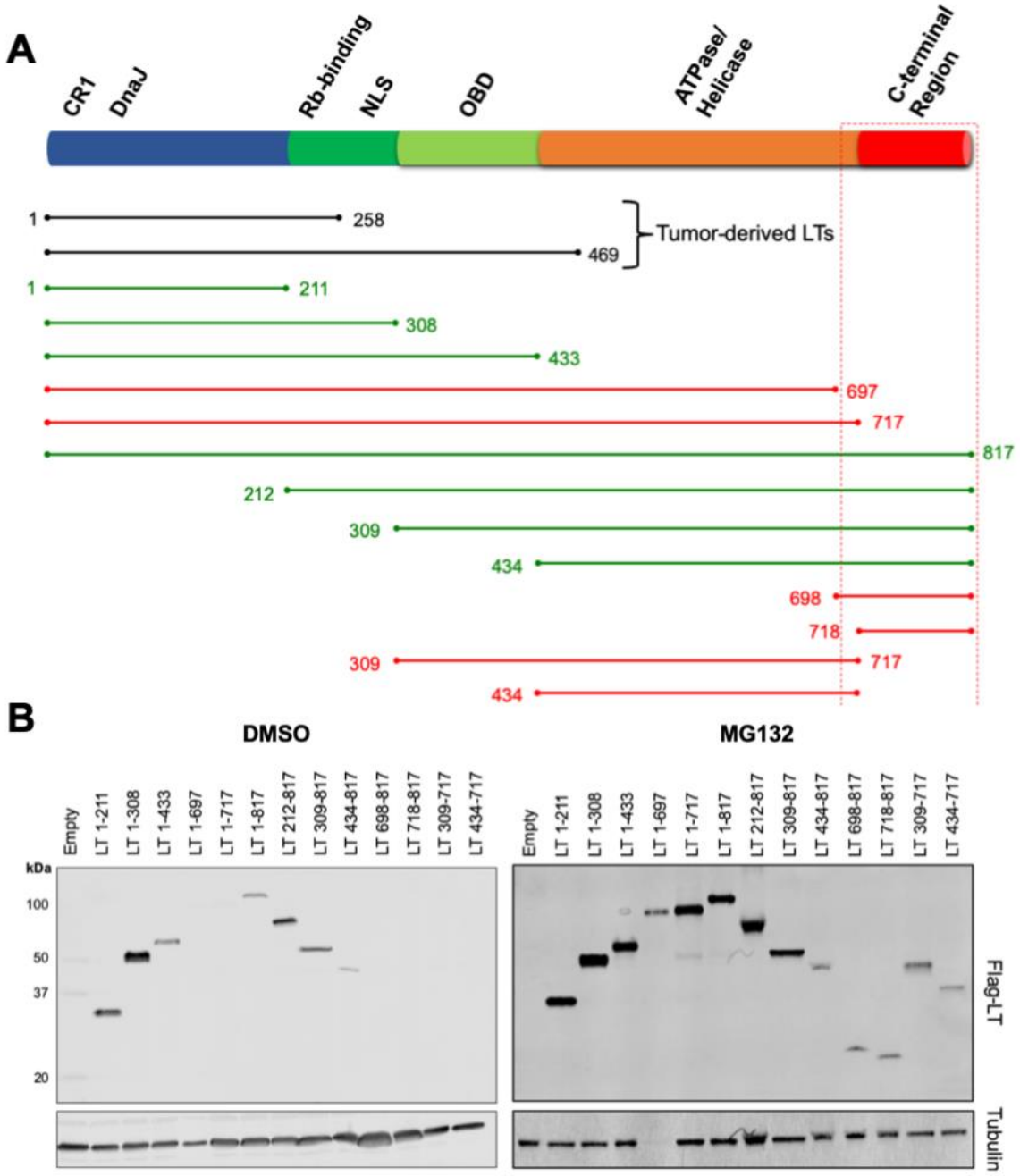


**Figure 14. C-terminal truncations compromise MCV LT stability.**

A. Diagram of Flag-tagged LT truncation mutants aligned with the corresponding functional domains of LT that each contains. Two tumor-derived LT protein sequences serve as reference. Constructs displayed in green show stable expression in 293 cells, whereas those shown in red are unstable. All unstable constructs have perturbations within the C-terminal 100 amino acids of LT or are limited to the C-terminal amino acids, highlighted by the red box. B. Immunoblots for Flag-LT truncation constructs expressed in 293 cells. Only 7 of 13 constructs are detected in control (DMSO) conditions, but LT protein levels for all constructs are restored upon proteasome inhibition by MG132.

showed that the LT mutants that failed to express under normal conditions were being expressed and synthesized, but were also being rapidly turned over by the cellular degradation machinery (**Figure 14B**). When looking at the map of truncations a clear pattern emerged in terms of the LT mutants that were rapidly degraded in that all contained deletions to the C-terminal 100 amino acids of LT, a region previously implicated in the growth-inhibitory phenotype associated with full-length MCV LT (258).

To more finely map the threshold required for stable LT expression, a second series of truncation mutants was created that featured systematic deletions of 17 amino acids, beginning from the C-terminus of LT and spanning the final 100 amino acids of the protein (**Figure 15A**). Expression of these truncation constructs in 293 cells revealed that the terminal ~35 amino acids of LT are required for stable expression, as truncation between 783-800 aa drastically reduced LT stability to undetectable levels by immunoblotting. As before, all truncation mutants became detectable after proteasome inhibition with MG132 (**Figure 15B**). To corroborate the immunoblotting data, immunofluorescence directed against Flag-tagged LT in transfected 293 cells was used. Full-length (1-817) LT was readily visible in nuclei of transfected cells, but only after MG132 treatment did LT 1-783 become visibly expressed (**Figure 15C**).

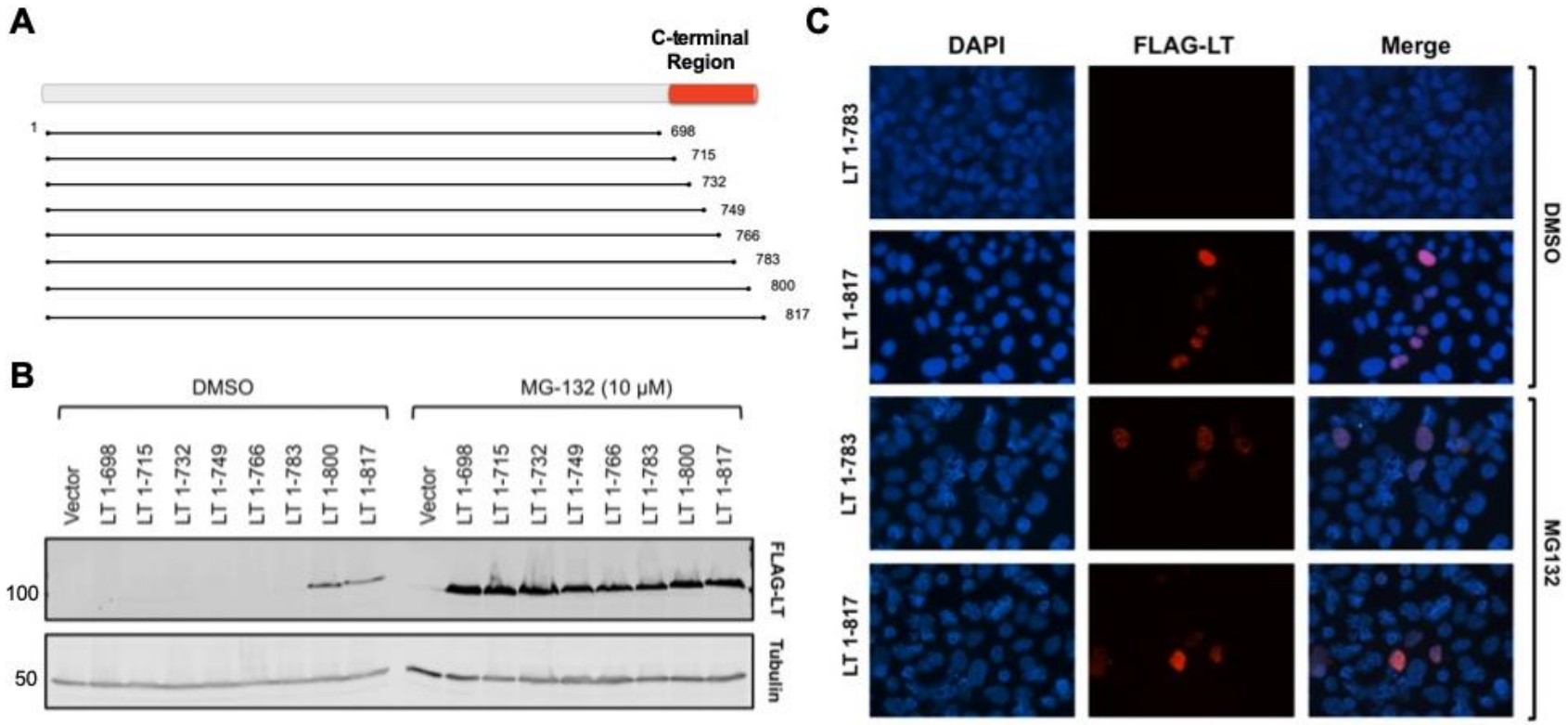


**Figure 15. Systematic C-terminal truncations reveal threshold for LT stability.**

A. Diagram of serial truncations to the C-terminus of LT. These Flag-tagged LT truncation mutants each vary by 17 amino acids and span the terminal 100 amino acids of LT. B. Immunoblot for Flag-LT truncation constructs expressed in 293 cells. Only full-length (1-817) LT and LT 1-800 show stable expression in control (DMSO) conditions, indicating the region between 783-800 aa is critical for stability. Protein levels for all constructs are restored by MG132 treatment. C. Immunofluorescence assay for Flag-LT in 293 cells. Compared to strong nuclear staining of full-length (1-817) LT expression in control conditions, the unstable LT 1-783 is only detected in cells after MG132 treatment.

### 3.3.2 Alanine mutagenesis reveals hotspots important for LT stability

While the truncation constructs were useful for defining a threshold of C-terminal amino acids required for LT stability, it could not be determined whether or not the loss of stability was due to the truncation of the protein chain itself or loss of a specific motif in that region. Alanine mutagenesis was then used in an attempt to identify a stability motif in the C-terminus of LT in context of the full-length protein. Stretches of 5-7 amino acids were mutated to alanine within the 781-817 aa region of full-length MCV LT (**Figure 16A**). Following transfection into 293 cells, it became clear that some of these mutations had a more pronounced destabilizing effect on the LT protein than others, but overall protein levels were again restored upon MG132 treatment in all cases (**Figure 16B**). Quantitation of LT protein levels as normalized to alpha-tubulin revealed two hotspot regions that when mutated to alanine resulted in ~80% reduction in LT protein levels: 786-795 aa and 811-817 aa (**Figure 16C**). These destabilizing mutations provided evidence that it was indeed loss of specific motifs in the C-terminus of LT that resulted in LT degradation.

Given that large mutations or truncations often alter or disrupt protein structure, leading to degradation, we wanted to see if mutation to any one residue in the C-terminal region of LT could impact its stability to the same degree as these larger mutations. Single amino acid alanine substitution mutants were then generated for residues falling within the first hotspot region for this purpose (786-795 aa). Conversely, single amino acid alanine substitution mutants were also generated for a region that did not impact LT stability when mutated (801-805 aa). As previously, these constructs were transfected into 293 cells; however, in this case all mutant LTs displayed stable protein levels in the

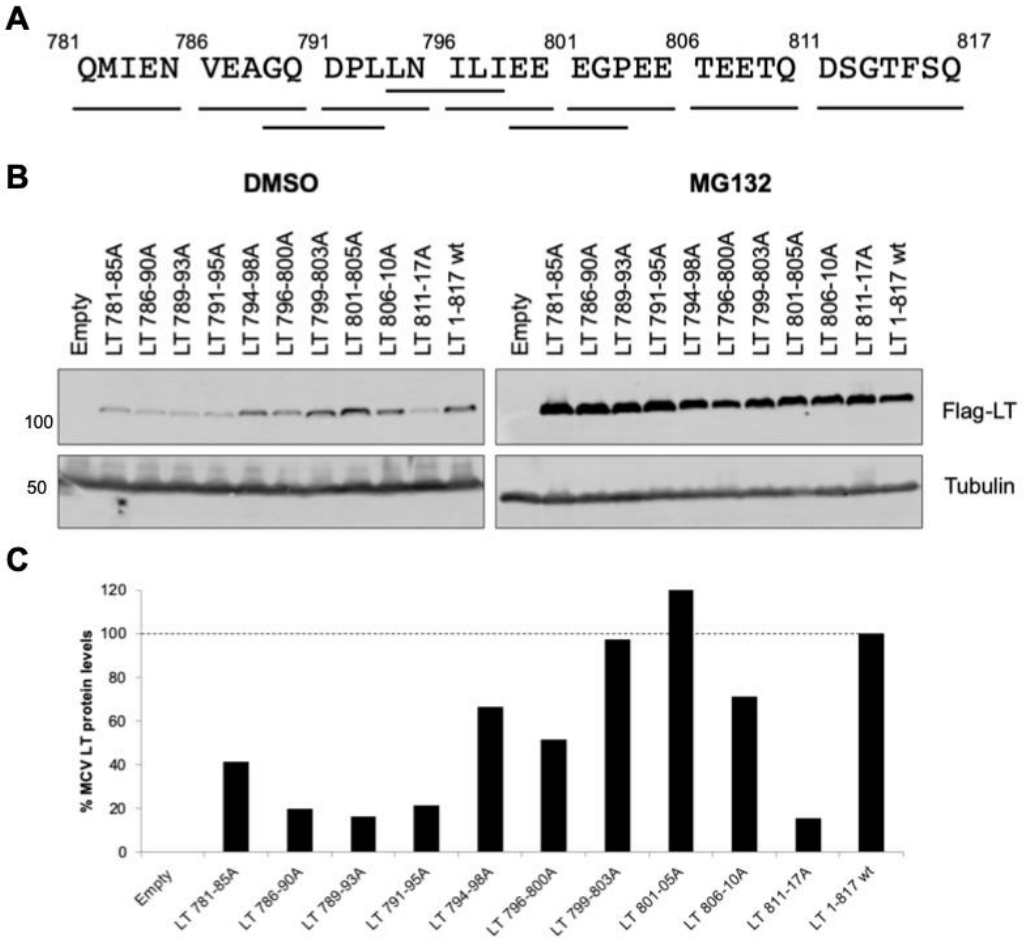


**Figure 16. Alanine mutagenesis reveals hotspot regions important for LT stability.**

A. LT C-terminal amino acid sequence spanning from 781-817 aa. Black lines beneath the sequence represent pentapeptide alanine substitution mutations that were generated throughout this region. B. Immunoblot for Flag-LT constructs expressed in 293 cells. Alanine substitution mutants show varied levels of LT protein compared to wild-type LT under normal (DMSO) conditions. Protein levels for all constructs are restored by MG132 treatment. C. Quantitative representation of LT protein levels for each mutant LT compared to wild-type LT reveals alanine substitution between 786-795 aa and 811-817 aa are highly destabilizing.

absence of proteasome inhibition, indicating that no single amino acid was directly responsible for the loss of LT stability upon mutation (**Figure 17**). Instead, the hotspot regions identified by larger tracts of alanine substitution represent the shortest peptide motifs that impact LT stability.

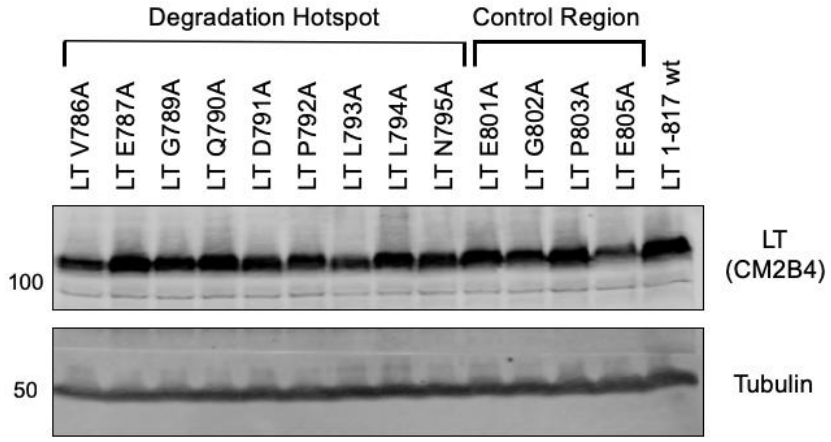


**Figure 17. Single alanine substitutions do not destabilize LT.**

Immunoblot of single alanine substitution LT mutants expressed in 293 cells, as detected by CM2B4 antibody. Constructs were sorted by whether or not the mutations fell within the hotspot region associated with increased degradation or an area that when mutated did not impact stability (control). In all cases, mutant LT protein levels were stably expressed.

### 3.3.3 Unstable LT mutants possess higher levels of ubiquitination

Proteins are most often targeted for degradation by the ubiquitin-proteasome pathway, where a series of covalently-linked ubiquitin moieties are attached to lysine residues on a protein to target it for proteasome recognition and degradation (300). Considering unstable LT mutants used in this study were consistently stabilized through proteasome inhibition, it followed that they were being targeted for degradation through this pathway. We next wanted to see whether or not the unstable LT mutants possessed a higher degree of poly-ubiquitination to further support this notion. 293 cells were transfected with either stable (wild-type, 799-803A) or unstable (781-85A, 786-90A, 789-93A, 791-95A) LT constructs along with HA-tagged ubiquitin and subject to 4 hours proteasome inhibition prior to lysis. Immunoprecipitation was performed against the Flag-tagged LT, followed by immunoblotting against the HA-tagged ubiquitin to visualize the

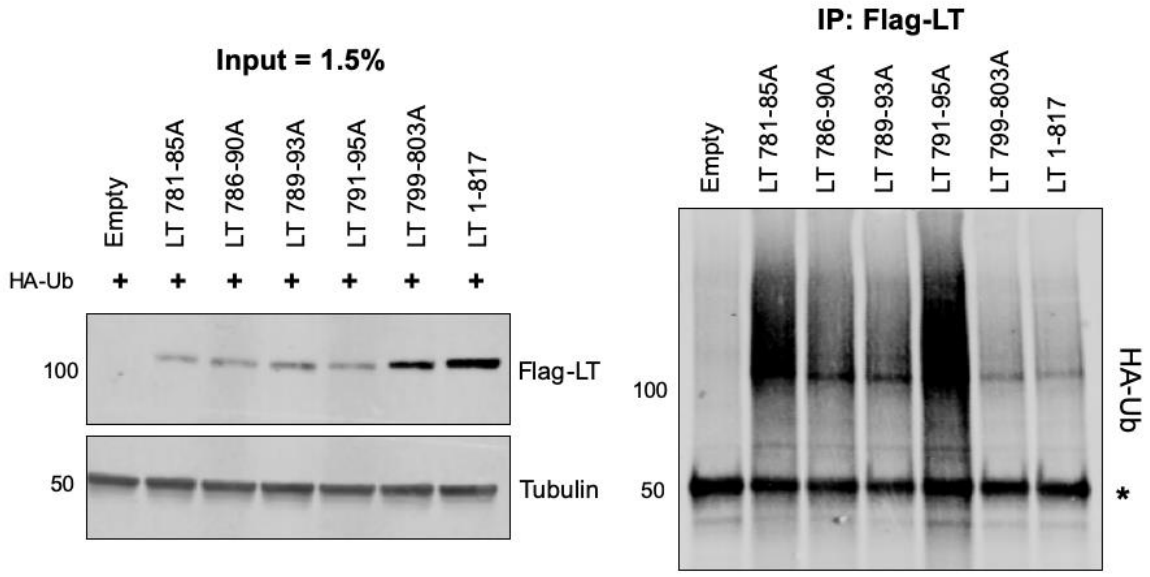


**Figure 18. Unstable LT mutants are highly ubiquitinated.**

Ubiquitination assay. 293 cells were transfected with wild-type, stable (LT 799-803A), and unstable (LT 781-85, LT 786-90A, LT 789-93A, LT 791-95A) LT constructs and HA-tagged ubiquitin. Cells were treated with MG132 (10 μM) for 4 hours prior to lysis. Input lysates (left) show Flag-LT protein levels within the whole cell lysate. Following IP against Flag and subsequent immunoblotting against HA-ubiquitin (right), characteristic smears make it clear that unstable LT mutants show more poly-ubiquitination than stable LT mutants or wild-type LT. Asterisk denotes nonspecific IgG heavy chain band.

presence of poly-ubiquitination on LT. Unstable LTs possessed a marked enrichment in ubiquitination compared to stable LTs (**Figure 18**), indicating that unstable mutants were being directly targeted for proteasomal degradation.

### 3.3.4 Attempts to stabilize LT mutants were unsuccessful

To better understand from a mechanistic standpoint why these truncation and alanine substitution mutations within the C-terminus of LT result in rapid turnover, a few attempts were made to counteract the destabilization phenotype. In some cases, single protein domains that lack inherent stability can become stabilized in the context of a

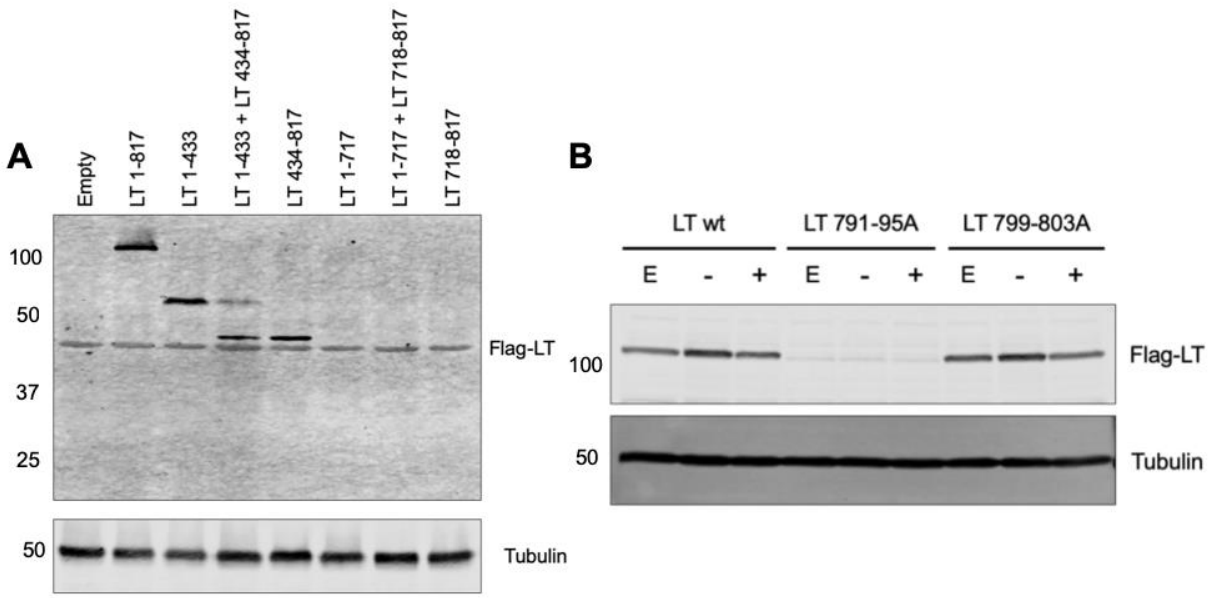


**Figure 19. LT stabilization attempts were unsuccessful.**

A. Immunoblot from 293 cells expressing single Flag-LT fragments or combinations of Flag-LT fragments that together constitute the full-length LT protein (1-817 aa). Co-expression of unstable LT 1-717 with corresponding LT 718-817 did not restore stable expression of either fragment. B. Immunoblot from 293 cells expressing wild-type LT, unstable LT 791-95A, or stable LT 799-803A in the presence of an empty vector, a mutant MCV replicon (-), or a wild-type MCV replicon (+). Co-expression of LT with MCV replicons did not result in significant stabilization of LT 791-95A.

multidomain protein (301), so we first tried co-expressing unstable domains of LT in trans to see if a complementation approach would increase their stability. However, co-expression of MCV LT 1-717 and 718-817 did not result in stabilization of either fragment, despite representing the complete amino acid sequence of LT (**Figure 19A**). We next sought to stabilize LT through co-transfection of a plasmid containing the viral origin of replication. As LT is known to form double hexamers and assemble at the viral origin (221, 302–305), we hypothesized that even mutant LTs could be stabilized in these higher ordered structures if origin sequences were present. Co-transfection of the unstable MCV LT 791-95A along with a wild-type origin plasmid did not result in an increase in LT protein

levels, however (**Figure 19B**). It remains undetermined why these mutations result in such a drastic destabilization of LT, resulting in its rapid turnover.

## 3.4 Discussion

What began as a methodology to express various functional domains of MCV LT led to the identification of specific sequences within the most C-terminal region of LT that are critical for stabilizing the entire protein. The simplest explanation for this phenomenon would be that these truncations and alanine mutations result in misfolding of LT, which leads to rapid poly-ubiquitination and degradation (306–308). Whether or not expression of unstable LT constructs results in an unfolded protein response (UPR) in cells has not been formally assayed for; however, the fact that not all mutations in this region compromise LT stability is evidence that the phenomenon may instead be sequence specific.

Much of what has been discovered about MCV biology to date has stemmed from comparisons with other polyomaviruses and tumor viruses. By aligning this C-terminal region of MCV LT with other human polyomavirus LT sequences, we found a limited amount of homology compared to other highly conserved regions of the protein (**Figure 20**). Though it does not allow for much inference about the function of this motif, it does indicate that these sequences may be unique to MCV LT. Additionally, with a limited amount of crystallographic data available for MCV LT, it is difficult to understand precisely what role this C-terminal tail plays in terms of coordinating the structure of the entire protein. Structural modeling through multiple predictive indices suggests that while part

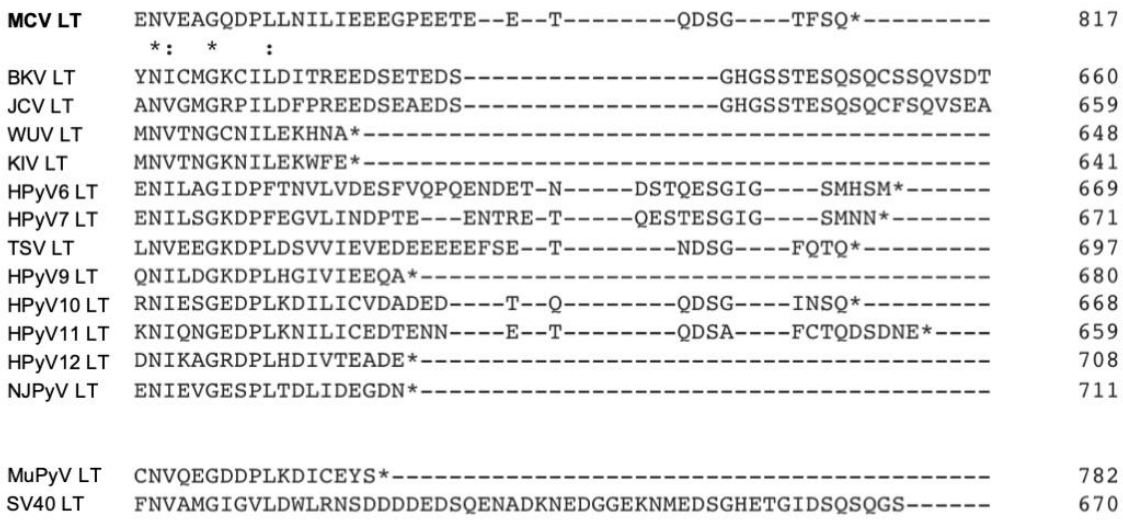


**Figure 20. Peptide sequence alignment of C-terminal regions from PyV LTs.**

Complete LT amino acid sequences from 13 human polyomaviruses and also SV40 and MuPyV were aligned using Clustal Omega aligment tool. The snapshot shown here highlights the C-terminal sequences of MCV LT that are critical for stability (top). Asterisks designate perfectly conserved residues. Colons indicate partial conservation. Only two asterisks and two colons appear for the entire C-terminal region. Overall, this region shows low sequence homology for MCV LT compared to the other polyomaviruses.

of this region is alpha-helical in nature, the majority of this tail is unstructured and does not participate in the larger globular structure of the major functional domains of LT (**Figure 21 A & B**). As naturally unstructured regions of proteins often serve as docking sites for other interactors (309–311), it follows that this motif could serve as a binding site for a protein that results in stabilization of LT. This is not unlike the human papillomavirus family, in which the length and nature of intrinsically disordered regions of E6 and E7 oncoproteins correlate directly with their affinity for cellular cofactors and overall tumorigenicity (312–314). Furthermore, the presence of post-translational modifications within this disordered region may also influence binding of cellular cofactors, and this region does contain multiple serine and threonine residues, which may serve as phosphorylation sites. Interestingly, Li *et. al* have identified an ATM phosphorylation site

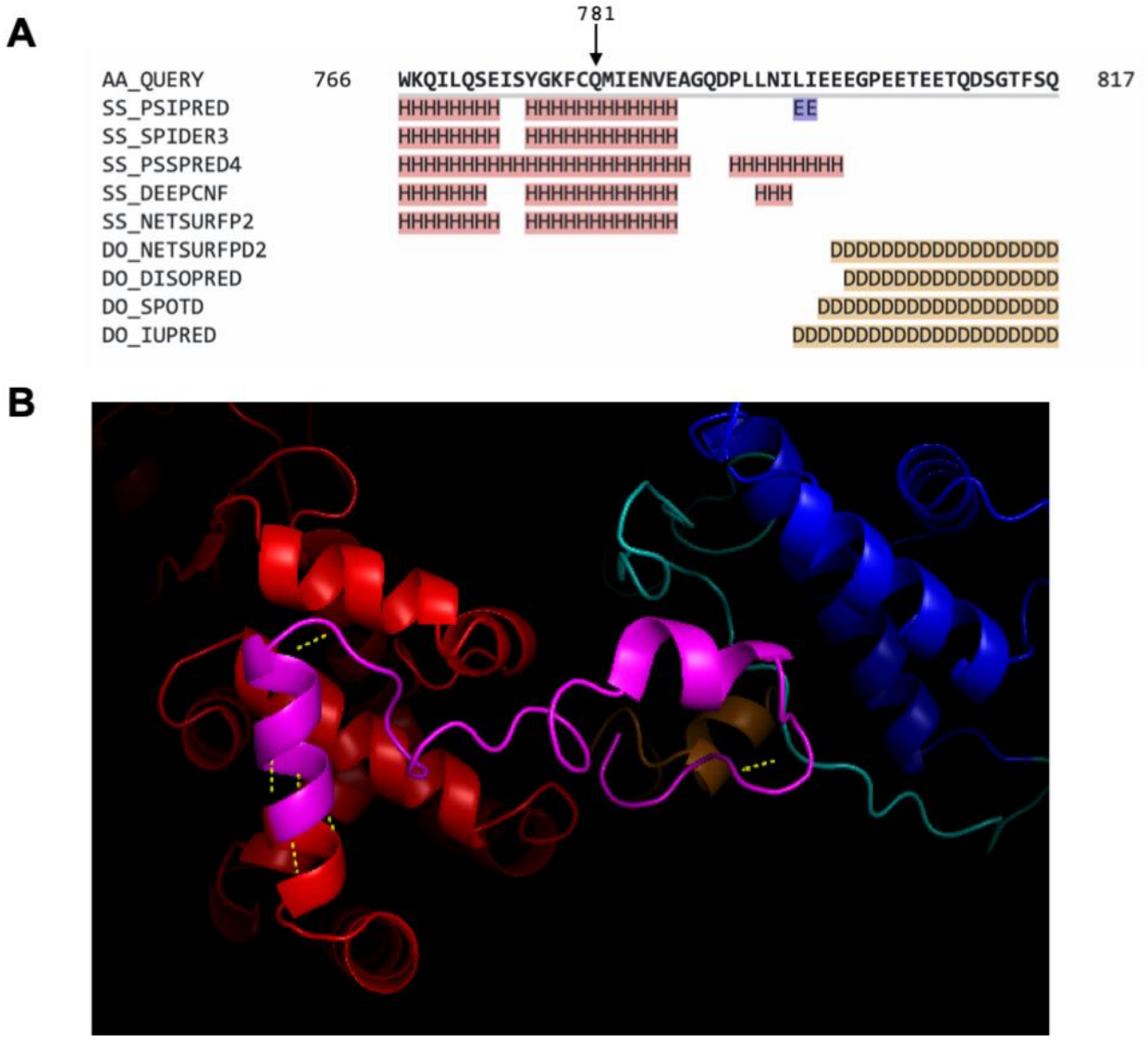


**Figure 21. Structural modeling of C-terminal tail of MCV LT.**

A. Secondary structural modeling of the C-terminal region of MCV LT from Quick2D. The black arrow at residue 781 denotes the beginning of the region involved in stability. Multiple predictive indices (left) indicate a portion of this region is alpha-helical (H). The majority of this sequence is disordered (D) in nature, however. EE designates an extended loop. B. Three-dimensional modeling of the C-terminal region of LT (pink) as predicted by Phyre2. While two small helices are present in this region, most of the sequence is unstructured. Any molecular contacts (yellow lines) between this region and the helicase domain (red) or the DnaJ domain (blue) are largely absent.

at S816 of MCV LT (315), which supports the idea that these other neighboring residues may also be phosphorylated by additional cellular kinases.

Protein degradation is generally governed by post-translational modifications at specific sites on target proteins that are then recognized by the cellular proteasomal machinery. Specific peptide motifs known as degrons can serve as recognition sites for E3 ubiquitin ligases, which coordinate poly-ubiquitination at key lysine residues to target proteins for degradation (316, 317). Likewise, some phosphorylation sites within proteins compose phosphodegron motifs that can also be recognized by particular E3 ligases to target proteins for degradation (318–320). Phosphorylation can also mask degron motifs and block E3 ligase binding in what is termed a phospho-inhibited degron (318). It has been reported that phosphorylation of several oncoproteins allows for interaction with the E3 ubiquitin ligase RNF4, which actually results in their stabilization (321). Immunoprecipitation experiments do not show evidence for interaction between MCVLT and RNF4, however (data not shown). In terms of LT degradation, it has been established that phosphorylation at residues S220 and S239 in the N-terminal region can be recognized by multiple cellular E3 ligases to target LT for degradation (222), but less is known about any C-terminal degron motifs. The C-terminal region identified in this study contains no lysine residues, but five potential phosphorylation sites are present (T806, T809, S812, T814, S816), the last of which has been validated (315). If and how any of these potential phosphorylation sites functions to promote or prevent LT degradation remains unknown.

While it has become clear through this study that the C-terminal tail of MCV LT plays an important role in stabilizing the protein, the precise mechanism governing this

process remains unknown. The destabilizing mutations identified here have made subsequent attempts at identifying novel binding partners in this region technically difficult. Also, given that the C-terminus of LT is canonically truncated in tumor specimens, it is unknown whether or not this region or any cofactors binding there have any relevance to MCV tumorigenesis. Instead, the C-terminus of LT may serve as a regulatory region for governing LT protein levels in the context of a natural MCV infection.

## 4.0 Differential targeting of p53 by polyomavirus Large T antigens

Work in this chapter is unpublished. Parts of the data presented here are in preparation for a manuscript submission in 2020.

**with authors Wendzicki JA, Moore PS, and Chang Y.**

J.A. Wendzicki performed all experiments described in this section. J.A. Wendzicki, P.S. Moore, and Y. Chang conceived the project, analyzed results, and have begun drafting the manuscript.

Targeting the p53 pathway is an essential component of the polyomavirus life cycle in lytic infections and tumorigenesis. In this chapter we compare mechanisms of p53 inhibition by the Large T (LT) antigens of two polyomaviruses: simian vacuolating virus 40 (SV40) and Merkel cell polyomavirus (MCV). In contrast with SV40 LT, MCV LT shows weak interaction with p53 and p300 in immunoprecipitation and proximity ligation assays. Quantitative PCR and chromatin immunoprecipitation further show that SV40 LT prevents binding of p53 to target gene promoters to prevent transcriptional activation, while MCV LT does not. A point mutation in the C-terminal domain of SV40 LT (P522L) disrupts its p53 binding ability, leading to a reversal of p53 accumulation and transcriptional inhibition. This mutant is also replication deficient but retains binding to retinoblastoma protein pRb. These data clarify the mechanism of p53 inhibition by SV40 LT and indicate that contact with p53 may be more specific than previously believed. It remains unclear how MCV inhibits the p53 pathway, but these results suggest it is not mediated through LT alone.

## 4.1 Introduction

As small, double-stranded DNA viruses, polyomaviruses must manipulate the host cell cycle and replication machinery to accomplish their viral life cycles. Polyomaviruses rely on the expression of multiple, alternatively-spliced transcripts from the early region of their genome known as tumor (T) antigens to accomplish this (82, 322). As one of the earliest discovered polyomaviruses (12), simian vacuolating virus 40 (SV40) has served as the touchstone of this virus family for investigating the precise biology of the polyomavirus life cycle and how this virus family elicits cellular transformation in a variety of hosts. Likewise, research on Merkel cell polyomavirus (MCV), the only human polyomavirus with a causal role for cancer in humans, has provided tremendous insight into novel mechanisms of tumorigenesis since its discovery (48, 105, 218).

One of the cellular proteins canonically targeted by the T antigens of polyomaviruses is p53, since its inhibition can prevent both host cell senescence and apoptosis (82, 323, 324). Either of these outcomes are otherwise dead ends for the viral life cycle, underscoring the importance of targeting the p53 pathway during a productive infection. As p53 is also at the center of maintenance of genome integrity (144, 325), inhibition of p53 is also a key factor in the tumorigenicity of these viruses. The p53 protein itself was first discovered and characterized as a result of interactions with the Large T (LT) antigen of SV40 (140, 141, 326). SV40 LT is known to contact p53 through bipartite motifs in its C-terminal domains, specifically amino acids 351-450 and 533-626 (103, 147, 327). Through this interaction, SV40 LT contacts regions of p53 that are involved in multimerization as well as DNA binding (148, 327–329), which is believed to be the method by which SV40 blocks p53 transcriptional activation. The ability of SV40 LT to

bind to p53 directly correlates with its efficiency of *in vitro* transformation in multiple cell lines (330).

While SV40 LT antigen has long been known to robustly bind to and inactivate p53, the relationship between MCV LT and p53 remains poorly understood. To date, the interaction between MCV LT and p53 has been described as weak to nonexistent (257, 258). There are also conflicting reports as to whether or not MCV LT can inhibit p53-dependent transcriptional activity (257, 331), but given that the vast majority of MCV-positive Merkel cell carcinoma (MCC) cases harbor wild-type p53 (245, 332, 333), it follows that there may be a yet undefined mechanism by which MCV antagonizes this pathway. On the other hand, it is known that MCV, like other polyomaviruses, induces a potent DNA damage response (DDR) and recruits DNA repair factors to facilitate its replication (71, 334–337). It has been reported that this DDR triggered by MCV LT results in p53 activation, downstream target upregulation, and apoptosis in certain cell lines (264, 315). Taken together, these data suggest the relationship between MCV LT and p53 both in the context of a lytic infection and tumorigenesis is multi-dimensional and represents an area in which further clarification is needed.

In this study, we highlight fundamental differences in the ability of the LT antigens of MCV and SV40 to inhibit the p53 pathway. We recapitulate the ability of SV40 LT to complex with p53 and its cofactor p300, for which interactions with either protein are significantly weaker in the case of MCV LT. SV40 LT also inhibits p53 site-specific DNA binding and activation of downstream targets, whereas MCV LT is deficient in this functionality. A point mutation at residue P522 in the C-terminal region of SV40 LT abrogates binding to p53, but retains binding to retinoblastoma protein pRb. This p53-

binding mutant LT reverses the p53 accumulation and inhibition phenotype seen with the wild-type protein. These results provide further insight into mechanisms of p53 inhibition by SV40 LT and effectively demonstrate that MCV LT does not play a direct role in inhibiting the p53 pathway.

## 4.2 Materials and methods

### 4.2.1 Cell culture and transfection

293 and U2OS cell lines were maintained in DMEM (Cellgro, #10-013), supplemented with 10% fetal bovine serum (FBS) (VWR Seradigm). The Short Tandem Repeat profiles of the 293 and U2OS cells were authenticated by the University of Arizona Genetics Core. Transfections were performed using Lipofectamine 2000 (Invitrogen) following the manufacturer's instruction.

### 4.2.2 Plasmids

Mammalian expression constructs used for MCV LT wt (265), MCV LT LXCXK (83), and SV40 LT wt (183) have been described previously, as referenced. Constructs MCV LT P689L, SV40 LT LXCXK, and SV40 LT P522L were generated through mutagenesis, using the QuikChange Lightning Mutagenesis Kit (Agilent). MCV (pMCV-Ori339(97)) (248) and SV40 (pSV01ΔEP) (338) origin plasmids used in the replication assay have been described previously, as referenced. The 4XBS2WT-luc plasmid

(Addgene #16593; (339)) used in p53 reporter assays was a kind gift from Dr. Jian Yu. The Flag-p53 plasmid was a kind gift from Dr. Ole Gjoerup.

### 4.2.3 Immunoblotting and antibodies

Cells were lysed in RIPA buffer [50 mM Tris-HCl (pH 8.0), 150 mM NaCl, 0.1% SDS, 1% NP-40, 0.5% sodium deoxycholate], supplemented with protease inhibitors pepstatin A, leupeptin, aprotinin, and phenylmethylsulfonyl fluoride (PMSF). Lysates were resolved by SDS-PAGE and transferred to nitrocellulose membranes (GE Healthcare). After blocking in 5% milk, membranes were incubated in primary antibodies for at least 2 hours at RT or overnight at 4°C. For quantitative Western blot detection, IRDye 800CW goat anti-mouse/rabbit or IRDye 800CW goat anti-mouse/rabbit antibodies (LI-COR) were used as secondary antibodies. Signal intensities were analyzed at 700 or 800 nm wavelengths, using the Odyssey IR Imaging System (LI-COR). The following primary antibodies were used: anti-MCV LT (CM2B4), anti-SV40 T antigen (pAb416 Calbiochem), anti-α tubulin (11H10 Cell Signaling; 12G10 DSHB), anti-pRb (Abcam), anti-p21 (EA10 Calbiochem), anti-PUMA (Ab3795), and anti-Flag (M2 Sigma). The following primary antibodies were used for p53 detection: total p53 (DO-1 Santa Cruz; FL-393 Santa Cruz), phospho-Ser15 (16G8 Cell Signaling), phospho-Ser20 (Cell Signaling), phospho-S392 (Cell Signaling), and acetyl-K373 (NY-CO-13 Millipore Sigma).

### 4.2.4 Immunoprecipitation

293 or U2OS cells were transfected with plasmids for expression of wild-type and mutant LTs of MCV and SV40. Cells were lysed in immunoprecipitation (IP) buffer (50 mM Tris-HCl [pH 7.4], 150 mM NaCl, 1% Triton X-100, 5 mM NaF) freshly supplemented with protease inhibitors pepstatin A, leupeptin, aprotinin, PMSF, and 1 mM benzamidine. Lysates were incubated overnight at 4°C with antibodies against p53 (DO-1 Santa Cruz), MCV LT (CM2B4), SV40 LT (pAb416 Calbiochem), or pRb (Abcam). This was followed by incubation with a slurry of Protein A/G Plus Agarose beads (Santa Cruz) for 3 additional hours. After a series of wash steps, bound proteins were eluted in 2×SDS loading buffer, resolved by SDS-PAGE, and immunoblotted as described above.

### 4.2.5 Proximity ligation assay

U2OS cells were seeded on glass slides and transfected with MCV or SV40 LT constructs. Cells were fixed in 4% paraformaldehyde for 10 minutes, followed by permeabilization in PBS containing 1% Triton X-100. Next, the Duolink PLA system (Sigma) was used to develop the PLA signal according to the manufacturer's instructions. After blocking with Duolink Blocking Solution, cells were incubated overnight at 4 °C with a combination of anti-LT antibodies (CM2B4; pAb416) and anti-p53 antibody (FL-393 Santa Cruz) or anti-LT antibodies and anti-p300 antibody (N-15 Santa Cruz). Cells were then incubated with Duolink anti-rabbit PLUS and anti-mouse MINUS secondary antibodies, followed by ligation, and rolling circle amplification to develop the PLA signal. Lastly, cells were incubated with Alexa Fluor 488 goat anti-mouse antibody to

counterstain against LT. Stained cells were mounted in Duolink PLA Mounting Medium with DAPI. Slides were analyzed by fluorescence imaging using an Olympus AX70 epifluorescence microscope.

### 4.2.6 RNA extraction and quantitative real-time PCR

RNA was extracted from cells using TRIzol Reagent (Ambion) according to the manufacturer's protocol. The TURBO DNA-free Kit (Invitrogen) was used to remove any DNA contamination, prior to cDNA synthesis with SuperScript IV Reverse Transcriptase (Invitrogen). Quantitative PCR (qPCR) was conducted on cDNA samples using the PowerUp SYBR Green Master Mix (Applied Biosystems) according to the manufacturer's instructions, using a QuantStudio 3 Real-Time PCR System (Applied Biosystems). Fold change in mRNA expression was calculated using the delta-delta CT method with target genes standardized to a GAPDH control.

### 4.2.7 Chromatin immunoprecipitation

Cells were fixed in 1% formaldehyde in PBS for 10 minutes to crosslink proteins and DNA. Nuclei were isolated as previous (222), followed by lysis in ChIP buffer (50 mM Tris-HCl [pH 8.1], 1% SDS, and 10 mM EDTA [pH 8.0] with protease inhibitors). Chromatin was sheared by sonication and then diluted 10-fold in dilution buffer (20 mM Tris [pH 8.1], 1% Triton X-100, 2 mM EDTA [pH 8.0], 150 mM NaCl with protease inhibitors). Soluble chromatin was precleared with protein A/G-agarose (Santa Cruz) and 2 µg of sonicated salmon sperm DNA (Stratagene) for 2 hours at 4 °C. Small aliquots

(5%) of the precleared chromatin were taken as input controls. The remainder was incubated overnight at 4°C with anti-p53 antibody (DO-1 Santa Cruz) or isotype IgG control (R&D Systems), after which A/G-agarose beads were added for another 4 hours at 4 °C. Following a series of wash steps, bound DNA was extracted twice with buffer (50 mM NaHCO3, 1% SDS, 50 mM Tris [pH 8.0], 1 mM EDTA) and incubated at 65 °C overnight to reverse crosslinking. Input and ChIP DNA samples were purified by phenol:chloroform extraction, followed by qPCR carried out with PowerUp SYBR Green Master Mix (Applied Biosystems) according to the manufacturer's instructions on a QuantStudio 3 Real-Time PCR System (Applied Biosystems). Results are reported using the percent input method, where ChIP samples are standardized to the input chromatin levels.

### 4.2.8 Replication assays

U2OS cells were transfected with wild-type or mutant MCV and SV40 LT constructs along with 50 ng origin-containing replicons for MCV (248) and SV40 (338). At 48 hours post-transfection cells were lysed in TE-SDS buffer (10 mM Tris [pH 8.0], 1 mM EDTA, 0.6% SDS), to which NaCl was added at 1M concentration to salt-precipitate chromatin DNA. After centrifugation, the episome-containing fraction was subject to phenol:chloroform extraction and ethanol precipitation. Digest with *DpnI* was used to remove input replicon DNA, and quantitative PCR with origin-specific primers for each virus was used to measure newly-replicated DNA. As above, qPCR was carried out with PowerUp SYBR Green Master Mix (Applied Biosystems) according to the manufacturer's instructions, using a QuantStudio 3 Real-Time PCR System (Applied Biosystems).

### 4.2.9 Luciferase assays

U2OS cells were transfected with equal amounts firefly luciferase reporter 4XBS2WT-luc (339) and control *Renilla* reporter pRL-null (Promega), along with MCV and SV40 LT constructs. Luciferase assays were performed using the Dual-Luciferase Reporter Assay System (Promega) according to the manufacturer's instructions. In short, cells were lysed in passive lysis buffer and lysates were loaded in triplicate in a 96-well plate. Firefly and *Renilla* luciferase reads were quantitated using a Synergy2 microplate reader (BioTek) equipped with a luciferase detection program. Firefly luciferase reads were standardized based on the *Renilla* luciferase reads. A portion of lysates from each condition were retained for immunoblotting to confirm LT expression.

### 4.2.10 Cycloheximide chase half-life studies

U2OS cells were transfected with expression plasmids for MCV and SV40 LT constructs. At 48 hours post-transfection, standard culture media was replaced with media containing 50 μg/mL cycloheximide (CHX) to block new protein synthesis. Cells were then washed once in 1X PBS, followed by direct lysis in RIPA buffer at the following time points: 0, 0.5, 1, 2, and 4 hours after CHX treatment. Lysates were resolved by SDS-PAGE, and immunoblotting was performed against LT, p53, and tubulin, as described above. Quantitative LI-COR detection allowed for measurement of p53 decay over time for each condition, normalized to tubulin.

## 4.3 Results

### 4.3.1 MCV LT does not strongly interact with p53 or p300

SV40 LT directly binds to and inactivates p53 through bi-partite motifs within its C-terminus (103, 147, 256, 340, 341), so we first wanted to see if MCV LT was capable of binding p53 in a similar manner. 293 cells were transfected with expression constructs for wild-type MCV LT or SV40 LT, followed by immunoprecipitation (IP) against endogenous p53. Immunoblotting for LT revealed that while SV40 LT was enriched through p53 pulldown, MCV LT showed a weak ability to co-IP with p53 (**Figure 22**). This finding is consistent with a previous study by Borchert *et. al* that failed to see direct interaction between MCV LT and p53, despite seeing inhibition of p53 activity through reporter assays (257).

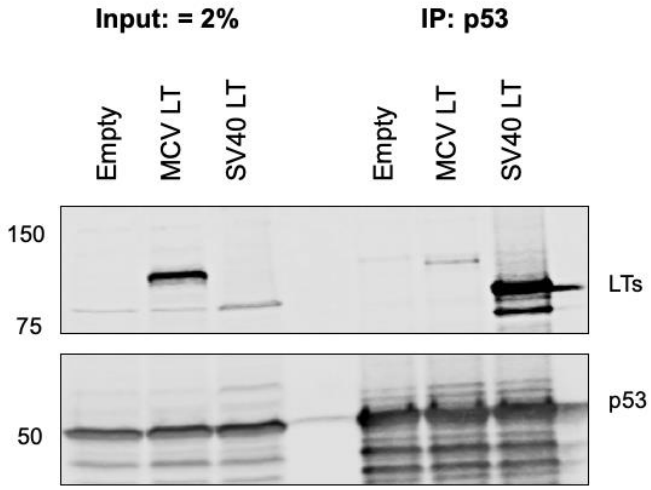


**Figure 22. MCV LT weakly immunoprecipitates with p53.**

293 cells were transfected with expression constructs for MCV LT, SV40 LT, or an empty vector. Input lysates show LT levels in the whole cell lysate (left). Following IP against endogenous p53 and immunoblotting against LT, SV40 LT was clearly enriched through pull-down, whereas MCV LT showed weak co-IP efficiency.

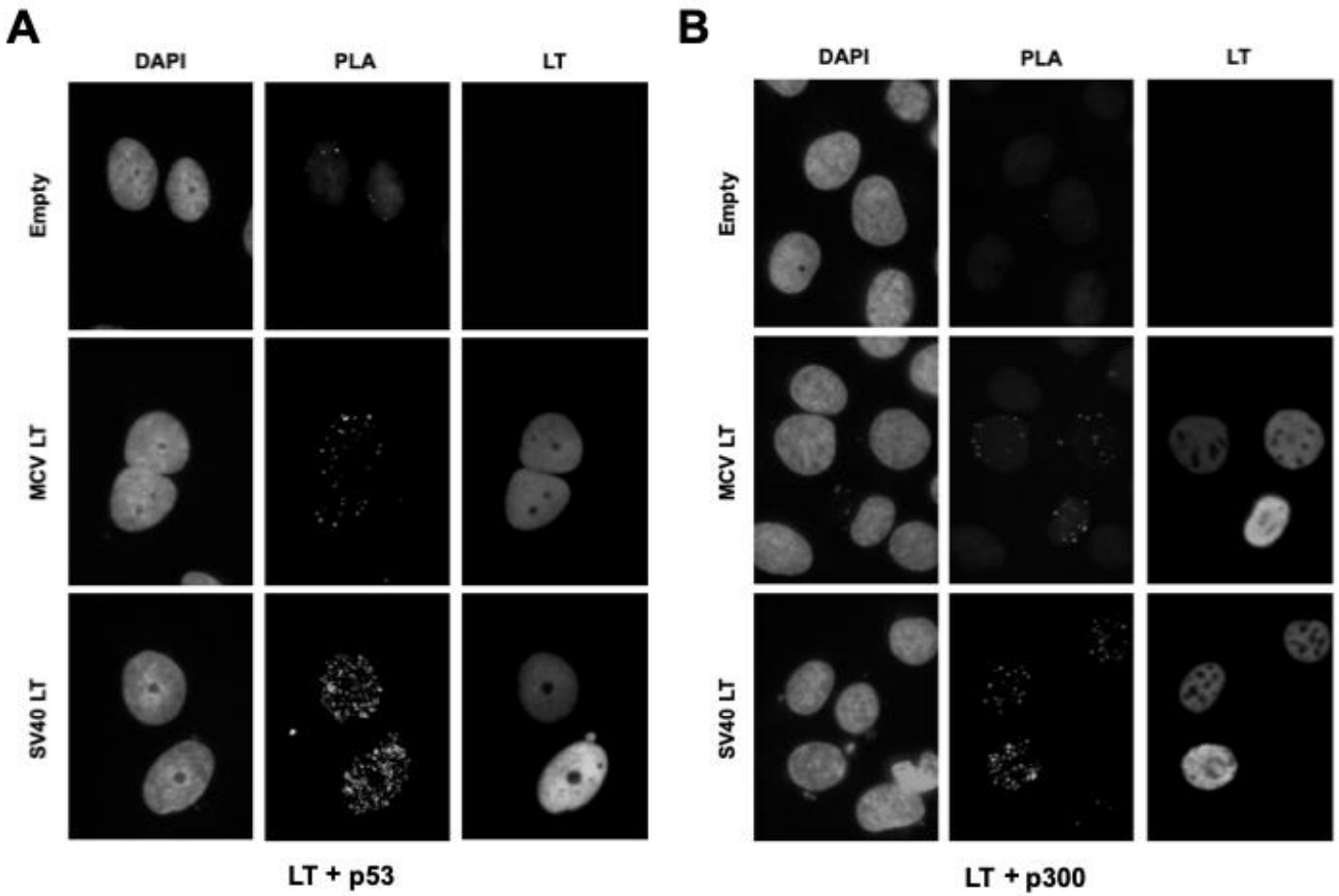


**Figure 23. MCV LT weakly interacts with p53 and p300.**

Immunofluorescence images following proximity ligation assay (PLA) in U2OS cells expressing MCV LT, SV40 LT, or an empty vector. Separate panels are displayed for each channel: DAPI (blue), PLA signal (red), and LT expression (green). Images captured at 1000X magnification. A. PLA was directed against LT and p53 interaction. PLA signal is much weaker for MCV LT compared to SV40 LT despite similar LT protein levels. B. PLA was directed against LT and p300 interaction. PLA signal is weaker for MCV LT compared to SV40 LT despite similar LT protein levels.

The LT antigen of MuPyV also does not directly bind p53, but rather targets the p53 co-activators CREB binding protein (CBP) and p300 through its C-terminus (342–346). SV40 LT has also been shown to participate in a complex with p300, but contact with p300 is mediated through direct binding to p53 (161, 170). We next wanted to see if MCV LT could also complex with p300 in some way, as this could represent a novel mechanism for antagonizing the p53 pathway by MCV. A technique called proximity ligation assay (PLA) was used to assay for interactions between LT, p53, and p300. This fluorescence microscopy technique relies on antibody-based detection of two target proteins, which when in close proximity (<40 nm) result in ligation and amplification of DNA oligos that are conjugated to the target-bound antibodies. The punctate staining pattern that results is a highly-specific surrogate marker for interaction between the two target proteins (347). Using PLA to probe for interactions between LT and p53 confirmed our initial IP results, as a strong PLA signal was detected in U2OS cells that expressed SV40 LT. Cells expressing MCV LT correspondingly showed a much weaker PLA signal for p53 interaction (**Figure 23A**). A second PLA between LT and p300 confirmed interaction between SV40 LT and p300, but there did not appear to be a similar robust interaction between MCV LT and p300 (**Figure 23B**). In this way it appears that MCV LT contrasts with other polyomavirus LTs in terms of targeting the p53 pathway.

### 4.3.2 SV40 LT inhibits p53 DNA binding and transactivation

Binding of SV40LT to p53 is undisputed, but the exact mechanism behind its functional inactivation is less clear. There are conflicting reports as to whether or not SV40 LT prevents p53-specific DNA binding to repress its transcriptional activity (151, 153,

156). It has also been reported that MCV LT prevents p53 transcriptional activity despite lack of evidence of a direct interaction (257). To better understand if and how MCV and SV40 LTs affect p53 DNA binding and transcriptional activation, we surveyed p53 target

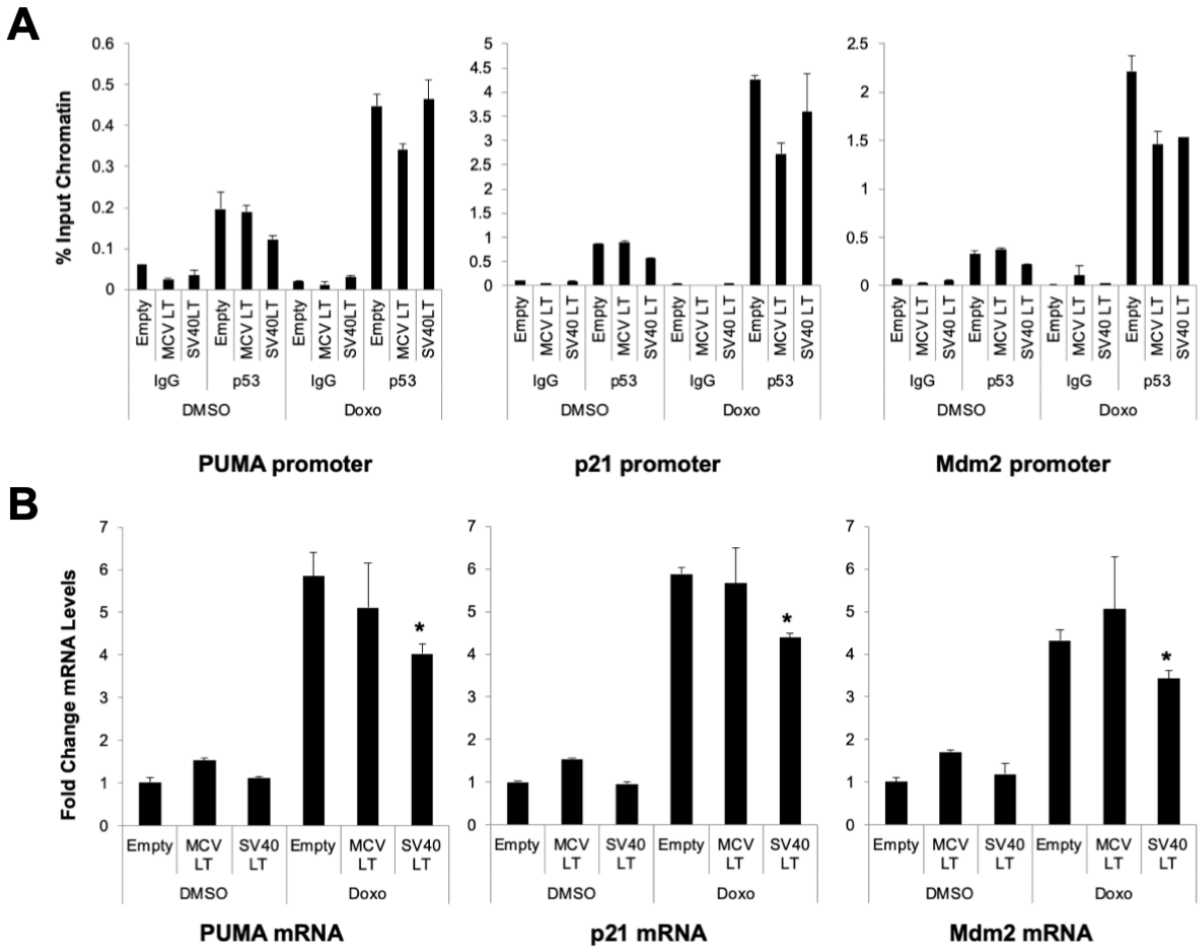


**Figure 24. SV40 LT downregulates p53 target transcripts during DNA damage response.**

U2OS cells were transiently-transfected with constructs for MCV LT, SV40 LT, or an empty vector. Cells were treated with doxorubicin to induce a DNA damage response or an equal amount of DMSO as a control prior to lysis. A. Chromatin immunoprecipitation (ChIP) results show level of p53 binding to promoter regions of PUMA, p21, and Mdm2 reported as % input chromatin levels. IP was directed against p53 protein or mouse IgG as an isotype negative control. B. qPCR results show fold change in mRNA levels for p53 target genes PUMA, p21, and Mdm2 normalized to GAPDH. Asterisks denote a significant decrease with respect to empty vector transfected cells as calculated by Student's t-test ($p<0.05$). Results show the mean ± standard error from two independent experiments with qPCR performed in triplicate.

gene transcript levels by quantitative real-time PCR (qPCR) and p53 binding at their corresponding promoters through chromatin immunoprecipitation (ChIP) (348–354). U2OS cells were transfected in duplicate with expression constructs for wild-type MCV LT, SV40 LT, or an empty vector. Prior to RNA extraction and fixation for ChIP, one set of cells with was treated overnight with doxorubicin (0.5 μM) to induce p53 activation through a DNA damage response (DDR) (355); the other set being treated with an equal amount of DMSO as a control. Binding of p53 to the promoters for PUMA (*BBC3*), p21 (*CDKN1A*), and Mdm2 (*MDM2*) was assessed by ChIP, which under normal conditions showed a limited decrease in binding of p53 to all three promoters in cells that expressed SV40 LT compared to empty vector or MCV LT-expressing cells (**Figure 24A**). As expected, doxorubicin treatment led to an increase in p53 occupancy at all three promoters, but expression of SV40 LT did not result in an inhibition of p53 binding to these promoters in this case. Despite subtle changes in p53 occupancy at target promoters, a significant decrease in transcript levels for each of these three genes was observed for cells expressing SV40 LT in the context of a DDR (**Figure 24B**). MCV LT on the other hand does not show evidence for preventing p53 transcriptional activation.

Though the results obtained from transient transfection were compelling, we sought to enhance our findings by generating stably-transfected U2OS cell lines that uniformly expressed LT. Stable cells expressing wild-type SV40 LT or an empty vector control were similarly processed for RNA extraction and ChIP in the absence of an active DDR. In this case, ChIP revealed significant decreases in p53 binding at the promoters for PUMA and p21, and a moderate decrease in occupancy at the Mdm2 promoter (**Figure 25A**). This loss of p53 binding at promoter sequences in SV40 LT-expressing

cells correlated with significant decreases in mRNA transcript levels for each of these three p53 target genes (**Figure 25B**). These data support the idea that SV40 LT inhibits p53 transactivation by preventing its binding to promoters of downstream target genes. Results from cells that stably express MCV LT are forthcoming, but it is not anticipated that major changes in p53 activity will be observed.

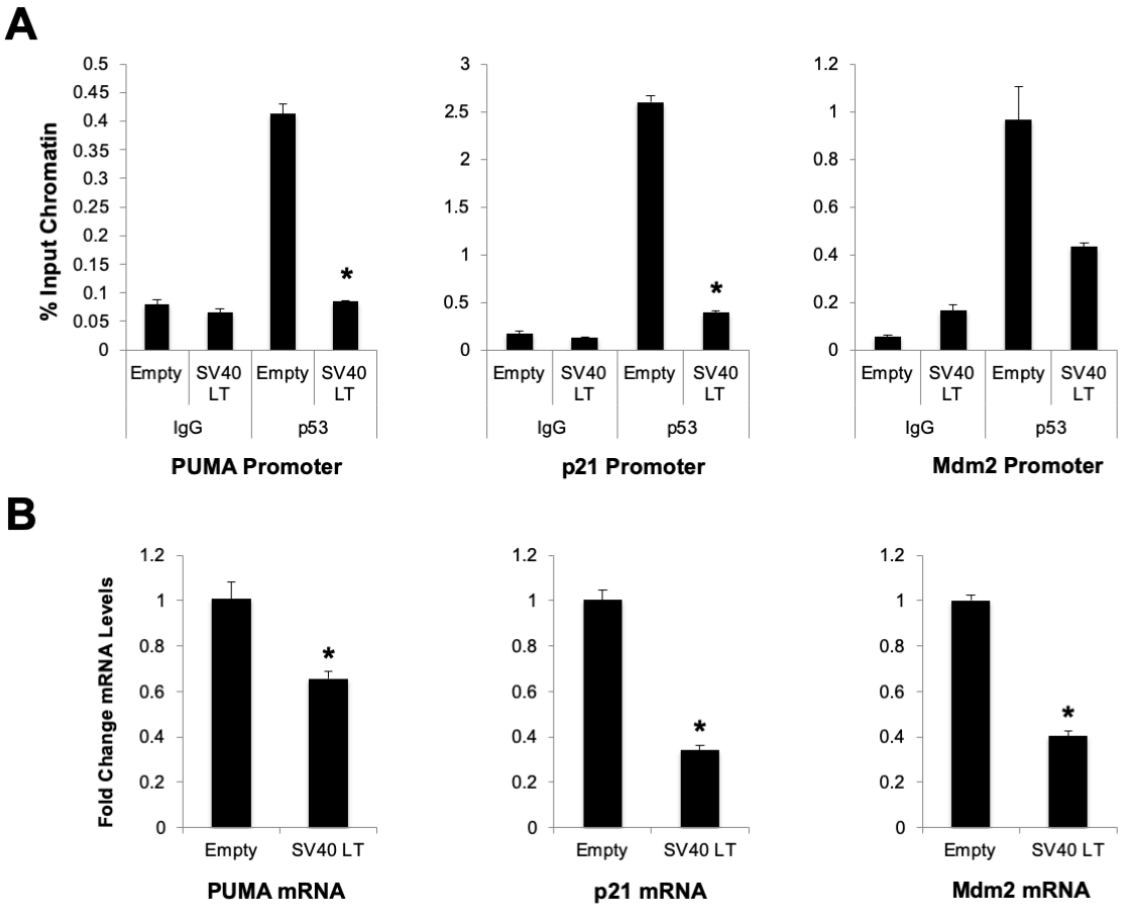


**Figure 25. Stably-transfected SV40 LT inhibits p53 binding and activation of target genes.**

U2OS cells were stably-transfected with SV40 LT or an empty vector. A. Chromatin immunoprecipitation (ChIP) results show level of p53 binding to promoter regions of target genes PUMA, p21, and Mdm2 reported as % input chromatin levels. IP was directed against p53 protein or mouse IgG as an isotype negative control. B. qPCR results show fold change in mRNA levels for p53 target genes PUMA, p21, and Mdm2 normalized to GAPDH. Asterisks in both panels denote a significant decrease with respect to empty vector transfected cells as calculated by Student's t-test ($p<0.05$). Results show the mean ± standard error from two independent experiments with qPCR performed in triplicate.

### 4.3.3 Characterization of a p53 binding mutant SV40 LT

Acetylation in the C-terminal domain of p53 by histone acetyltransferases (HATs) like CBP and p300 is essential for its stabilization and activation. Though neither MCV nor SV40 LT appear to directly bind to p300, we noticed both proteins possess the same Q(L/I)FP motif that is responsible for binding p300 by MuPyV LT (**Figure 26**). Upon

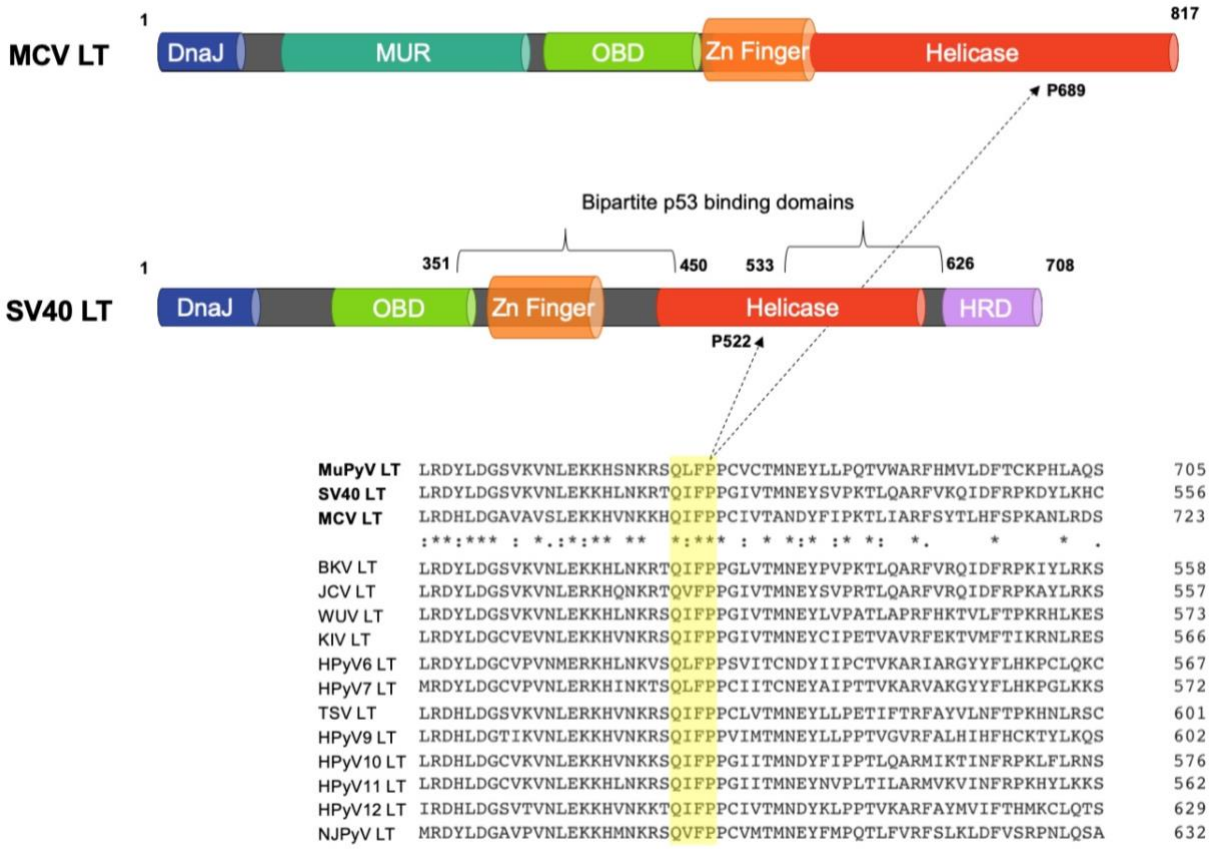


**Figure 26. Polyomavirus LT antigens possess a conserved p300 binding motif.**

Top: Schematic representations of MCV and SV40 LT antigens and their relevant functional domains. The bipartite binding motifs for p53 binding by SV40 LT are noted with brackets. Bottom: Sequence alignment of MuPyV, SV40, MCV, and human PyV LT amino acid sequences clustered around the Q(L/I)FP motif (yellow box) that MuPyV LT uses to bind p300. Asterisks denote perfectly conserved residues and colons denote partially conserved residues. This region is highly conserved across all PyVs shown here. Dotted arrows show the location of the conserved proline required for p300 interaction by MuPyV LT in MCV (P689) and SV40 LT (P522).

mutation of the proline residue in this motif to leucine or cytosine, binding between MuPyV LT and p300 was abrogated (342). We next wanted to see whether or not the same mutation at P689 and P522 of MCV and SV40 LT respectively would impact p53 targeting by either protein in any way. Surprisingly, it was revealed through co-IP experiments against LT in U2OS cells that p53 interaction was severely compromised by P522L mutation on SV40 LT (**Figure 27A**). A reciprocal co-IP experiment against p53 further

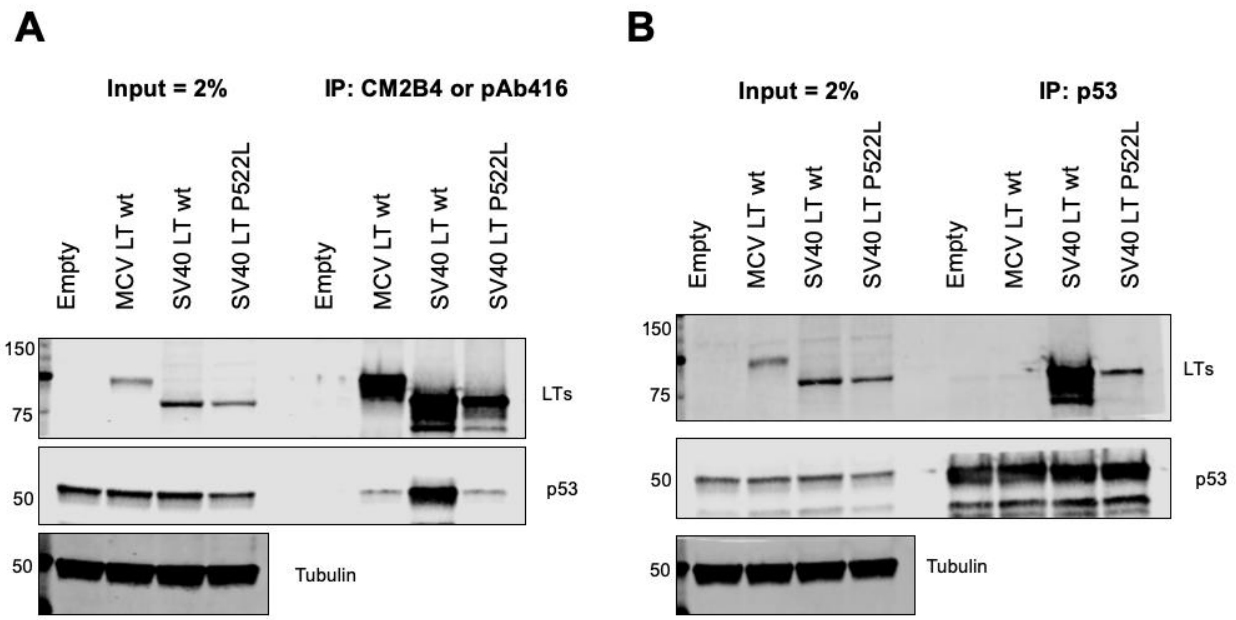


**Figure 27. P522L mutation in SV40 LT disrupts p53 binding.**

Reciprocal immunoprecipitation (IP) experiments to examine p53 binding by MCV LT wt, SV40 LT wt, or SV40 LT P522L. A. IP against MCV LT (CM2B4) and SV40 LT (pAb416) and immunoblotting against p53 shows that SV40 LT P522L has a p53 binding defect compared to its wild-type counterpart. Input lysates show LT and p53 protein levels in the whole cell lysate. B. IP against p53 and immunoblotting against LTs similarly shows that SV40 LT P522L co-IPs with p53 at a greatly reduced efficiency compared to SV40 LT wt. In neither case does MCV LT strongly co-IP with p53, matching earlier data. Input lysates show LT and p53 protein levels in the whole cell lysate.

supported the finding that this mutation in SV40 LT impairs its ability to bind p53 (**Figure 27B**). This P522 residue falls just outside the canonical bi-partite sequences on SV40 LT known to be essential for p53 binding (103), and these data suggest that p53 binding by SV40 LT may be more precise than previously believed.

Having identified a point-mutation critical for binding p53 in SV40 LT, it was imperative to determine whether or not this mutation also affected other functions of LT.

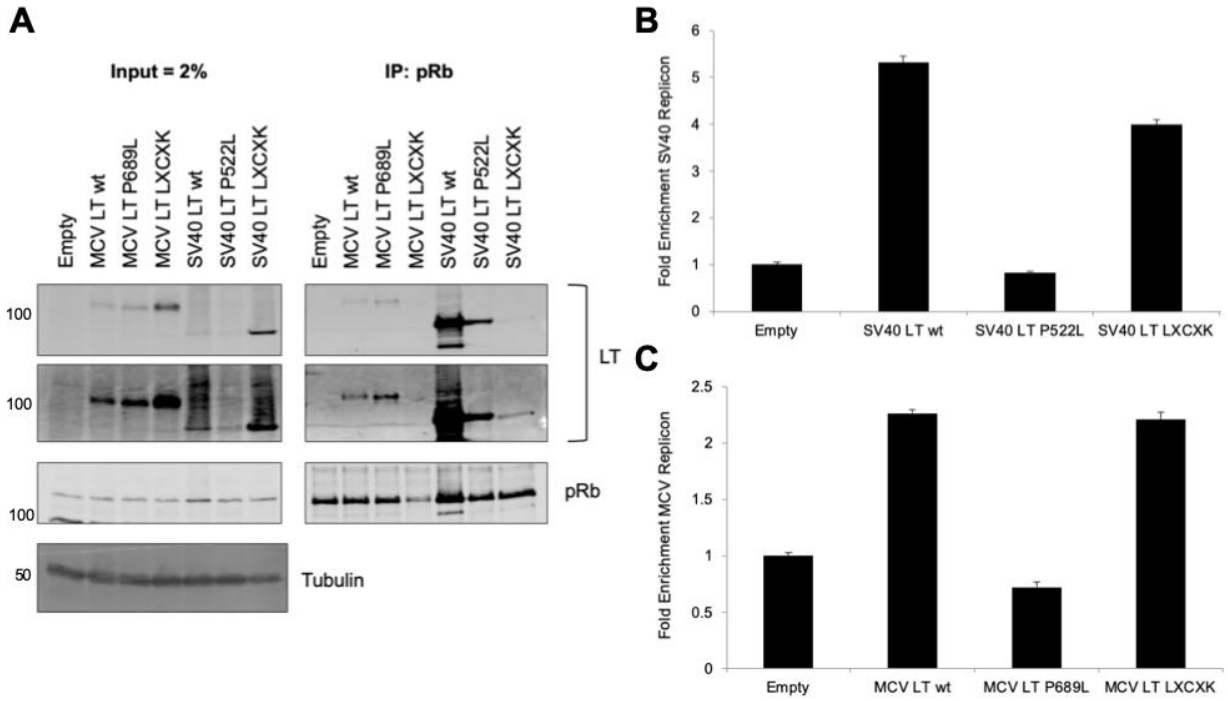


**Figure 28. Mutant LTs bind pRb but fail to replicate DNA.**

A. Immunoprecipitation (IP) experiment to examine pRb binding efficiency of wt, P→L mutant, or LXCXE mutant LTs from MCV and SV40. IP against pRb and immunoblotting against LT shows only LXCXE mutant LTs fail to co-IP with pRb. Two different exposures are shown as signal intensities varied between MCV and SV40 LTs. Input lysates show LT and pRb protein levels in the whole cell lysate. B. SV40 replication assay. Results are shown as fold enrichment in SV40 replicon DNA over empty vector transfected cells. SV40 LT wt and SV40 LT LXCXK both efficiently amplify the replicon, but SV40 LT P522L shows no replication activity. C. MCV replication assay. Results are shown as fold enrichment in MCV replicon DNA over empty vector transfected cells. MCV LT wt and MCV LT LXCXK both amplify the replicon, MCV LT P689L shows no replication activity.

Apart from binding p53, another function of SV40 LT is to bind to and sequester the retinoblastoma (Rb) family of proteins to facilitate the replication process (90, 137, 356). IP experiments were used to determine if mutant LTs from MCV and SV40 were still capable of binding to pRb. U2OS cells were transfected with wild-type, P→L mutant, or Rb-binding mutant (LXCXK) LTs from MCV or SV40 and subject to pulldown against endogenous pRb. Immunoblotting revealed that both MCV LT P689L and SV40 LT P522L were still capable of pRb interaction, unlike the corresponding LXCXK mutant LTs (**Figure 28A**). The main function of LT in the context of a productive infection is to initiate the viral replication process, so replication assays were used to determine if these mutations had an impact on this process. In these assays, qPCR was used to measure the efficiency of replication of an origin-containing replicon in the presence of either LT (222, 248). It became clear that both MCV LT P689L and SV40 LT P522L were deficient in DNA replication, compared to wild-type LTs (**Figure 28 B & C**). This is consistent with findings that mutations in the helicase region of LT often hinder replication efficiency (262, 330, 341). Overall, these mutations appear to disrupt multiple functions of LT, but they do not render the protein completely functionally inactive either.

### 4.3.4 SV40 LT mutation reverses p53 stabilization and inhibition

Inhibition of p53 activity by SV40 LT is dependent upon direct binding between the two proteins, so we next examined the consequences of a p53-binding mutant LT on p53 activation. Using a luciferase reporter that contains four copies of the p53 binding site (BS2) from the PUMA (*BBC3*) promoter, p53-dependent transcriptional activation in the presence of wild-type and mutant LTs from MCV and SV40 could be measured. While

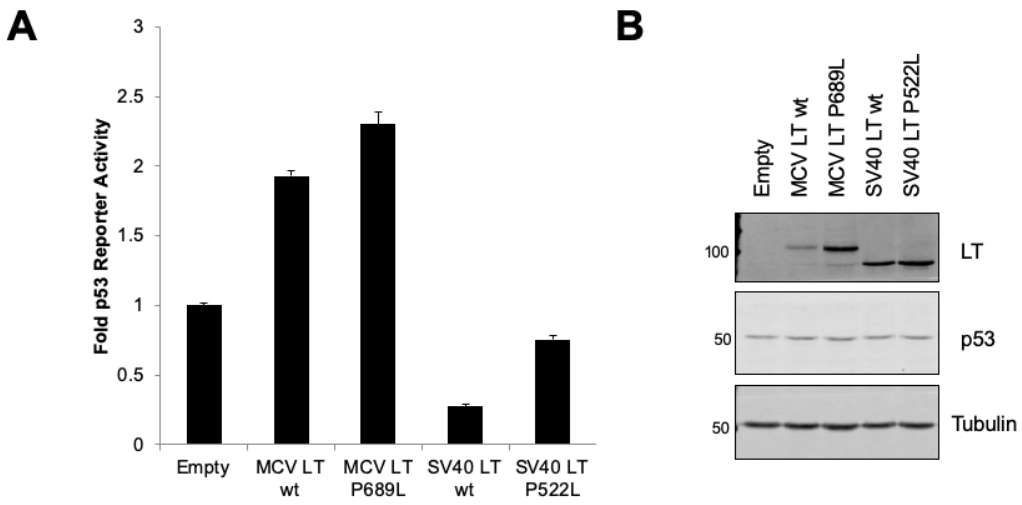


**Figure 29. P522L mutation in SV40 LT reverses p53 transcriptional inhibition.**

A. Luciferase assay results for p53-dependent transcription using the 4xBS2 reporter system. U2OS cells expressing either MCV LT show a 2-fold increase in p53 reporter activity compared to empty vector control. SV40 LT wt shows potent inhibition (~75% decrease) of p53 reporter activity, which is reversed to near baseline levels upon P522L mutation. B. Corresponding immunoblot for cells used in the luciferase assay, showing the LT and p53 protein levels in these cells. LT protein levels are relatively equal between all conditions.

wild-type SV40 LT showed greater than 70% reduction in reporter activity (**Figure 29A**), the P522L mutant failed to inhibit transcriptional activation to the same degree, despite equal LT protein levels (**Figure 29B**). By contrast, both wild-type and P689L MCV LT showed a 2-fold increase in reporter activity, which is consistent with the notion that full-length MCV can trigger p53 activation through a DNA damage response (264).

The transactivation capability of p53 is primarily governed by post-translational modifications such as phosphorylation and acetylation that promote p53 multimerization, DNA binding, and recruitment of multiple cofactors (146, 357, 358). Post-translational modifications on p53 were profiled by immunoblotting, using lysates derived from U2OS cells transfected with wild-type or P→L mutant LTs from MCV and SV40 both with and without a doxorubicin-induced DDR (**Figure 30**). Under normal conditions in empty

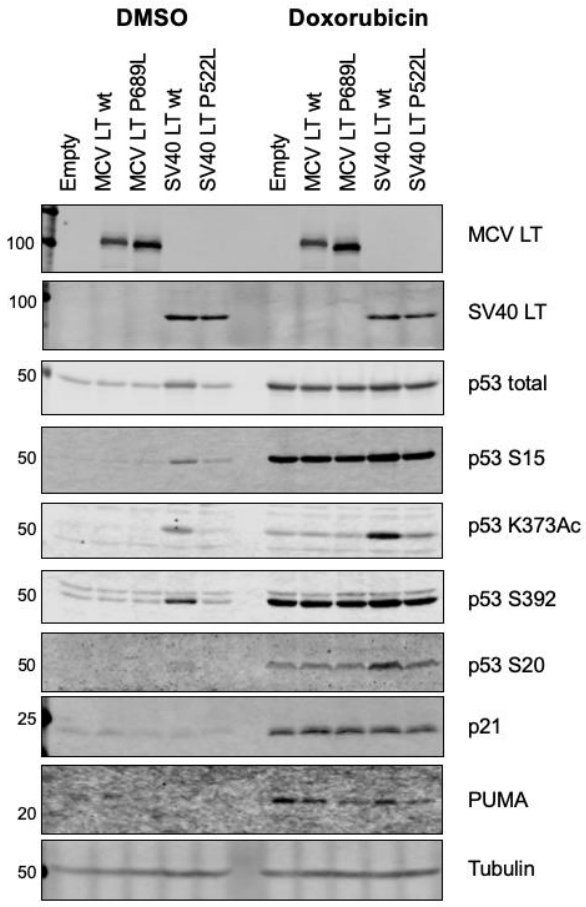


**Figure 30. Post-translational modifications on p53 vary in the presence of LTs.**

Immunoblots of lysates generated from U2OS cells transfected with MCV LT wt, MCV LT P689L, SV40 LT wt, SV40 LT P522L, or an empty vector. Cells were either treated with doxorubicin to induce a DNA damage response or an equal amount of DMSO. The first two panels show protein levels for MCV and SV40 LTs. The next five panels show total p53 protein levels as well as phosphorylation at S15, S20, S392, and acetylation at K373. Protein levels of p53 targets PUMA and p21 are shown below. Tubulin serves as a loading control.

vector-transfected cells, total p53 protein levels remained low and markers of activation were largely absent. This was also seen for cells expressing either wild-type or P689L MCV LT, but cells that expressed wild-type SV40 LT showed an increase in total p53 protein levels along with the presence of several activating post-translational modifications. This is consistent with reports that describe p53 bound to SV40 LT as possessing activation markers despite overall functional inhibition (161, 170). By

comparison, cells expressing P522L mutant SV40 LT show diminished total p53 levels and a reduction in activation markers, providing further evidence that this mutation impairs p53 inactivation by LT. Following doxorubicin treatment, total p53 levels became increased across all conditions, as did protein levels for downstream targets PUMA and p21. Likewise, consistent with a DDR, post-translational markers of activation are present on p53 in all conditions here, with a specific enrichment at phospho-S20 and acetyl-K373 in cells expressing wild-type SV40 LT. We hypothesize that the increased signal at these sites is a consequence of inhibition of p53 degradation by SV40 LT.

Unlike high-risk HPV E6 proteins that target p53 for degradation (359–361), SV40 LT simultaneously prevents its transcriptional activation and degradation through direct binding (155, 156, 158, 362). This p53 accumulation with SV40 LT was observed in our immunoblots, but it was reversed by P522L mutation (**Figure 30**). We next explored changes in p53 half-life in the presence of wild-type and P→L mutant LTs from MCV and SV40 through cycloheximide (CHX) chase assays. As p53 is generally a short-lived protein (363), p53 protein levels readily decreased over the 4 hour course of CHX treatment in empty vector-transfected cells (**Figure 31A**). Similar kinetics of p53 degradation were observed in cells that expressed either wild-type or P689L MCV LT. Cells that expressed wild-type SV40 LT, however, showed a substantial stabilization of p53 across the entire time course. This stabilization phenotype was reversed upon P522L mutation of SV40 LT, indicating that this p53 binding mutant is insufficient at blocking p53 degradation. RNA extraction was simultaneously performed at each time point, so that p53 mRNA transcript levels could be monitored throughout. At no time point were

substantial changes in p53 transcripts observed between the different conditions (**Figure 31B**), suggesting observed changes in p53 protein levels occurred post-transcriptionally.

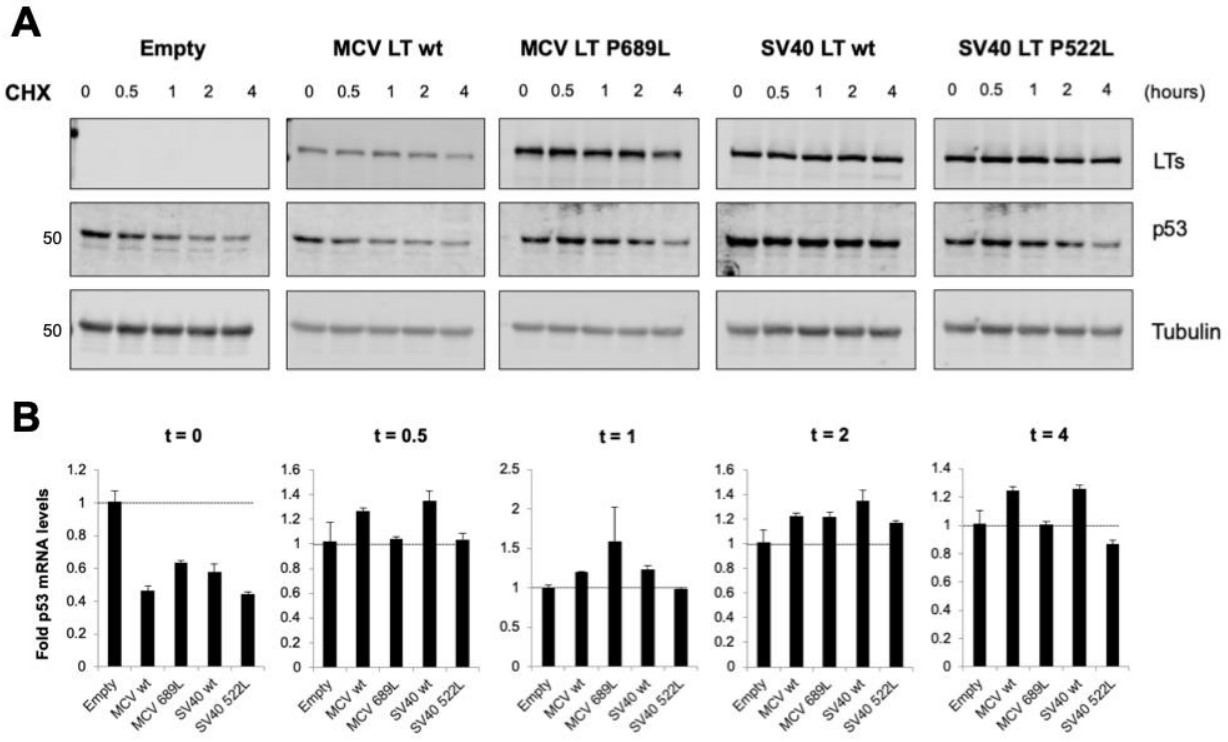


**Figure 31. P522L mutation in SV40 LT sensitizes p53 to degradation.**

Cycloheximide (CHX) chase experiment to study p53 half-life in U2OS cells expressing MCV LT wt, MCV LT P689L, SV40 LT wt, SV40 LT P522L, or an empty vector. Time points were taken at 0, 0.5, 1, 2, and 4 hours post-CHX treatment. A. Immunoblots for each condition show LT and p53 protein levels over the 4-hour time course. Tubulin serves as a loading control. Half-life of p53 is stabilized only by SV40 LT wt. B. qPCR results for p53 mRNA levels at each time point, normalized to GAPDH. Dotted line corresponds to p53 mRNA level in empty vector transfected cells, normalized to 1. Significant changes in p53 mRNA were not detected at any time point for any condition relative to the empty vector control.

## 4.4 Discussion

T antigens and p53 have been married from the start, and as in any marriage their relationship is multidimensional, enduring, and profound. This study sought to compare the LT antigens from the classic polyomavirus SV40 with the more recently discovered MCV primarily in an attempt to reach a greater understanding of how these proteins manipulate the p53 pathway, but also to reconcile some of the conflicting data that has existed in the field regarding mechanisms of p53 inhibition by both viruses. Rather than revealing concerted mechanisms of p53 targeting by MCV and SV40, the data presented here show that the LT antigens from these two viruses possess entirely disparate mechanisms for antagonizing the p53 pathway.

The relationship between MCV and the p53 pathway remains complicated, but these results show clearly that there is little evidence of a role for LT alone when it comes to p53 inhibition. Despite putative binding motifs for both p53 and p300 based on sequence homology to other polyomaviruses, IP and PLA results demonstrate that if LT does complex with either of these proteins, it is with significantly less affinity than SV40 LT. This is not an entirely unexpected finding, as other groups have reported a lack of binding between MCV LT and p53 (257, 258). However, unlike the results from the study by Borchert *et al.* that additionally show a decrease in p53-dependent transcription in the presence of LT by reporter assays, we see no evidence of any reduction in the mRNA transcript levels of p53 target genes in cells that express MCV LT. In contrast to their findings, the reporter assay results described here suggest an increase in p53-dependent transcription in LT-expressing cells. Transcript levels of p53 target genes were slightly elevated in MCV LT-transfected cells under normal conditions, as well. These results are

more consistent with studies that have shown that full-length MCV LT does not inhibit p53 but rather induces p53 activation downstream of ATR activation in U2OS cells (255, 264). It is believed that MCV-induced p53 activation is mediated by and requires an intact, functional C-terminal helicase domain.

Recent work by Park *et al.* suggests that there may be a role for the small T (sT) antigen of MCV in inhibiting the p53 response through transcriptional modulation of Mdm2 and Mdm4 through a sT-MYCL-EP400 complex (277, 278). Their results show that co-expression of sT with LT can dampen the p53 activation phenotype that was observed by expression of LT alone (278). A similar level of interplay between sT and LT functionalities has also been seen in the enhancement of viral replication by MCV LT through co-expression of sT (219). Taken together, these findings emphasize the utility of examining the functions of LT and sT proteins in conjunction with one another rather than attempting to separate their roles.

Seminal works involving SV40 have been the foundation for studying cancer biology in general and have prompted the discovery of a litany of new polyomaviruses throughout the animal kingdom during the past few decades (79, 364). Although a multitude of research has been published on the human polyomaviruses, there remains much more to be gained from further study of SV40. Portions of this study recapitulate established dogma about p53 targeting by SV40 LT, but these results go further to definitively show that SV40 LT prevents binding of p53 to cognate sequences in the promoter regions of established target genes, which corresponds to a significant decrease in mRNA transcripts from those same loci. Furthermore, attempts to investigate p300 binding led to the identification of a p53-binding point mutant SV40 LT (P522L) that

is deficient in stabilizing p53 protein levels and inhibiting its transactivating functions. Although this mutation also renders LT replication incompetent, it still retains the important N-terminal function of binding to pRb. This P522L mutant LT also displays a similar half-life to the wild-type protein in CHX chase experiments, adding further support to the idea that this mutation does not completely destabilize and disable LT.

As LT is a complex, multidomain protein, it is possible for a mutation to eliminate functionalities within one domain without completely eliminating all functions of the protein as a whole. Extensive mutagenic studies on SV40 LT have made this concept clear, as mutations that disrupted ATPase activity or p53 binding by LT resulted in proteins that in some cases were still competent for replication and even transformation of particular cell lines (330, 341). Furthermore, work by Manos and Gluzman has identified multiple mutants of SV40 LT that were defective in replication but were competent in transformation, including a P522S mutant LT (262, 365). Given that this mutation has been classified as an ATPase mutant and not a p53 binding mutant, it would appear that serine versus leucine substitution mutations at this residue produce different effects on LT function. How the P522L mutant LT identified in this study may impact cellular transformation by SV40 remains to be seen.

# 5.0 Merkel cell polyomavirus small T antigen induces genome instability by E3 ubiquitin ligase targeting

Work described in this chapter was published in Oncogene

**Oncogene. 2017 Dec 7;36(49):6784-6792.**

**with authors Kwun HJ, Wendzicki JA, Shuda Y, Moore PS, and Chang Y.**

H.J. Kwun and J.A. Wendzicki contributed equally to this work.

H.J. Kwun and J.A. Wendzicki performed transfection and transduction of cell lines, immunofluorescence staining and centrosome counts, and immunoblotting. J.A. Wendzicki performed flow cytometry. J.A. Wendzicki prepared cells for karyotype analysis, which was carried out by the Cytogenomics Laboratory at the University of Minnesota Masonic Cancer Center. Y. Shuda maintained mice used in this study and assisted in blood and organ sample collection, which were processed and analyzed by J.A. Wendzicki with help from Litron Laboratories. H.J. Kwun performed knockdown, immunoprecipitation, RT-qPCR, and half-life experiments. H.J Kwun, J.A. Wendzicki, P.S. Moore, and Y. Chang conceived the project, analyzed results, and wrote the manuscript.

The formation of a bipolar mitotic spindle is an essential process for the equal segregation of duplicated DNA into two daughter cells during mitosis. As a result of deregulated cellular signaling pathways, cancer cells often suffer a loss of genome integrity that might etiologically contribute to carcinogenesis. This chapter describes how Merkel cell polyomavirus MCV sT oncoprotein induces centrosome overduplication, aneuploidy, chromosome breakage and the formation of micronuclei by targeting cellular ligases through a sT domain that also inhibits MCV LT oncoprotein turnover. These results provide important insight as to how centrosome number and chromosomal stability can be affected by the E3 ligase targeting capacity of viral oncoproteins such as MCV sT, which may contribute to Merkel cell carcinogenesis.

## 5.1 Introduction

Merkel cell polyomavirus (MCV) is the causative agent of most Merkel cell carcinomas (MCCs), a highly aggressive human cancer (48). Shortly after the discovery of MCV, the large T (LT) and small T (sT) antigens encoded by the early region of the virus were identified as the two major oncoproteins responsible for tumorigenesis and tumor maintenance (235). Both LT and sT are expressed in virtually every MCV-infected MCC (333, 366). MCC tumors are characterized by the clonal integration of viral DNA within the host genome as well as by mutations in the viral early coding region that result in the expression of a C-terminally truncated form of LT; however, the coding region for sT is left intact (83).

The sT antigen of MCV alone is able to transform rodent fibroblasts (265). While sT transgenic mice show dermal hyperproliferation (239), expression of sT combined with homozygous deletion of p53 in a transgenic mouse model leads to the development of fully transformed, highly anaplastic tumors in livers and spleens (238). The transformation activity of sT is independent of its ability to interact with PP2A (198, 265), but is localized to a short region of sT from amino acids 91–95 termed the LT-stabilization domain (LSD) (237). The LSD allows sT to inhibit the cellular ubiquitin ligase complex SCF-Fbw7 (237), which governs the degradation of several cellular oncoproteins, including c-myc and cyclin E (194). The LSD is also responsible for inhibiting the anaphase-promoting complex/cyclosome E3 ligase, which leads to increased mitogenesis and hyperphosphorylation of the major translation regulator 4E-BP1 (273).

Many cancer cells display evidence of genomic instability (367), such as the presence of centrosome amplification and multipolar mitotic spindles. Supernumerary centrosomes can lead to the assembly of multipolar mitotic spindles, which may in turn result in chromosome mis-segregation, aneuploidy and, over time, cancer development (368). MCC, similar to many other cancers, has been shown to exhibit a chromosomal instability tumor phenotype (369), which can be attributed in part to the properties of viral oncoproteins as commonly seen in other virus-induced human cancers. The Skp, Cullin, F-box containing complex (SCF) family of E3 ligases has been known to have an important role in the regulation of many of the major proteins involved in cell cycle (370, 371). In many cancers, mutational loss of SCF is associated with genomic instability resulting from the accumulation of its substrates, including cyclin E, cyclin D1, Polo-like kinase 4 (PLK4) and several others (372, 373). A number of viral oncoproteins implicated

in human cancer have previously been shown to cause multipolar mitoses and aneuploidy by deregulation of host systems involved in ubiquitin-mediated degradation. Human papillomavirus 16 (HPV16) E7 induces centriole multiplication mediated by altered expression of PLK4, a target of SCF-β-TrCP (374, 375), hepatitis B virus HBx binding to DDB1 (ultraviolet-damaged DNA-binding protein1) E3 ubiquitin ligase complex subunit results in chromosome segregation defects (376), and human T-cell leukemia virus type-1 Tax oncoprotein directly binds and activates the Cdc20-associated anaphase-promoting complex (377) resulting in mitotic abnormalities (378–380). In addition, primary endothelial cells infected with Kaposi's sarcoma-associated herpesvirus display abnormal mitotic spindle assembly, supernumerary centrosomes and chromosome instability (381). These findings underscore the importance of the intricate network of host cell machinery in maintaining genome integrity, which, when deregulated by viral proteins, can lead to tumorigenesis.

MCV sT expression stabilizes SCF-Fbw7 targets such as c-myc and cyclin E (237) and promotes microtubule destabilization (276). These effects implicate the induction of genomic instability as an important mechanism for MCV sT-induced oncogenesis. Here we show using several assays of genomic instability that MCV sT, through the targeting E3 ligases, fosters a genomically unstable phenotype. Expression of sT in vitro results in the formation of supernumerary centrosomes and increased aneuploidy and chromosomal breakage in an LSD-dependent manner. Inducible expression of sT in vivo leads to the development of micronuclei in reticulocytes. Loss of Fbw7 either by knockout or by knockdown leads to the formation of supernumerary centrosomes, an effect that can be recapitulated by sT expression when Fbw7 is replete.

## 5.2 Materials and methods

### 5.2.1 Cell culture and transfection

293 and WI38 (American Type Culture Collection CCL-75, Manassas, VA, USA) cell lines were maintained in Dulbecco's modified Eagle's medium (Cellgro, #10-013, Manassas, VA, USA), supplemented with 10% fetal bovine serum (VWR Seradigm, Radnor, PA, USA). hCDC4+/+ and hCDC4−/− HCT116 cells (kindly provided by Dr. Bert Vogelstein and obtained from Johns Hopkins University Genetic Resources Core Facility) were grown in McCoy's 5A medium with 10% fetal bovine serum. NIH3T3 cells were maintained in Dulbecco's modified Eagle's medium with 5% calf serum (Gibco, Gaithersburg, MD, USA). Transfections were performed using Lipofectamine 2000 (Invitrogen, Carlsbad, CA, USA) following the manufacturer's instructions. The short tandem repeat profiles of the 293 and WI38 cells were authenticated by the University of Arizona Genetics Core and NIH3T3 cells by IDEXX (Westbrook, ME, USA). All cells used in experiments were confirmed to be negative for mycoplasma at the time of each experiment.

### 5.2.2 Plasmids and lentivirus production

Codon-optimized cDNAs for MCV sT WT (GenBank accession number AEM01096.1, Addgene, Cambridge, MA, USA, #40201), sT L142A (198), sT LSDm (237) and for SV40 sT (GenBank accession number KM359729) (198), and HPV E7 (NCBI reference sequence NP_041326.1) (382) plasmids for lentiviral transduction and

transfection were described previously, as referenced. shRNA-targeting sequences of CDC20 (TRCN0000003790, UniProtKB ID: Q12834) and BTRC (TRCN0000006541, UniProtKB ID: Q9Y297) cloned in pLKO.1 vector (265) were used for the knockdown study. shRNAs for human Fbw7 (UniProtKB ID: Q969H0) were described previously (237), and a control shRNA construct was obtained from Addgene (#1864). Lentiviral and retroviral particles were generated in 293FT (Invitrogen) cells maintained in Dulbecco's modified Eagle's medium with 10% fetal bovine serum by cotransfection with the packaging vector plasmids psPAX2 and pMD2 or pCLAmpho (Addgene) using Lipofectamine 2000 (Invitrogen).

### 5.2.3 Immunoblotting and antibodies

Cells were lysed in buffer (50 mM Tris-HCl (pH 8.0), 150 mM NaCl, 0.6% SDS and 5 mM NaF) containing protease inhibitors (Roche, Basel, Switzerland). Lysates were resolved by SDS-polyacrylamide gel electrophoresis and transferred to nitrocellulose membranes (GE Healthcare, Chicago, IL, USA), then incubated in primary antibodies for at least 2 h at room temperature. For quantitative infrared western blot detection, IRDye 800CW goat antimouse (926-32210, LI-COR) or IRDye 800CW goat anti-rabbit antibody (929- 32211, LI-COR) were used as secondary antibodies. Signal intensities were analyzed at 800 nm, using the Odyssey IR Imaging System (LI-COR, Lincoln, NE, USA). The following primary antibodies were used: anti-MCV sT CM8E6 (248); anti-α tubulin (B-5-1-2, T5168, Sigma-Aldrich, St Louis, MO, USA); pAb419 (sc-58665, Santa Cruz, Dallas, TX, USA); Myc (9E10, sc-40, Santa Cruz); FLAG (M2, F3165, Sigma, St Louis, MO, USA);

anti-HA (16B12, MMS-101R, Biolegend, San Diego, CA, USA); and Hsc70 (sc-7298, Santa Cruz).

### 5.2.4 Flow cytometry

Cells were trypsinized and stained with a fixable viability dye (eBioscience, Thermo Fisher Scientific, Waltham, MA, USA) according to the manufacturer's instructions. Fixation was performed in cold 70% (vol/vol) ethanol. Fixed cells were washed with phosphate-buffered saline (PBS) containing 1% bovine serum albumin and permeabilized by addition of 0.25% Triton X-100 for 30 min on ice. To label DNA, cells were resuspended in propidium iodide/RNaseA staining solution (0.05 mg/ml propidium iodide, 0.1 mg/ml RNaseA in 1 × PBS) and incubated for 30 min at room temperature and analyzed using a Becton Dickinson (Franklin Lakes, NJ, USA) Accuri C6 flow cytometer.

### 5.2.5 Immunofluorescence microscopy

Cells were seeded on glass slides and transfected or transduced with designated plasmids. Cells were fixed with 4% buffered formalin for 10 min and permeabilized with PBS with 0.1% Triton X-100 for 10 min. After blocking with 10% goat serum in PBS-T (PBS with 0.5% Tween 20), cells were incubated overnight at 4 °C with primary antibody γ-tubulin (ab84355, Abcam, Cambridge, MA, USA) or CEP170 (72-413-1, Thermo Fisher Scientific, Waltham, MA, USA) for staining, followed by secondary antibody incubation (Alexa Fluor 488- or 568-conjugated goat anti-rabbit (A11034 or A11036) or anti-mouse (A11029 or A11004, 1:1000, Invitrogen) for 1 h at room temperature. Stained cells were

mounted in aqueous medium containing 4,6-diamidino-2-phenylindole (DAPI) (Vector Laboratories, Burlingame, CA, USA). Cells were analyzed by fluorescence imaging using an Olympus AX70 epifluorescence microscope equipped with a U-CMAD3 camera (Olympus, Tokyo, Japan). Centrosome counting was performed in a blinded manner by two observers.

### 5.2.6 Karyotype analysis

Cells were seeded in flasks and transduced with specified lentiviruses. The following day cells were shipped to the Cytogenomics Laboratory at the University of Minnesota Masonic Cancer Center, and culture medium was replaced upon arrival. At 48 h post transduction, cells were subjected to overnight (15 h) treatment with colcemid to arrest cells in metaphase. Cells were then collected, fixed and dropped on slides according to standard cytogenetic protocol. Fifty metaphases per condition were analyzed for chromosomal gaps, breakages and losses by G-banding at 400 band resolution.

### 5.2.7 Mouse studies

All mice were maintained in accordance with protocols approved by the Institutional Animal Care and Use Committee at the University of Pittsburgh. In brief, a previously characterized tamoxifen-inducible, cre-loxP recombination system was used to achieve ubiquitous expression of MCV sT from the ROSA26 locus in C57BL/6 mice (238). Two main cohorts of mice (8–10 weeks of age) were used: $Ubc^{CreERT2-/+}ROSA^{sT/+}$ for sT expression alone (five female and four male) and $Ubc^{CreERT2-/+}p53^{flox/flox}ROSA^{sT/+}$

(six female and four male) for additional p53 knockout. $Ubc^{CreERT2-/-}$ mice (four female and seven male) from either genetic background served as negative controls, as they lack expression of Cre recombinase. All mice were subjected to intraperitoneal injection of tamoxifen (0.2 mg/g), followed by sacrifice after 48 h. Mouse tissues were isolated and processed for immunoblotting as described previously (238). Mouse blood samples were isolated via cardiac puncture, fixed in ultracold methanol and analyzed by Litron Laboratories (Rochester, NY, USA). All mice used for experiments were randomly assigned to non-blinded treatment groups. Sample size determined by Mead's resource equation.

### 5.2.8 Immunoprecipitation

293 were transfected with plasmids for expression of MCV sT WT or sT LSDm along with HA-tagged β-TrCP. Cells were lysed in immunoprecipitation buffer (50 mM Tris-HCl (pH 7.4), 150 mM NaCl and 1% Triton X-100) freshly supplemented with protease inhibitor cocktail (Roche), 1 mM phenylmethylsulfonyl fluoride and 1 mM benzamidine. Lysates were incubated overnight at 4 °C with HA-specific antibody, followed by incubation with a slurry of Protein A/G Plus Agarose beads (Santa Cruz) for 3 additional hours. Following a series of wash steps, bound proteins were eluted in 2 × SDS loading buffer, resolved by SDS-polyacrylamide gel electrophoresis, and immunoblotted for MCV sT as described above.

### 5.2.9 Quantitative real-time PCR analysis

shRNA-transfected cells were selected with puromycin (2 μg/ml) for 4 days after infection. Total RNA was isolated 2 days after transduction using TRIzol LS reagent (Invitrogen) and treated with DNase I (NEB, Ipswich, MA, USA). The cDNA was generated using random hexamer primers and Superscript III First-Strand Synthesis reverse transcriptase (Invitrogen). Quantitative PCR with cDNA (0.1 μg) was carried out using SsoFast EvaGreen Supermix (Bio-Rad, Hercules, CA, USA) and a CFX96 real-time PCR detection system (Bio-Rad) according to the manufacturer's protocol with primer pairs for Fbw7 (5′-AAAGAGTTGTTAGCGGTTCTCG-3′ and 5′-CCACAT GGATACCATCAAACTG-3′), β-TrCP (5′-TGCCGAAGTGAAACAAGC-3′ and 5′-CCTGTGAGAATTCGCTTG-3′), cdc20 (5′- CGCCAACCGATCCCACAG-3′ and 5′-CAGGTTCAAAGCCCAGGC-3′) and GAPDH (5′-ACTTCAACAGCGACACCC-3′ and 5′-TCTTCCTCTTGTGCTCTTGC-3′) cDNA detection.

## 5.3 Results

### 5.3.1 Overexpression of MCV sT induces centrosomal aberration and aneuploidy

To determine whether MCV sT causes centrosome amplification, NIH3T3 cells were stably transduced with lentiviruses for wild-type (WT) MCV sT, a PP2A-binding mutant sT (L142A), an LSD mutant sT (LSDm), HPV16 E7, SV40 sT or an empty vector. These stably transduced NIH3T3 cells were enriched for mitosis by arrest with the cyclin-

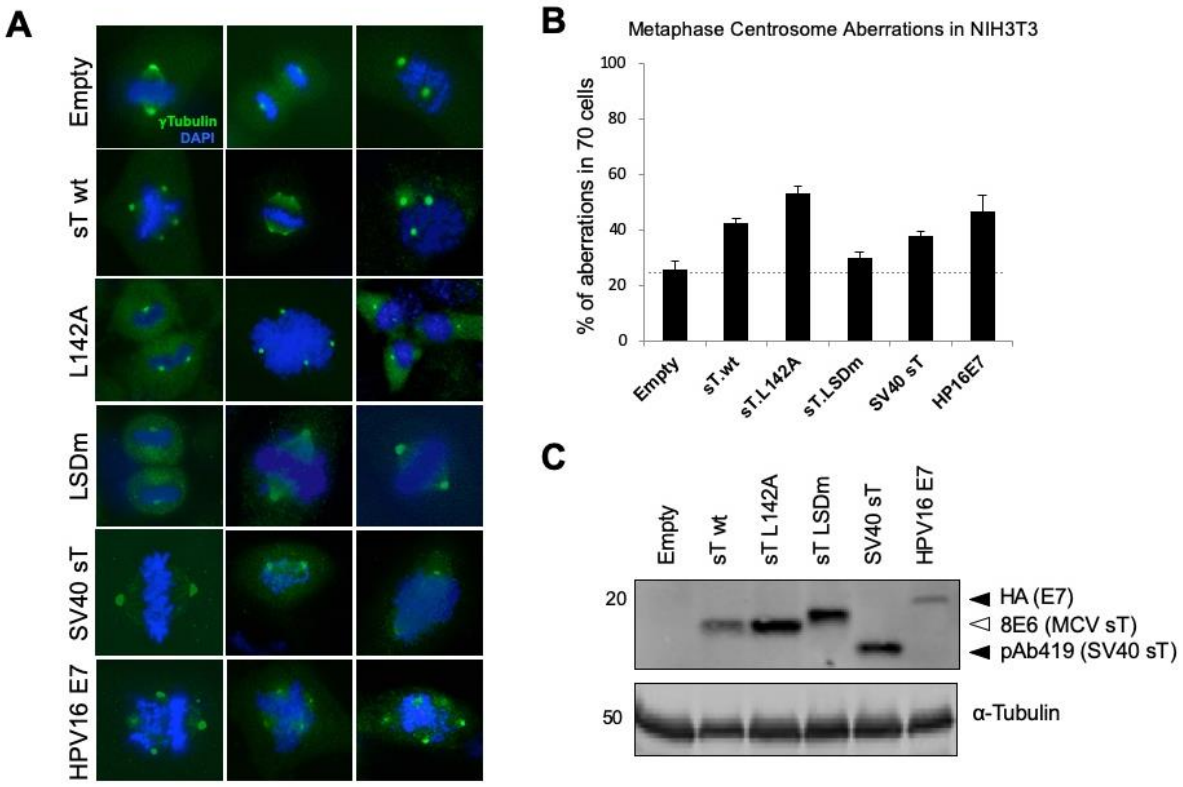


**Figure 32. Overexpression of sT causes centrosomal aberration in NIH3T3 cells.**

A. Multipolar mitosis with centrosome amplification by viral oncoproteins. Stably transduced NIH3T3 cells were stained for centrosomes (γ-tubulin, green) and DNA (4,6-diamidino-2-phenylindole (DAPI), blue). SV40 sT antigen and HPV16 E7 were used as controls. Supernumerary centrosomes were readily visible in cells expressing WT or L142A mutant MCV sT as well as HPV16 E7 (× 1000 magnification). B. Quantification of cells with abnormal numbers (⩾3) of centrosomes in metaphase out of 70 cells. Data show the mean ±s.e. from three experiments. C. Expression of oncoproteins was analyzed using specific antibodies (8E6, pAb419 and HA for MCV sTs, SV40 sT and E7, respectively) by immunoblotting from the same samples used for immunofluorescence.

dependent kinase 1 inhibitor RO-3306 (10 μM) at the mitotic boundary and subsequently released. Cells were then fixed and immunostained for γ-tubulin, a principle protein component of centrosomes. Abnormal centrosome numbers and multipolar mitotic assemblies were readily detected in metaphase spreads from cells expressing WT MCV sT or L142A mutant sT (**Figure 32A**), reaching frequencies >40% of the 70 mitotic cells counted in each experiment (**Figure 32B**). This 1.5- to 2-fold enrichment of

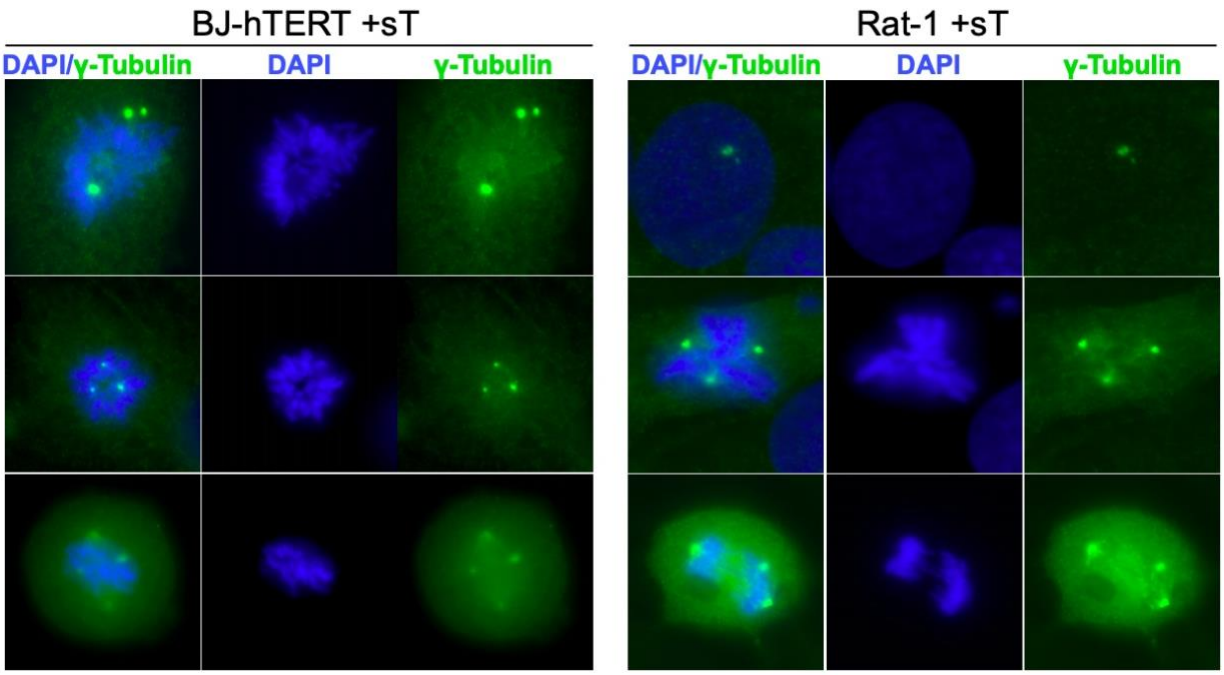


**Figure 33. Centrosome aberration in BJ-hTERT and Rat-1 fibroblasts.**

An increase in the frequency of supernumerary centrosomes (γ-Tubulin, green) is detected by fluorescence microscopy in wild-type sT-expressing BJ-hTERT and Rat-1 cells. Formation of supernumerary centrosomes was observed at 2 days post-transduction. DAPI nuclear counterstaining is shown in blue.

supernumerary centrosomes observed in cells expressing MCV sT or a mutant unable to interact with PP2A (198) was comparable to cells that expressed the HPV16 E7 oncoprotein, which has previously been reported to cause centrosome amplification (378). Mutation of the LSD of sT by alanine substitution at amino acids 91–95 (237) resulted in a loss of this phenotype, with the frequency of centrosome abnormalities matching cells transduced by an empty vector. Transiently-transfected BJ-hTERT and Rat-1 fibroblasts also showed the formation of supernumerary centrosomes upon WT sT expression (**Figure 33**).

The presence of supernumerary centrosomes during mitosis can result in mistakes in spindle assembly and chromosome missegregation, which in many cases leads to cell

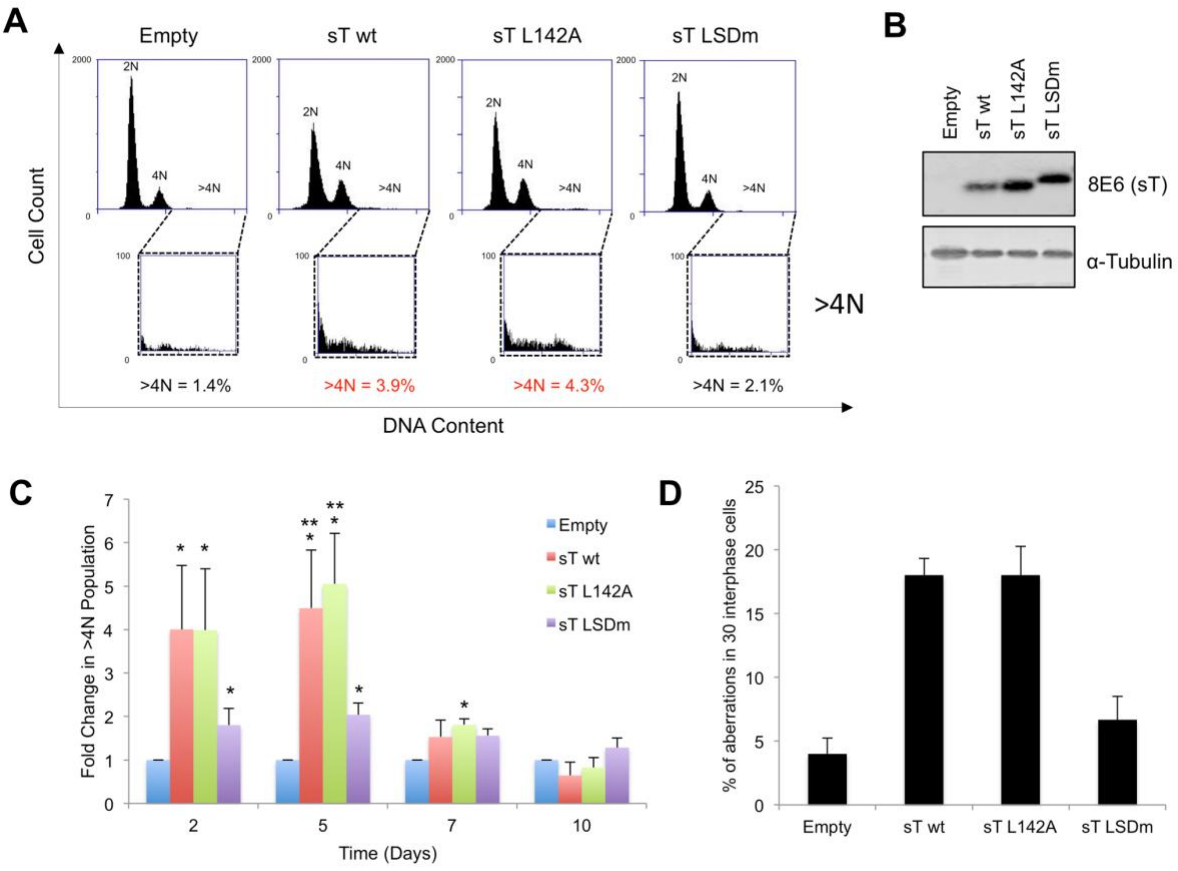


**Figure 34. sT increases aneuploidy and number of centrosomes in human diploid WI38 cells.**

A. Ploidy analysis. Cells transiently transduced with WT sT, L142A sT, LSDm sT or empty expression vectors were stained for DNA content by propidium iodide and analyzed by flow cytometry. Representative cell cycle profiles are shown for cells isolated at 2 days post transduction, with 2N, 4N and >4N populations annotated. The population of cells with >4N DNA content is magnified as respective inserts, and is most elevated for WT sT- and L142A sT-expressing cells. B. Expression of sT. Immunoblotting was simultaneously performed on a portion of the cells used for flow cytometry to validate sT expression using mouse monoclonal, anti-sT antibody (CM8E6). Results are representative of expression at 2 days post transduction from four independent experiments. C. Fold changes in the percentage of cells with >4N content were calculated for 2, 5, 7 and 10 days after transduction in each condition. A single asterisk denotes a significant increase over empty vector control cells ($P<0.05$), and a double asterisk denotes a significant increase over LSDm-expressing cells ($P<0.05$). Results represent the mean ±s.e. from three independent experiments. D. Transiently transduced cells were fixed at 2 days post transduction and stained for γ-tubulin, a centrosome marker. The number of centrosomes per cell was analyzed by microscopy and counted in 30 interphase cells to determine the frequency of supernumerary centrosomes. Results represent the mean ±s.e. from five independent experiments.

death by mitotic catastrophe (383–387). In the rare cases when an aberrant mitotic event progresses, the daughter cells that result often display an aneuploid karyotype, which has been proposed to have a causal role in tumorigenesis and tumor evolution (388, 389). To ascertain the ability of MCV sT to induce an increase in aneuploidy, early-passage WI38 human diploid fibroblast cells were selected to more easily monitor changes in DNA content. These cells were first transiently transduced with lentiviruses for wild-type MCV sT, L142A sT, LSDm sT or an empty vector. Changes in ploidy were monitored over the course of 10 days, using flow cytometric analysis to detect changes in DNA content. A four-fold increase in the aneuploid population, evidenced by >4N staining, was present in wild-type sT and L142A sT-expressing cells as early as 2 days post transduction

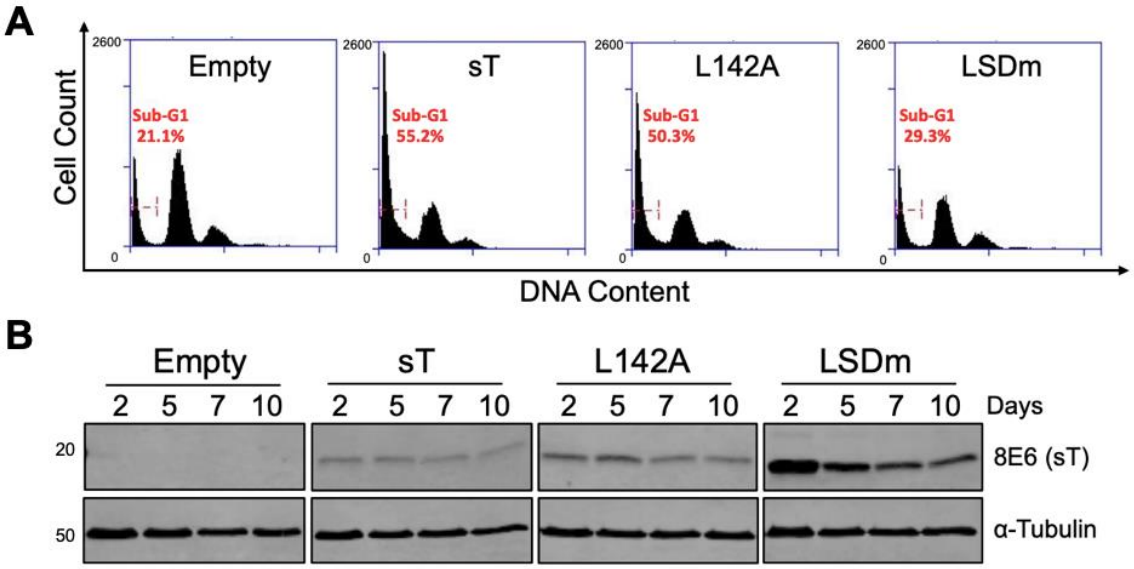


**Figure 35. MCV sT expression acutely increases cell death in WI38 fibroblasts.**

A. An increase in the population of Sub G1-phase (red) is shown by flow cytometry when either wild-type or L142A mutant sT is expressed in cells. sT expression induces loss of DNA due to DNA fragmentation and results in cell death. Sub G1-phase cell population is doubled to reach almost ~50% of the population in cells expressing either wild-type or L142A mutant sT, but not LSDm. B. sT proteins were detected from the same lysates used in Fig. 34C as controls. Expression of sT has retained at 10 days post-transduction.

(**Figure 34 A & B)**. This increase in genome DNA content by sT expression was maintained through to 5 days post transduction, but declined at later time points with an elevated proportion of dead cells (**Figure 35A**), likely triggered by acute induction of aneuploidy and genotoxic stress (383) and not the by loss of sT protein levels (**Figure 35B**). The degree of aneuploidy that is observed with LSDm sT is increased two-fold or less compared to the empty control (**Figure 34C**). In addition to increased aneuploidy, an increase in the frequency of supernumerary centrosomes was present in interphase WI38

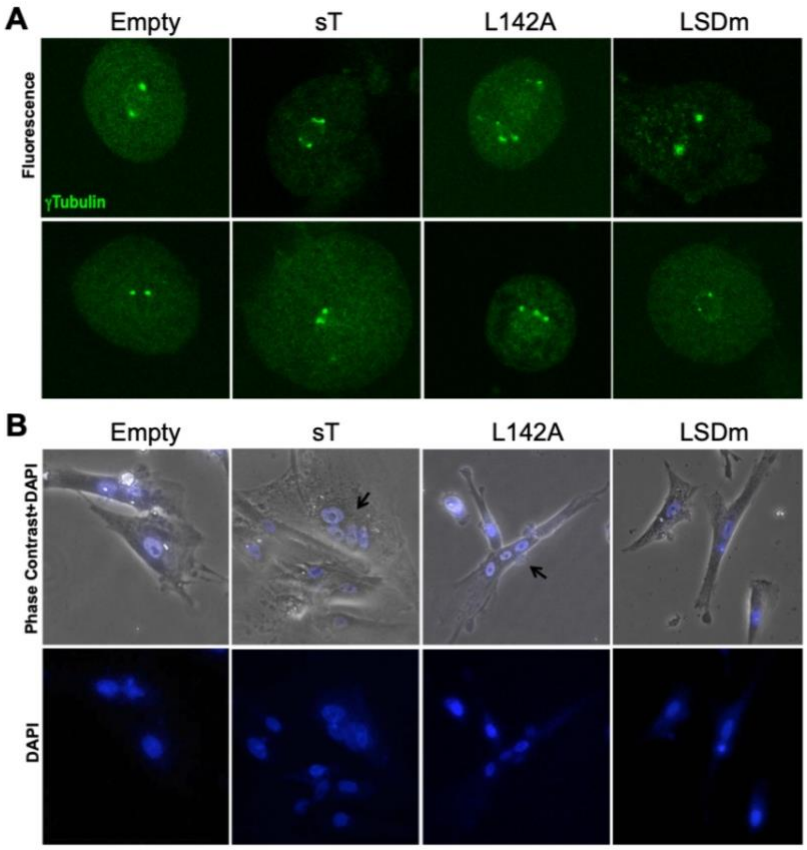


**Figure 36. Centrosome and nuclear aberrations in MCV sT-expressing WI38 fibroblasts.**

An increase in the frequency of supernumerary centrosomes (γ-Tubulin, green) is detected by fluorescence microscopy using an Olympus AX70 epifluorescence microscope (A) and phase contrast microscopy (Nikon Eclipse TS100 with DAPI filter) (B) in both wild-type and L142A mutant sT-expressing WI38 cells but not in LSDm. Formation of multinucleated cells were observed at 2 days post-transduction.

cells (**Figure 34D; Figure 36A**), and the formation of multinucleated cells (**Figure 36B**) was observed at 2 days post transduction by both WT and L142A sTs but not by LSDm sT expression.

To better characterize the type of genetic damage occurring in cells from the aneuploidy analysis, karyotype (**Figure 37)** and metaphase chromosome spread analysis were also performed on WI38 cells. Cells were first transduced with lentiviral vectors for WT MCV sT, LSDm sT or an empty vector. At 2 days post transduction, cells were arrested in metaphase with colcemid and collected for cytogenetic analysis. Representative karyotypes were collected for each condition, and cells expressing WT MCV sT showed an elevated level of chromosomal breakage, aneuploidy and even loss of an X chromosome (**Figure 37**). Out of the 50 metaphase spreads that were analyzed for each condition, WT sT-expressing cells showed an increase in total number of chromosome breakages and gaps, a greater number of breakages within a single cell and an overall higher average number of breakages per cell (**Table 2)** that did not reach statistical significance compared to empty control. The number of breakage and gaps in LSDm sT-expressing cells was not elevated above empty control levels. In looking at the specific loci of gaps and breaks, WT sT-expressing cells had a higher frequency of breaks at telomeres and known fragile sites (390) (**Tables 2-5**), but this increase was not statistically significant. Complex rearrangements, such as translocation events, were entirely absent in the empty control cells, but were observed in three instances in cells that expressed WT sT (**Table 2**).

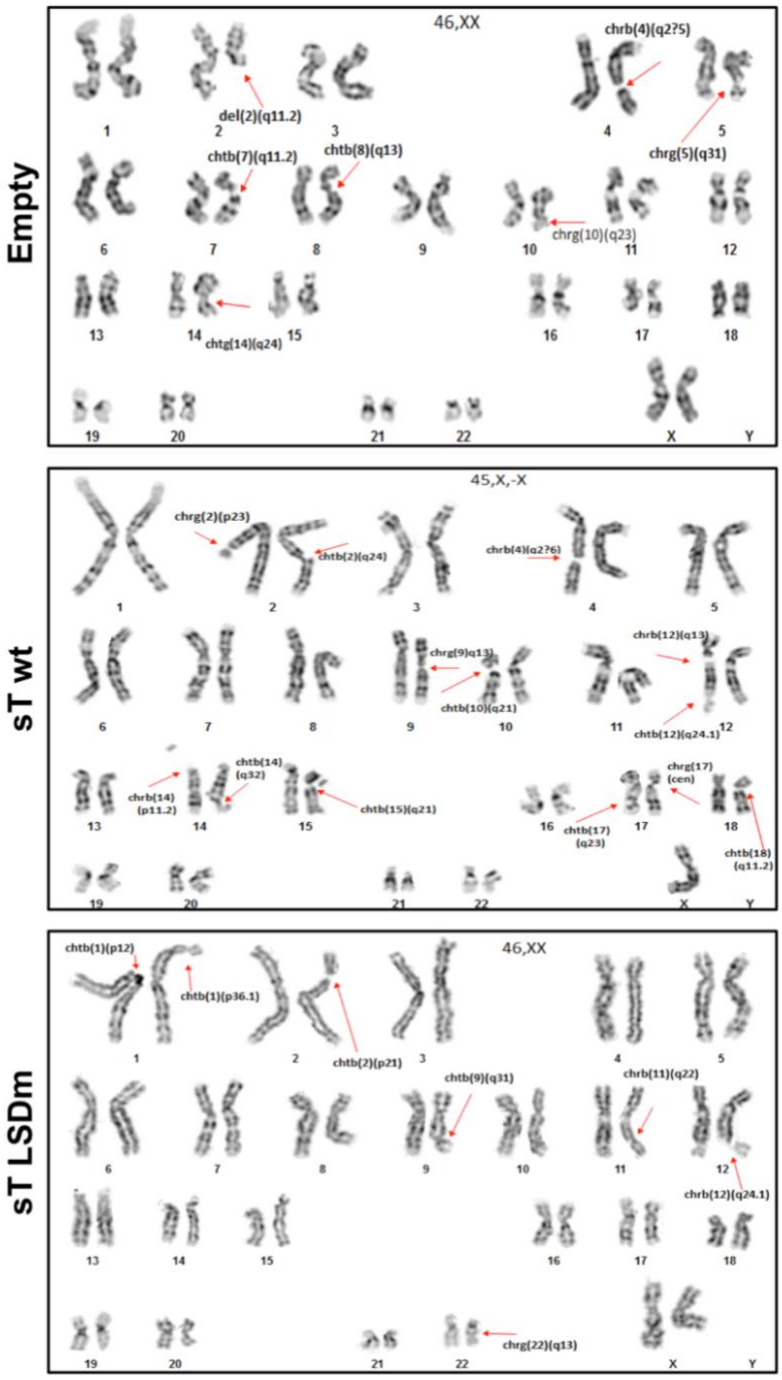


**Figure 37. sT expression results in increased chromosomal instability in WI38 cells.**

Karyotyping and G-banding analysis were performed on cells at 2 days post transduction with indicated lentivirus constructs. Representative karyotypes are shown for each condition, and chromosome breaks are indicated by red arrows. The greatest amount of breakage was seen in cells that express WT MCV sT, which is also missing an X chromosome.

**Table 2. Karyotype analysis in WI38 cells**

| | Empty Vector | sT wt | sT LSDm |
|---|---|---|---|
| **No. of metaphase cells analyzed** | 50 | 50 | 50 |
| Total number of gaps and breaks | 146 | 148* | 144* |
| Range of breaks per cell | 0-9 | 0-13 | 0-8 |
| Average no. of breaks per abnormal cell | 3.39 | 3.61 | 3.34 |
| Unique gap and breakage loci | 37 | 43** | 45** |
| Telomeric regions affected | 6 | 9** | 5** |
| Total number of gaps and breaks at fragile sites (390) | 28 | 33** | 28** |
| 46, XX normal | 7 | 6 | 6 |
| 46, XX with breakage | 43 | 41 | 43 |
| 46, XX with other structural rearrangements | 0 | 3<br>der(3), del(6)<br>der(X;1)<br>der(X;10) | 1<br>ring(X) |

*Not statistically increased over empty vector control levels when compared against number of cells analyzed by $\chi^2$-test ($p>0.05$).
**Not statistically increased over empty vector control levels when compared against the total number of gaps and breaks present in each group by $\chi^2$-test or Fisher's exact test ($p>0.05$).

**Table 3. Table of all breaks listed by chromosome for WI38 cells with an empty vector**

| Chromosome | | | | | | | | | | | | | | | # breaks |
|---|---|---|---|---|---|---|---|---|---|---|---|---|---|---|---|
| 1 | 1q12 | 1p34 | 1q25 | 1p32 | 1q32 | 1p13 | 1p34 | 1p32 | 1q21 | 1p22 | 1q42 | 1p22 | | | 12 |
| 2 | 2p13 | 2q11.2 | 2q32 | 2p13 | 2q21 | 2p15 | 2q11.2 | 2p15 | 2p23 | 2p21 | 2q31 | 2p21 | 2p13 | 2q23 | 14 |
| 3 | 3p10 | 3q21 | 3p25 | 3q26 | 3p26 | 3q29** | 3p22 | 3q26 | 3p25 | 3p23 | 3p25 | 3q21 | 3q25 | 3p13 | 14 |
| 4 | 4q25 | 4q27 | 4q27 | 4q27 | 4q27 | 4q33 | 4q25 | 4p15 | 4p12 | 4q21 | 4p16** | 4q12 | 4q28 | | 13 |
| 5 | 5q31 | 5q23 | 5q11.2 | 5q15 | 5q13 | 5p13 | 5q22 | 5q33 | 5p13 | 5q14 | 5q13 | 5p14 | 5q33 | | 13 |
| 6 | 6p21 | 6q22 | 6p21 | 6q23 | 6p21.3 | 6q21 | 6p21.1 | 6p22 | 6q21 | 6q25 | 6q21 | | | | 11 |
| 7 | 7q21 | 7q11-12 | 7p13 | 7q34 | 7q22 | 7q31 | 7p21 | | | | | | | | 7 |
| 8 | 8q13 | 8p11.2 | 8q21 | 8p23 | 8q22 | 8q24.1 | 8q22 | 8q22 | 8q23 | 8q13 | | | | | 10 |
| 9 | 9q22 | 9q22 | 9q22 (x2) | 9q12 | 9q22 | 9q12 | | | | | | | | | 7 |
| 10 | 10q23 | 10q23 | 10q24 | 10p15** | 10q11.2 | 10q24 | 10q24 | 10q11.2 | | | | | | | 8 |
| 11 | 11p15** | 11q21 | 11q13 | 11q24 | | | | | | | | | | | 4 |
| 12 | 12q15 | 12p13** | 12q15 | 12q22 | 12p11.2 | | | | | | | | | | 5 |
| 13 | 13q22.2 | 13q14 | 13q22 | 13q21 | 13q32 | 13q14 | 13q22 | | | | | | | | 7 |
| 14 | 14q13 | | | | | | | | | | | | | | 1 |
| 15 | 15q21 | 15q21 | 15q11.2 | | | | | | | | | | | | 3 |
| 16 | | | | | | | | | | | | | | | 0 |
| 17 | 17q23 | 17q21 | | | | | | | | | | | | | 2 |
| 18 | 18p11.3 | 18q21 | 18q11.2 | | | | | | | | | | | | 3 |
| 19 | | | | | | | | | | | | | | | 0 |
| 20 | | | | | | | | | | | | | | | 0 |
| 21 | 21q21 | | | | | | | | | | | | | | 1 |
| 22 | 22q11.2 | 22q11.2 | 22q11.2 | | | | | | | | | | | | 3 |
| X | Xq12 | Xq28** | Xp22.1 | Xp22.1 | Xq24 | Xq26 | Xq26 | Xq26 | | | | | | | 8 |
| | | | | | | | | | | | | | | total | 146 |

| | |
|---|---|
| **Other structural rearrangements:** | None |
| ** = telomeric regions | 6 |
| Fragile Sites induced by Aphidicolin | 10 |
| Fragile Sites induced by Oncoproteins (Cyclin E/Ras) | 12 |
| Common to both | 6 |
| **Total** | **28** |

**Table 4. Table of all breakpoints listed by chromosome for WI38 cells with MCV sT wt expression**

| Chromosome | | | | | | | | | | | | | | | | | | | | # Breaks | OTHER |
|---|---|---|---|---|---|---|---|---|---|---|---|---|---|---|---|---|---|---|---|---|---|
| 1 | 1q44** | 1q12 | 1p22 | 1q44** | 1p34 | 1q21 | 1q12 | 1p31 | 1p34 | | | | | | | | | | | 9 | der(1pter) |
| 2 | 2q31 | 2p23 | 2q24 | 2q11.2 | 2q11.2 | 2q32 | 2q11.1 | 2p23 | 2p23 | 2q33 | 2q37** | 2p11.2 | 2p23 | 2q33 | 2q33 | 2q22 | 2q21 | 2q37** | | 18 | |
| 3 | 3q25 | 3p25 | 3q25 | 3q27 | 3q26 | 3q27 | 3q21 | 3p13 | 3q13.2 | | | | | | | | | | | 9 | der(3)(q29) |
| 4 | 4q26 | 4p15 | 4p14 | 4q21 | 4q28 | 4q13 | 4q21 | 4q27 | | | | | | | | | | | | 8 | |
| 5 | 5q21-22 | 5q31 | 5p15.1 | 5q23 | 5q35** | 5q31.1 | 5p11.2 | 5p11.2 | 5q31 | 5q35** | 5p12 | | | | | | | | | 11 | |
| 6 | 6q13 | 6q25 | 6q25 | 6q13 | 6q21 | 6q24 | 6p21.3 | 6q15 | 6q21 | | | | | | | | | | | 9 | del(6)(q21) |
| 7 | 7q11.2 | 7q31 | 7p15 | 7q32 (x2) | 7p15 | 7q22 | 7p15 | 7q32 | | | | | | | | | | | | 9 | |
| 8 | 8q13 | 8p21 | 8q22 | 8p21 | 8q13 | 8q21.1 | 8q24 | 8q13 | 8q22 | 8p11 | 8p21 | 8q13 | 8p21 | | | | | | | 13 | |
| 9 | 9q13 | 9q13 | 9q22 | 9p10 | 9q11 | 9p21 | 9q13 | 9q32 | | | | | | | | | | | | 8 | |
| 10 | 10q21 | 10p13 | 10q21 | 10q24 | | | | | | | | | | | | | | | | 4 | der(10pter) |
| 11 | 11q21 | 11p15** | 11q13 | 11q13 | 11q23 | 11q12 | 11p13 | 11q14 | | | | | | | | | | | | 8 | |
| 12 | 12q13 | 12q24.1 | 12q24.1 | 12q24.1 | 12q22 | 12q21 | | | | | | | | | | | | | | 6 | |
| 13 | 13q12 | 13q13 | 13q31 | 13q14 | | | | | | | | | | | | | | | | 4 | |
| 14 | 14p11.2 | 14q32** | 14q24 | 14q21 | 14q32** | 14q21 | 14q22 | 14q22 | | | | | | | | | | | | 8 | |
| 15 | 15q21 | 15q22 | 15p11.2 | 15q15 | 15q22 | 15p11.2 | | | | | | | | | | | | | | 6 | |
| 16 | 16q12-13 | 16p13.1 | 16q11.2 | | | | | | | | | | | | | | | | | 3 | |
| 17 | 17cen | 17q23 | | | | | | | | | | | | | | | | | | 2 | |
| 18 | 18q11.2 | 18q12 | | | | | | | | | | | | | | | | | | 2 | |
| 19 | | | | | | | | | | | | | | | | | | | | 2 | |
| 20 | 20q11.2 | 20q11.2 | 20q13.1 | | | | | | | | | | | | | | | | | 0 | |
| 21 | | | | | | | | | | | | | | | | | | | | 2 | |
| 22 | | | | | | | | | | | | | | | | | | | | 0 | |
| X | Xq21 | Xq24 | Xq22 | Xq21 | Xq26 | Xp11.4 | Xp21 | | | | | | | | | | | | | 7 | der(Xpter), der(Xpter) |
| | | | | | | | | | | | | | | | | | | | Total | 148 | |

| | |
|---|---|
| **Other structural rearrangements:** | |
| t(3;6)(q29;q21) | |
| der(X;1)(p22.3;p36.3) | |
| der(X;10)(p22.3;p15.3) | |
| ** = telomeric regions | 9 |
| Fragile Sites induced by Aphidicolin | 10 |
| Fragile Sites induced by Oncoproteins (Cyclin E/Ras) | 11 |
| Common to both | 12 |
| **Total** | **33** |

**Table 5. Table of all breaks listed by chromosome for WI38 cells with MCV sT LSDm expression**

| Chromosome | | | | | | | | | | | | | | | | | | | | # breaks | | OTHER | |
|---|---|---|---|---|---|---|---|---|---|---|---|---|---|---|---|---|---|---|---|---|---|---|---|
| 1 | 1p34 | 1q31 | 1q41 | 1p12 | 1p36.1 | 1p13 | 1q25 | 1p12 | 1p32 | 1q42 | 1p22 | 1q42 | 1p32 | 1p34 | 1p32 | 1q25 | 1q32 | 1p34 | | 18 | | | |
| 2 | 2p21 | 2p23 | 2p23 | 2p12 | 2q23 | 2p15 | 2p11.2 | | | | | | | | | | | | | 7 | | | |
| 3 | 3q23 | 3q13.2 | 3p11 | 3q21 | 3p13 | 3p21 | 3q25 | | | | | | | | | | | | | 7 | | | |
| 4 | 4q31 | 4q31 | 4q12 | 4q25 | 4q33 | 4q31 | 4p14 | 4q23 | 4p15 | 4q21 | 4q21 | 4p14 | 4q11 | | | | | | | 13 | | | |
| 5 | 5q31 | 5q31 | 5q33 | 5q22 | 5q33 | 5p14 | | | | | | | | | | | | | | 6 | | | |
| 6 | 6q13 | 6q15 | 6q23 | 6q21 | 6q21 | 6q24 | 6q25 | 6q13 | 6q11.2 | | | | | | | | | | | 9 | | | |
| 7 | 7p13 | 7q22 | 7q11.2 | 7p11 | 7q36 | 7p21 | 7p11.2 | | | | | | | | | | | | | 8 | | | |
| 8 | 8p22 | 8q22 | 8p11 | 8q24.1 | 8q24.1 | 8q21 | | | | | | | | | | | | | | 6 | | | |
| 9 | 9q34** | 9q31 | 9p24** | 9q12 | | | | | | | | | | | | | | | | 1 | | | |
| 10 | 10p13 | 10q24 | 10q21 | 10p11.2 | 10q24 | 10q11.2 | 10p15** | 10p13 | | | | | | | | | | | | 8 | | | |
| 11 | 11q22 | 11q23 | 11p11.2 | 11q14 | 11q21 | 11p11.2 | | | | | | | | | | | | | | 6 | | | |
| 12 | 12q24.1 | 12q24.1 | 12q15 | 12q24.1 | | | | | | | | | | | | | | | | 4 | | | |
| 13 | 13q32 | 13q12 | 13q34 | 13p11 | 13q12 | 13q13 | | | | | | | | | | | | | | 6 | | | |
| 14 | 14q32** | 14q24 | 14q24 | 14q11.2 | 14q24 | 14q24 | 14q24 | 14q22 | | | | | | | | | | | | 8 | | | |
| 15 | 15q26.1 | 15q11.2 | 15q15 | 15q21 | 15q15 | 15q13 | | | | | | | | | | | | | | 6 | | | |
| 16 | 16q12-13 | 16p13 | 16q24 | 16q12.1 | | | | | | | | | | | | | | | | 4 | | | |
| 17 | 17p11.2 | 17q23 | 17q24 | | | | | | | | | | | | | | | | | 3 | | | |
| 18 | 18q21 | 18q21 | 18p11.2 | 18q21 | | | | | | | | | | | | | | | | 4 | | | |
| 19 | 19q13.1 | 19q13.1 | 19q13.1 | 19q12 | 19q13.3 | | | | | | | | | | | | | | | 5 | | | |
| 20 | | | | | | | | | | | | | | | | | | | | 0 | | | |
| 21 | 21q11.2 | | | | | | | | | | | | | | | | | | | 1 | | | |
| 22 | 22p11.2 | 22q13** | 22q12 | | | | | | | | | | | | | | | | | 3 | | | |
| X | Xq24 | Xp11 | Xp21 | Xp21 | Xq13 | Xq21 | Xp22.1 | Xq11 | Xq22 | Xq26 | Xp11.2 | | | | | | | | | 11 | | r(X) | |
| | | | | | | | | | | | | | | | | | | | | | | | |
| | | | | | | | | | | | | | | | | | | | total | 144 | | | |
| | | | | | | | | | | | | | | | | | | | | | | **Other structural** | |
| | | | | | | | | | | | | | | | | | | | | | | **rearrangements:** | r(X) |
| | | | | | | | | | | | | | | | | | | | | | | ** = telomeric regions | 5 |
| | | | | | | | | | | | | | | | | | | | | | | Fragile Sites induced by Aphidicolin | 10 |
| | | | | | | | | | | | | | | | | | | | | | | Fragile Sites induced by Oncoproteins (Cyclin E/Ras) | 10 |
| | | | | | | | | | | | | | | | | | | | | | | Common to both | 8 |
| | | | | | | | | | | | | | | | | | | | | | | **Total** | **28** |

### 5.3.2 sT increases aneuploidy in mice

Mis-segregation of chromosomes during mitosis can also lead to chromosomal breakage or loss, and these fractured or lagging chromosomes can become packaged in micronuclei, which appear adjacent to the main nucleus following cell division (391, 392). Therefore, the presence of micronuclei is a definitive and, more important, quantifiable marker of genomic instability. To determine whether sT expression leads to the formation of micronuclei, we made use of an inducible MCV sT transgenic mouse model for an in vivo micronucleus assay. This assay quantitatively detects the presence of micronuclei retained after enucleation occurs during erythrocyte maturation by flow cytometric analysis of peripheral blood cells (393). The primary cohort of mice used in this study allowed for ubiquitous, tamoxifen-inducible expression of MCV sT (**red; Figure 38A**). Because of the fact that in vivo tumor development has only been observed when sT is expressed and p53 is concurrently ablated (238), a second cohort of mice (blue) with this phenotype was also included to determine whether loss of p53 affected the frequency of micronuclei formation. Mice lacking cassettes for Cre recombinase in each of those backgrounds served as negative controls (black and gray). At 48 h post induction of sT expression, a significant increase in the presence of micronuclei in reticulocytes could be detected at nearly equal levels in mice both with and without p53 (**Figure 38B**). The frequency of micronuclei in reticulocytes was increased 3.3-fold upon sT expression alone (red) and 2.1-fold when combined with a p53 knockout (blue). In the same mice from which erythrocytes were collected, immunoblotting was performed on lysates extracted from a panel of tissues following necropsy to confirm that sT expression was induced

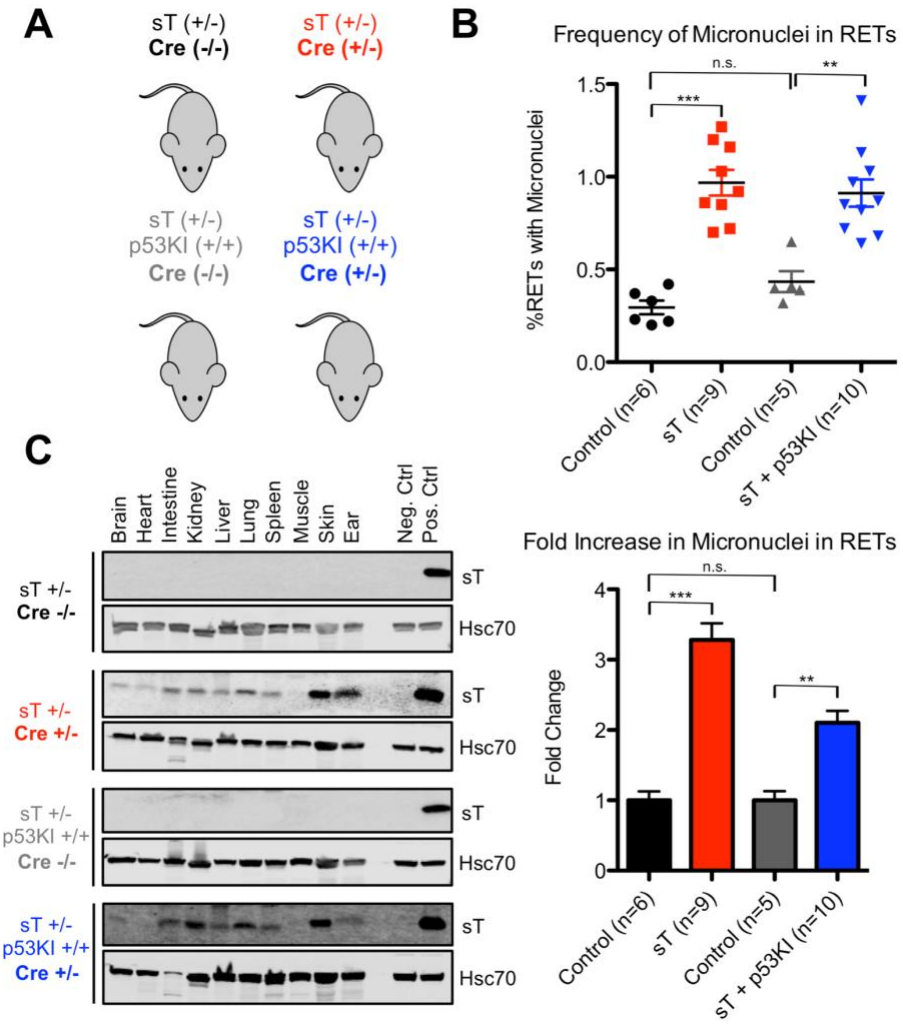


**Figure 38. sT expression in transgenic mouse model increases frequency of micronuclei.**

A. Schematic of the transgenic mice used in this study. All mice were subjected to intraperitoneal injection of tamoxifen (0.2 mg/g) with blood and tissue samples collected 48 h later at necropsy. B. In vivo micronucleus assay. Frequency of micronuclei in reticulocytes (RETs) was measured by staining DNA (MicroFlow kits, Litron Laboratories, Rochester, NY, USA) using flow cytometry. An increase in the frequency of micronucleated RETs was detected in mice after sT induction (~1%) compared to control mice (~0.3%). This corresponds to a threefold increase for sT expression alone (***P<0.0001) and twofold when p53 is concurrently knocked out (**P=0.0005). Numbers of mice within each group are indicated. C. Near-ubiquitous expression of sT was detected in panel of mouse organs from Cre+/− mice only but not from Cre−/− controls. Representative results are shown for each mouse background. Statistical significance between two groups was determined using two-tailed Student's t-tests in either GraphPad Prism or Excel.

ubiquitously in all experimental mice (Cre +/− ) and not in tissues from control mice (Cre−/−) (**Figure 38C**). Together, these data indicate that MCV sT is capable of inducing chromosomal damage in an in vivo setting.

### 5.3.3 sT targets E3 ligases to induce centrosome abnormality

MCV sT through its LSD has been shown to inhibit multiple ubiquitin ligases, including the SCFFbw7 complex (237) and the cdc20 subunit of the anaphase-promoting complex/cyclosome (273), which govern a number of substrates involved in centrosome duplication and cell division (394–397). To examine the effect of E3 ligases targeted by sT in centrosome amplification, HCT116 cells deleted for the FBW7 gene (372) were used. Supernumerary centrosomes form spontaneously in FBW7-null cells (−/−), but sT expression drives further centrosome amplification in this FBW7-null background, where LSDm sT cannot (**Figure 39A**). Expression of WT but not LSDm sT in the parental FBW7 WT (+/+) cells also results in the formation of supernumerary centrosomes. Together these results underscore the importance of Fbw7 in the regulation of centrosome duplication, although it is not the sole target of MCV sT in causing a genomically unstable phenotype. Additional immunostaining against Cep170 (red) in WT sT-expressing HCT116 cells allowed us to distinguish mature ‘mother’ centrioles from newly formed daughter centrioles, which were correspondingly labeled with green fluorescent protein-tagged centrin (green). In all cases, we observed a single ‘mother’ centriole with multiple daughter centrioles, indicative of centriole overduplication as opposed to accumulation (398) (**Figure 39B**). HPV16 E7-induced centriole overduplication requires aberrant PLK4 (374), a substrate of β-TrCP E3 ubiquitin ligase and so we examined potential interaction

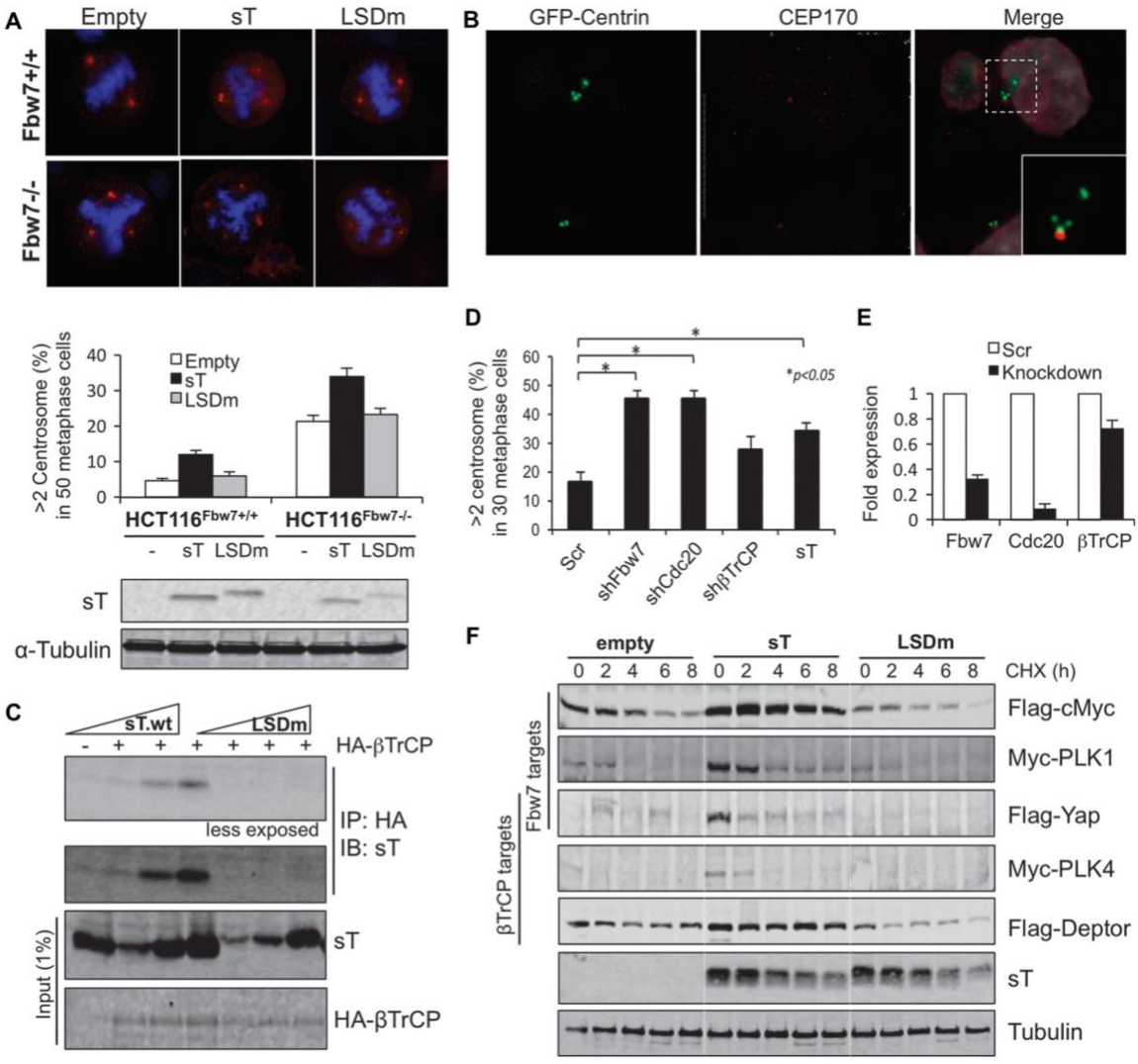


**Figure 39. sT targets E3 ligases to induce centrosome abnormality.**

A. Centrosome abnormality induced by sT expression or loss of Fbw7. HCT116 cells were stained for centrosomes (γ-tubulin, red) and DNA (4,6-diamidino-2-phenylindole (DAPI), blue). Supernumerary centrosomes form spontaneously in an Fbw7-null clone (FBW7−/−). Expression of WT sT, but not LSDm sT, results increased supernumerary centrosomes over empty vector control levels in both the parental (FBW7+/+) and knockout (FBW7−/−) cell lines. Images were captured at × 1000 magnification with oil. B. sT induces centrosome overduplication. HCT116 were transfected with GFP-centrin to visualize centrioles (green) along with MCV sT. CEP170 protein (red) was stained to specifically visualize 'mother' centrioles. The single mother with multiple daughter centrioles is induced by sT overexpression. Images were captured at × 1000 magnification. C. MCV sT interacts with β-TrCP in an LSD-dependent manner. HEK293 cells were transfected with increasing amounts of WT sT (1, 3 and 5 μg) or LSDm (2, 6 and 10 μg) along with HA-tagged β-TrCP (5 μg with sT WT and 10 μg with LSDm) to obtain comparable levels of protein expression. D. E3 ligase knockdown is sufficient for centrosome amplification. Depletion of Fbw7, or cdc20 by shRNA induces a significant increase in centrosome amplification, as does sT overexpression alone ($P<0.05$). Data show the mean ±s.e. from three experiments, where the number of centrosomes in 30 metaphase cells was counted. E. Efficiency of knockdown was

**Figure 39 (Continued)**
determined by quantitative PCR instead of immunoblotting due to the low expression of cellular E3 ligases and the limited availability of Fbw7 antibody(237). F. sT stabilizes Fbw7 and β-TrCP substrate targets relevant for genome stability. The half-lives of the target proteins of these E3 ligases are extended by expression of WT sT but not empty vector or LSDm sT. Specific targets of Fbw7, β-TrCP or both are indicated by side brackets (left). 293 cells were treated with cycloheximide (CHX; 100 μg/ml) and collected at the indicated time points. A representative α-tubulin loading control is shown. Representative results are shown from three independent experiments.

between MCV sT and β-TrCP by immunoprecipitation. When MCV sT is coexpressed with hemagglutinin (HA)-tagged β-TrCP in 293 cells, sT was readily detectable after coimmunoprecipitation with HA antibody, and mutation of the LSD specifically impaired its binding to β-TrCP (**Figure 39C**). Further, we tested the effect of sT-targeting E3 ligase knockdown in centrosome amplification. Either knockdown of Fbw7 or cdc20 resulted in a two-fold increase in abnormal centrosome numbers in 293 cells, with the frequency of centrosomal aberrations in these cells comparable to that achieved by expression of WT MCV sT alone (**Figure 39D**). Unexpectedly, knockdown of β-TrCP by short hairpin RNA (shRNA) lentiviral induction caused cell death, sustained the low efficiency of target gene silencing and resulted in a modest increase in supernumerary centrosomes (**Figure 39E**). The effect of sT expression on the stability of cellular Fbw7 and β-TrCP targets associated with genomic instability, including c-myc, PLK1, PLK4, YAP and Deptor, was examined in 293 cells. Consistent with our previous data (237) sT inhibited the turnover of proteins targeted by E3 ligase in the presence cycloheximide in an LSD-dependent manner (**Figure 39F; Figure 40**).

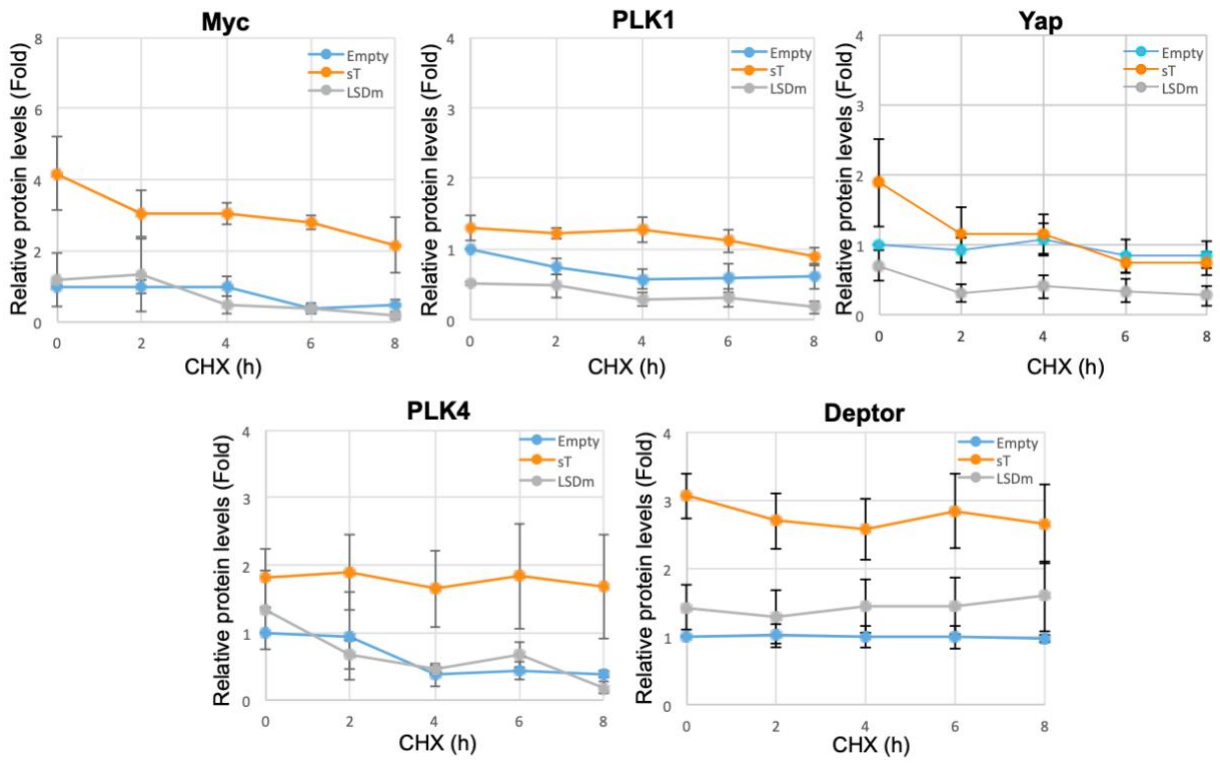


**Figure 40. sT stabilizes Fbw7 and β-TrCP substrate targets relevant for genome stability.**

The half-lives of the target proteins of Fbw7 and β-TrCP E3 ligases are extended by expression of wild-type sT but not empty vector or LSDm. 293 cells were treated with CHX (100 µg/mL) and harvested at the indicated time points. In the presence of sT expression, substrates turnover was inhibited and the steady-state levels of each substrate was increased. Protein expression level at time points was quantitated and normalized by control, α-tubulin, using Odyssey LI-COR IR imaging system. Graphs were plotted with relative expression value to non-CHX treated empty sample (Empty, time 0). Error bars represent SEM; n = 3.

## 5.4 Discussion

As a recognized hallmark of cancer, the genomic instability phenotype induced by MCV sT may be a contributing factor to its transformation activity in the context of MCC development. Genomic instability is frequently characterized by centrosomal aberrations,

namely the presence of supernumerary centrosomes. While a diverse set of proteins contribute to the tight regulation of centrosome duplication, it is known that members of the SCF complex are integral to this process (373). Specifically, inactivation of SCF/Fbw7 has previously been shown to be associated with increased centrosome amplification due to increased levels of c-myc, cyclin E (372), PLK2 (397) and possibly PLK4 (370). Our results demonstrate that sT expression results in the presence of supernumerary centrosomes in multiple cell lines in an LSD-dependent manner. It has been shown that the LSD is required for the binding of sT to Fbw7 (237), and our results further show that turnover of Fbw7 target proteins, including c-myc, PLK1 and YAP is attenuated in the presence of sT. The accumulation of these substrates as a result of Fbw7 inhibition could in part be responsible for centrosome overduplication in sT-expressing cells.

The overlap between multiple E3 ligase pathways that regulate mitotic controls makes it particularly difficult to implicate the targeting of any single E3 ligase by MCV sT as a cause for genome instability. For example, because both Fbw7 and β-TrCP are F-box proteins that function as part of the SCF complex (399), there is overlap in the proteins they target for degradation. Similarly, although β-TrCP has been identified as the E3 ligase responsible for PLK4 degradation, which allows for tight control of centriole duplication (400), it also has been proposed that Fbw7 may participate in PLK4 regulation (370). A combination of promiscuous targeting of such E3 ligases by sT along with overlap within those E3 ligase networks may contribute to the ability of sT to produce an unstable genomic phenotype. Although sT targeting of any single E3 ligase cannot be shown to be exclusively responsible for its disturbance of genome stability, what is clear from our

results, however, is that the observed phenotype requires the presence of the LSD of sT in multiple assays.

Not only is the presence of supernumerary centrosomes a marker for genomic instability in its own right, it has also been proposed as a precursor to the development of aneuploidy (401). Our results indicate that sT is capable of acutely inducing an aneuploid cell population. A subset of these populations is lost over time, which is consistent with cell death following acute genotoxic stress, in which cells with the most severe genetic abnormalities die (383). We also noted that WT or L142A sT expression both led to an increased proportion of cells in the G2/M population, which is in line with the ability of sT to promote mitogenesis as a result of targeting the anaphase-promoting complex/cyclosome (273). Our karyotyping analysis showed that WT sT-expressing cells contained more breakages at fragile sites that are uniquely induced by oncogene expression (such as cyclin E or Ras) as well as general replicative stress (390) (**Tables 3-5**). In addition, WT sT-expressing cells exhibited a higher number of breaks in telomeric regions, which is of interest because telomere dysfunction has been associated with tumorigenesis (402). Although the differences noted in our karyotype analysis are not statistically significant, they show a trend toward the types of genetic damage that likely result from sT expression over time and are consistent with the small population of cells with aberrant DNA content detected by flow cytometry (**Figure 34A**). These single-oncoprotein overexpression experiments may not completely recapitulate the precise biology of the virus in the context of MCC, in which the LT antigen is also expressed, but these data do provide evidence that sT expression alone is capable of inducing a genomically unstable phenotype.

# 6.0 Conclusions and perspectives

## 6.1 The C-terminus of MCV LT

Studies on SV40 over the past few decades have consistently shown that the LT antigen is a dynamic, multifunctional powerhouse in terms of the ways it can use its many domains and motifs to target cellular proteins. Some have even referred to it as the most amazing molecule in the universe. While the LT antigen of MCV differs from that of SV40 in terms of its intrinsic transforming capabilities, it remains an integral part of the MCV life cycle and plays an important role in MCC tumorigenesis. The study included in Chapter 3 began as an attempt to clone and isolate the various functional domains of MCV LT so that they could be better characterized. Novel functions in the C-terminus of LT were of particular interest, as this region is canonically truncated in MCC tumor samples (83). While elimination of replication following integration of the viral genome within the host genome is a clear reason for LT truncation, there is evidence to support other anti-tumorigenic functions may be localized to the C-terminus that further prompts their elimination for tumor outgrowth to occur (258, 264).

This study identified a region at the very C-terminal tail of MCV LT downstream of the helicase domain that is critical for maintaining the stability of the full-length LT protein. Mutagenesis in this region revealed two hotspot areas (786-795 aa and 811-817 aa) in which the native LT amino acid sequence was essential for producing a stable full-length LT protein. Thus far, no single amino acid has been implicated in being critical for stability, so it is most likely the loss of a larger peptide motif that compromises LT stability. While

these MCV LT expression studies were carried out in 293 cells, which express adenovirus E1A and E1B proteins, we do not believe these additional viral proteins play a role in the destabilization of LT. Expression of LT truncation constructs in U2OS cells, which do not express other viral oncoproteins, yielded similar results in terms of destabilization of LT protein levels (data not shown).

There is no crystallographic data for MCV LT that contains the regions in question, making any inference about how this region contributes to the overall structure of LT quite difficult. As this region is also divergent from other polyomavirus species, it becomes even harder to try and draw comparisons in terms of its potential structure and function. From what can be predicted, it appears that this region exists as an unstructured, flexible tail downstream of the helicase domain and does not serve to contact other regions of LT.

While the motifs within the C-terminus of MCV LT that are required for stability are divergent from those of other polyomavirus LTs, the concept that mutations to the LT amino acid sequence can compromise its stability is not new. Seminal works on SV40 describe multiple LT mutants that are expressed at lower levels, are more rapidly turned over, and have defects in facilitating viral replication compared to wild-type LT in the context of a lytic infection. Notably, these effects are temperature-dependent and can be mitigated by reducing the temperature at which infected cells are cultured to 34 °C (403–405). The experiments performed with MCV LT in Chapter 3 were all conducted at 37 °C, so it would be of interest to determine whether or not the destabilizing mutations identified here render LT temperature-sensitive. Culturing transfected cells at a lower temperature may serve as a means to stabilize these otherwise unstable LT mutants, and, if

successful, this method would provide an avenue for exploring the functional consequences of these mutations in terms of MCV biology.

Given the presence of a number of putative phosphorylation sites within this region, one plausible hypothesis to explain our findings is that this region may contain a phospho-inhibitor degron module (318). In this type of a model, phosphorylation at one or more of these sites may sterically block binding of an E3 ligase at some other site on LT. Mutation of those sequences would therefore eliminate this block, and LT would be readily targeted for degradation. This is further supported by the fact that LT is known to be phosphorylated at multiple sites throughout its amino acid sequence, and some of these have been validated as recognition sites for cellular E3 ligases (222, 237).

Future experiments designed at validating these putative phosphorylation sites and their contributions to LT stability may be of value. It would also be interesting to try to identify novel binding partners of LT within this region. Unstable LT mutants may fail to bind a stabilizing cofactor or instead display increased affinity for a host protein that targets LT for degradation. A differential mass spectrometric approach would be an excellent means to identify novel interactors that are specific to either wild-type or mutant LT antigens. As the 57kT antigen of MCV also shares the same C-terminal sequences but lacks the DNA binding and helicase domains present in LT, it may be informative to see if the same C-terminal mutations that compromise LT stability also affect 57kT stability. Overall, additional study of this region is required to obtain a more complete understanding of its biological relevance for MCV, but given what has been described here, it follows that this region may have a regulatory function in terms of governing LT protein levels within cells, especially during the context of a lytic infection.

## 6.2 Large T antigens and p53

Tumor suppressor p53 has long been regarded as the “guardian of the genome” due to the fact that it sits at the center of a number of important cellular signaling pathways that work to maintain tight regulation of all aspects of the cell cycle (144). In the case of cell cycle dysregulation or DNA damage, p53 has been implicated in determining the fate of such cells by initiating cell death or senescence pathways. The natural function of p53 is at odds with the polyomavirus life cycle, which requires the unscheduled entry into S-phase for efficient genome replication. Thus, T antigens of polyomaviruses have canonically inhibited p53 function in one way or another. The study in Chapter 4 sought to better understand how MCV LT may contribute to p53 inhibition by comparison to SV40 LT, whose p53-targeting capacities have been well studied. In doing so, it also helped to resolve ongoing conflicts in the literature regarding p53 targeting by both MCV and SV40 LT antigens.

For the case of MCV, it became clear that its LT antigen does not target p53 via a similar mechanism as SV40 LT. IP and PLA experiments both showed that MCV LT does not strongly interact with p53 or the co-adaptor p300. Our experiments further demonstrated that MCV LT is defective for inhibiting p53-specific DNA binding to target gene promoters and blocking their transcription. In reporter assays, we even saw an increase in p53-dependent transcription, which is consistent with reports of MCV LT inducing a DNA damage response in cells (264). Overall, these results demonstrate the lack of a role for MCV LT alone in antagonizing the p53 pathway. Given recent findings on the effects of MCV sT activation of Mdm2 and Mdm4 as an indirect means of targeting p53, it may be of interest to express MCV sT in some of these assays or co-express both

T antigens to see how p53 activation and downstream transcriptional activity may be impacted.

For the case of SV40, our results have provided greater insight into how its LT antigen is capable of directly binding to p53 and inhibiting its transactivating properties. Our results confirm the well-characterized binding between LT and p53 and the metabolic stabilization of inactive p53 in LT-expressing cells. ChIP and qPCR data support the model that SV40 LT directly inhibits p53 binding to target gene promoters as the mechanism for inhibiting p53-dependent transcription (151). Furthermore, the identification of a point mutant LT (P552L) that disrupts p53 binding is evidence that the precise residues responsible for facilitating contact with p53 may have a greater specificity than previously described (147). Not only is this mutant LT incapable of binding p53, it also compromises the ability of LT to stabilize p53 and block transcriptional activation. The interaction between SV40 LT and p53 may impede the ability of Mdm2 to bind p53 and target it for degradation, resulting in its stabilization (406). It follows that the P522L mutant LT that no longer binds p53 would be defective at blocking Mdm2 recognition of p53, leading to a return to steady-state degradation kinetics. It would be informative to profile Mdm2 binding to p53 and examine p53 poly-ubiquitination states in the presence of wild-type and mutant LTs in future experiments to elucidate this mechanism. Ongoing experiments seek to better characterize this mutant LT and to further define the functional consequences of this mutation in terms of modulating p53 activity.

The results presented in Chapter 4 describe a striking contrast between the mechanism of p53 targeting by SV40 and MCV LT antigens and provides further insight

into the biology of both of these polyomaviruses. Still, there remain a number of items that need to be addressed before moving forward to publish these findings. First, we are working on a more complete functional characterization of the P522L mutant of SV40 LT in terms of its ability to bind other known interactors of LT as well as its ability to multimerize into a double hexamer formation. A more complete understanding of the precise LT functionalities that are abrogated by this mutation will allow for a more informed interpretation of our findings. Secondly, we plan to incorporate the P522L mutant of SV40 LT into the PLA, ChIP, and qPCR experiments described for the wild-type LTs in this chapter to examine the functional consequences of this mutation on the p53 pathway. How this mutation may impact the transformation efficiency of LT is also a potential avenue for continued research.

Lastly, we also want to address the technical difficulties imposed by transient transfection used in many of these experiments. While 293 cells contain wild-type p53, they also express adenovirus E1A and E1B proteins, which metabolically stabilize and inactivate p53 function (407). This makes 293 cells less than ideal candidates for studying the effects of T antigens on p53 biology. Thus, many of the studies performed here were conducted with U2OS cells, due to the fact that they can readily be transfected, harbor wild-type p53, and do not express other viral oncoproteins. We are currently developing a tet-inducible expression system for the LTs described in this study. This system will be used to create stably-transduced cell lines in which LT expression can be uniformly initiated. This approach would allow us to standardize our approach in terms of LT expression and eliminate the potentially confounding factor that the transfection process itself may have on p53 activation. This inducible system would also allow us to extend

our experiments to non-transformed, primary cell lines, which may provide even greater insight into the functional relevance of our findings. We anticipate that the results of these additional experiments will serve to bring this study to completion.

### 6.3 MCV sT and genomic instability

Genomic instability has been enumerated as an emerging hallmark of cancer (408), and many cancers show the presence of key features of genomic instability: centrosome amplification, multipolar mitotic events, and aneuploidy. Multiple oncoproteins from tumor viruses have been implicated in inducing hallmarks of genomic instability by targeting cellular proteins that regulate cell division, which may contribute to their tumorigenic potential. Chapter 5 described how the sT antigen of MCV is capable of inducing a genomically unstable phenotype through its promiscuous E3 ligase targeting function.

Previous studies from our laboratory and others have demonstrated the tumorigenic potential of the sT antigen of MCV, which is underscored by the fact that continued proliferation of MCC cell lines requires sT expression (236). One of the unique features of MCV sT in comparison to other polyomavirus sT antigens is the presence of a flexible linker sequence termed the LT-stabilization domain or LSD. This domain is responsible for interacting with and inhibiting multiple E3 ligases within cells, including Fbw7, β-TrCP, and cdc20 (237). In this study, we showed how dysregulation of these E3 ligase networks by MCV sT can lead to the induction of a multiple hallmarks of genomic instability.

Expression of sT in rodent and human fibroblasts shows evidence for centrosome amplification, aberrant mitotic events, and the development of aneuploidy in an LSD-dependent manner. Use of a sT-inducible mouse model revealed that sT is capable of increasing the frequency of micronuclei in reticulocytes. While the results of our karyotype analysis did not reach statistical significance, we did see an increasing trend in the number of chromosomal breakages and rearrangements in cells that expressed wild-type sT compared to an LSD mutant. By directly knocking down E3 ligases known to be targeted by sT, the same aberrant mitotic events seen in the presence of sT began to emerge. Lastly, sT expression resulted in the stabilization of several targets of these E3 ligases that are known to be important in regulating cell division. Taken together, these data provide evidence for the induction of genomic instability as an oncogenic mechanism of sT that may influence MCC tumorigenesis.

Though this study has effectively been completed, there are additional experiments that could provide a deeper insight into the mechanism presented in this chapter. One experiment that could most convincingly corroborate our findings would be to perform live cell microscopy on sT-expressing cells to monitor the induction of aberrant mitotic events in real time. Additionally, now that PLA has been adopted by our laboratory, it may serve as an excellent tool for examining interactions between sT and various E3 ligases. This technique would also add an additional layer of information about these interactions by showing precisely where in cells these interactions are taking place. Lastly, as MCV LT has also been implicated in promoting a DNA damage response in cells (264), it may be of interest to co-express LT and sT to see if any of the findings here are in any way amplified further.

There is one final point of contention raised by the data presented in this study, which is the fact that these results conflict with data that shows a low rate of somatic mutations in MCV-positive MCC samples (243, 244). The fact of the matter is that no one single oncogenic mechanism described for MCV is responsible for causing MCC. It is likely a multifactorial combination of multiple mechanisms employed by the T antigens that contributes to tumorigenesis. It is important to note that the results presented in this chapter were generated by overexpression of sT as a means of amplifying the phenotype to a level that could be experimentally observed. In all likelihood, the frequency of such events is probably quite low, but our results suggest that dysregulation of E3 ligase networks by sT may be one contributing factor that sets the stage for MCC tumorigenesis.

### 6.4 Semper prorsum

It has now been just over a decade since the identification of MCV, and the staggering amount of work during this time has vastly enhanced our knowledge of the newest member on the list of human tumor viruses. For as much as we have learned, though, there remain scores of questions about MCV biology that require answers. Similar to the way in which MCV LT initiates bidirectional replication of the viral genome, research on MCV has moved in two directions since its discovery. Many groups have worked to identify initiating events in MCC tumorigenesis by studying the oncogenic mechanisms of MCV T antigens. Others have instead begun by studying the biology of established MCC tumors and tracing backwards to infer about the origins of this rare cancer and the role MCV plays in its development. As time has progressed, these two directions of research

have started to meet in the middle and inform each other more and more to give a clearer picture of MCV biology.

Two of the biggest roadblocks for the MCV field moving forward are the lack of an infectious model system and lack of information about the natural host cells for MCV. To get around this, many of the foundational studies regarding MCV T antigen biology have relied on the use of expression plasmids, derived either from genomic MCV sequences or cDNA. In some ways, this approach has been an excellent tool for being able to dissect the particular functionalities of each T antigen alone. In fact, several of these foundational characterization studies of tumorigenic mechanisms of MCV T antigens were performed in our laboratory using codon-optimized expression constructs for either LT or sT antigens. The work contained in this dissertation reflects that methodology. While such results are informative, they do not completely recapitulate the natural biology of the virus, and there is likely a lot of additional information we are missing by taking this approach. This is underscored by the fact that the field has significant gaps in its understanding of the functions of the other MCV T antigens, namely 57kT and ALTO. Both in the context of a productive infection and in MCC tumors, T antigens are expressed together, and it is imperative to focus on how they may influence one another in terms of manipulating the host cell moving forward.

## Bibliography


1. Weinberg RA. 2014. Biology of the CancerGarland Science.

2. Plummer M, de Martel C, Vignat J, Ferlay J, Bray F, Franceschi S. 2016. Global burden of cancers attributable to infections in 2012: a synthetic analysis. Lancet Glob Heal.

3. De Flora S, La Maestra S. 2015. Epidemiology of cancers of infectious origin and prevention strategies. J Prev Med Hyg.

4. Rous P. 1911. A sarcoma of the fowl transmissible by an agent separable from the tumor cells. J Exp Med.

5. Rubin H. 2011. The early history of tumor virology: Rous, RIF, and RAV. Proc Natl Acad Sci U S A.

6. Javier RT, Butel JS. 2008. The history of tumor virology. Cancer Res.

7. Shope RE, Hurst EW. 1933. Infectious papillomatosis of rabbits. J Exp Med.

8. Rous P, Beard JW. 1935. The progression to carcinoma of virus-induced rabbit papillomas (shope). J Exp Med.

9. Bittner JJ. 1936. Some possible effects of nursing on the mammary gland tumor incidence in mice. Science (80- ).

10. Gross L. 1951. “Spontaneous” Leukemia Developing in G3H Mice Following Inoculation, In Infancy, with AK-Emkemic. Proc Soc Exp Biol Med.

11. Gross L. 1953. A filterable agent, recovered from Ak leukemic extracts, causing salivary gland carcinomas in C3H mice. Proc Soc Exp Biol Med 83:414–421.

12. Sweet BH, Hilleman MR. 1960. The vacuolating virus, S.V. 40. Proc Soc Exp Biol Med 105:420–427.

13. Epstein MA, Achong BG, Barr YM. 1964. VIRUS PARTICLES IN CULTURED LYMPHOBLASTS FROM BURKITT’S LYMPHOMA. Lancet.

14. Henle W, Diehl V, Kohn G, Hausen H Zur, Henle G. 1967. Herpes-type virus and chromosome marker in normal leukocytes after growth with irradiated burkitt cells. Science (80- ).

15. Griffin BE. 2000. Epstein-Barr virus (EBV) and human disease: Facts, opinions and problems. Mutat Res - Rev Mutat Res.

16. Moore PS, Chang Y. 2010. Why do viruses cause cancer? Highlights of the first century of human tumour virology. Nat Rev Cancer 10:878–889.

17. 1997. Proceedings of the IARC Working Group on the Evaluation of Carcinogenic Risks to Humans. Epstein-Barr Virus and Kaposi's Sarcoma Herpesvirus/Human Herpesvirus 8. Lyon, France, 17-24 June 1997.IARC monographs on the evaluation of carcinogenic risks to humans / World Health Organization, International Agency for Research on Cancer.

18. Moore PS, Chang Y. 2014. The conundrum of causality in tumor virology: the cases of KSHV and MCV. Semin Cancer Biol 26:4–12.

19. Blumberg BS, Alter HJ, Visnich S. 1965. A "New" Antigen in Leukemia Sera. JAMA J Am Med Assoc.

20. Prince AM. 1968. An antigen detected in the blood during the incubation period of serum hepatitis. Proc Natl Acad Sci U S A.

21. Blumberg BS, Larouze B, London WT, Werner B, Hesser JE, Millman I, Saimot G, Payet M. 1975. The relation of infection with the hepatitis B agent to primary hepatic carcinoma. Am J Pathol.

22. Beasley RP, Lin CC, Hwang LY, Chien CS. 1981. HEPATOCELLULAR CARCINOMA AND HEPATITIS B VIRUS. A Prospective Study of 22 707 Men in Taiwan. Lancet.

23. Choo QL, Kuo G, Weiner AJ, Overby LR, Bradley DW, Houghton M. 1989. Isolation of a cDNA clone derived from a blood-borne non-A, non-B viral hepatitis genome. Science (80- ).

24. Alter HJ, Purcell RH, Shih JW, Melpolder JC, Houghton M, Choo QL, Kuo G. 1989. Detection of Antibody to Hepatitis C Virus in Prospectively Followed Transfusion Recipients with Acute and Chronic Non-A, Non-B Hepatitis. N Engl J Med.

25. Colombo M, Choo QL, Del Ninno E, Dioguardi N, Kuo G, Donato MF, Tommasini MA, Houghton M. 1989. PREVALENCE OF ANTIBODIES TO HEPATITIS C VIRUS IN ITALIAN PATIENTS WITH HEPATOCELLULAR CARCINOMA. Lancet.

26. Goossens N, Hoshida Y. 2015. Hepatitis C virus-induced hepatocellular carcinoma. Clin Mol Hepatol.

27. Perz JF, Armstrong GL, Farrington LA, Hutin YJF, Bell BP. 2006. The contributions of hepatitis B virus and hepatitis C virus infections to cirrhosis and primary liver cancer worldwide. J Hepatol.

28. Olson C, Pamukcu AM, Brobst DF, Kowalczyk T, Satter EJ, Price JM. 1959. A Urinary Bladder Tumor Induced by a Bovine Cutaneous Papilloma Agent. Cancer Res.

29. zur Hausen H. 2009. Papillomaviruses in the causation of human cancers - a brief historical account. Virology.

30. Durst M, Gissmann L, Ikenberg H, Zur Hausen H. 1983. A papillomavirus DNA from a cervical carcinoma and its prevalence in cancer biopsy samples from different geographic regions. Proc Natl Acad Sci U S A.

31. Boshart M, Gissmann L, Ikenberg H, Kleinheinz A, Scheurlen W, zur Hausen H. 1984. A new type of papillomavirus DNA, its presence in genital cancer biopsies and in cell lines derived from cervical cancer. EMBO J.

32. Ghittoni R, Accardi R, Chiocca S, Tommasino M. 2015. Role of human papillomaviruses in carcinogenesis. Ecancermedicalscience.

33. Al Moustafa AE, Al-Awadhi R, Missaoui N, Adam I, Durusoy R, Ghabreau L, Akil N, Gadelkarim Ahmed H, Yasmeen A, Alsbeih G. 2014. Human papillomaviruses-related cancers Presence and prevention strategies in the Middle East and North African Regions. Hum Vaccines Immunother.

34. Zur Hausen H. 1999. Papillomaviruses in human cancers. Proc Assoc Am Physicians. Blackwell Publishing Inc.

35. Poiesz BJ, Ruscetti FW, Gazdar AF, Bunn PA, Minna JD, Gallo RC. 1980. Detection and isolation of type C retrovirus particles from fresh and cultured lymphocytes of a patient with cutaneous T-cell lymphoma. Proc Natl Acad Sci U S A.

36. Hinuma Y, Nagata K, Hanaoka M, Nakai M, Matsumoto T, Kinoshita KI, Shirakawa S, Miyoshi I. 1981. Adult T-cell leukemia: Antigen in an ATL cell line and detection of antibodies to the antigen in human sera. Proc Natl Acad Sci U S A.

37. Matsuoka M. 2005. Human T-cell leukemia virus type I (HTLV-I) infection and the onset of adult T-cell leukemia (ATL). Retrovirology.

38. Uchiyama T, Yodoi J, Sagawa K, Takatsuki K, Uchino H. 1977. Adult T-cell leukemia: Clinical and hematologic features of 16 cases. Blood.

39. Kaposi. 1872. Idiopathisches multiples Pigmentsarkom der Haut. Arch Dermatol Syph.

40. Ganem D. 2006. KSHV INFECTION AND THE PATHOGENESIS OF KAPOSI'S SARCOMA. Annu Rev Pathol Mech Dis.

41. Beral V, Peterman TA, Berkelman RL, Jaffe HW. 1990. Kaposi's sarcoma among persons with AIDS: a sexually transmitted infection? Lancet.

42. Chang Y, Cesarman E, Pessin MS, Lee F, Culpepper J, Knowles DM, Moore PS. 1994. Identification of herpesvirus-like DNA sequences in AIDS-associated Kaposi's sarcoma. Science (80- ).

43. Russo JJ, Bohenzky RA, Chien MC, Chen J, Yan M, Maddalena D, Parry JP, Peruzzi D, Edelman IS, Chang Y, Moore PS. 1996. Nucleotide sequence of the Kaposi sarcoma-associated herpesvirus (HHV8)Proceedings of the National Academy of Sciences of the United States of America.

44. Sarid R, Olsen SJ, Moore PS. 1999. Kaposi's sarcoma-associated herpesvirus: epidemiology, virology, and molecular biology. Adv Virus Res.

45. Moore PS, Chang Y. 1995. Detection of herpesvirus-like dna sequences in kaposi's sarcoma in patients with and those without hiv infection. N Engl J Med.

46. Cesarman E, Chang Y, Moore PS, Said JW, Knowles DM. 1995. Kaposi's sarcoma—associated herpesvirus-like DNA sequences in AIDS-related body-cavity—based lymphomas. N Engl J Med.

47. Soulier J, Grollet L, Oksenhendler E, Cacoub P, Cazals-Hatem D, Babinet P, D'Agay MF, Clauvel JP, Raphael M, Degos L, Sigaux F. 1995. Kaposi's sarcoma-associated herpesvirus-like DNA sequences in multicentric Castleman's disease. Blood.

48. Feng H, Shuda M, Chang Y, Moore PS. 2008. Clonal integration of a polyomavirus in human Merkel cell carcinoma. Science (80- ) 319:1096–1100.

49. Chang MH, You SL, Chen CJ, Liu CJ, Lee CM, Lin SM, Chu HC, Wu TC, Yang SS, Kuo HS, Chen DS. 2009. Decreased incidence of hepatocellular carcinoma in hepatitis B vaccinees: A 20-year follow-up study. J Natl Cancer Inst.

50. Herrero R, González P, Markowitz LE. 2015. Present status of human papillomavirus vaccine development and implementation. Lancet Oncol.

51. Stewart SE, Eddy BE, Borgese N. 1958. Neoplasms in mice inoculated with a tumor agent carried in tissue culture. J Natl Cancer Inst.

52. Eddy BE. 1962. Tumors Produced in Hamsters by Sv40. Fed Proc 21:930-.

53. Eddy BE, Borman GS, Grubbs GE, Young RD. 1962. Identification of the oncogenic substance in rhesus monkey kidney cell cultures as simian virus 40. Virology.

54. Girardi AJ, Sweet BH, Slotnick VB, Hilleman MR. 1962. Development of Tumors in Hamsters Inoculated in the Neonatal Period with Vacuolating Virus, SV40. Proc Soc Exp Biol Med.

55. Gardner SD, Field AM, Coleman D V, Hulme B. 1971. New human papovavirus (B.K.) isolated from urine after renal transplantation. Lancet 1:1253–1257.

56. Padgett BL, Walker DL, ZuRhein GM, Eckroade RJ, Dessel BH. 1971. Cultivation of papova-like virus from human brain with progressive multifocal leucoencephalopathy. Lancet 1:1257–1260.

57. De Paoli P, Carbone A. 2013. Carcinogenic viruses and solid cancers without sufficient evidence of causal association. Int J Cancer.

58. Abend JR, Jiang M, Imperiale MJ. 2009. BK virus and human cancer: Innocent until proven guilty. Semin Cancer Biol.

59. Kuypers DRJ. 2012. Management of polyomavirus-associated nephropathy in renal transplant recipients. Nat Rev Nephrol.

60. Ferenczy MW, Marshall LJ, Nelson CDS, Atwood WJ, Nath A, Khalili K, Majora EO. 2012. Molecular biology, epidemiology, and pathogenesis of progressive multifocal leukoencephalopathy, the JC virus-induced demyelinating disease of the human brain. Clin Microbiol Rev.

61. White MK, Khalili K. 2004. Polyomaviruses and human cancer: Molecular mechanisms underlying patterns of tumorigenesis. Virology.

62. Allander T, Andreasson K, Gupta S, Bjerkner A, Bogdanovic G, Persson MA, Dalianis T, Ramqvist T, Andersson B. 2007. Identification of a third human polyomavirus. J Virol 81:4130–4136.

63. Gaynor AM, Nissen MD, Whiley DM, Mackay IM, Lambert SB, Wu G, Brennan DC, Storch GA, Sloots TP, Wang D. 2007. Identification of a novel polyomavirus from patients with acute respiratory tract infections. PLoS Pathog 3:e64.

64. Nguyen NL, Le BM, Wang D. 2009. Serologic evidence of frequent human infection with WU and KI polyomaviruses. Emerg Infect Dis.

65. Norja P, Ubillos I, Templeton K, Simmonds P. 2007. No evidence for an association between infections with WU and KI polyomaviruses and respiratory disease. J Clin Virol.

66. Schowalter RM, Pastrana D V, Pumphrey KA, Moyer AL, Buck CB. 2010. Merkel cell polyomavirus and two previously unknown polyomaviruses are chronically shed from human skin. Cell Host Microbe 7:509–515.

67. van der Meijden E, Janssens RW, Lauber C, Bouwes Bavinck JN, Gorbalenya AE, Feltkamp MC. 2010. Discovery of a new human polyomavirus associated with trichodysplasia spinulosa in an immunocompromized patient. PLoS Pathog 6:e1001024.

68. Sauvage V, Foulongne V, Cheval J, Ar Gouilh M, Pariente K, Dereure O, Manuguerra JC, Richardson J, Lecuit M, Burguiere A, Caro V, Eloit M. 2011. Human polyomavirus related to African green monkey lymphotropic polyomavirus. Emerg Infect Dis 17:1364–1370.

69. Siebrasse EA, Reyes A, Lim ES, Zhao G, Mkakosya RS, Manary MJ, Gordon JI, Wang D. 2012. Identification of MW polyomavirus, a novel polyomavirus in human stool. J Virol 86:10321–10326.

70. Yu G, Greninger AL, Isa P, Phan TG, Martinez MA, de la Luz Sanchez M, Contreras JF, Santos-Preciado JI, Parsonnet J, Miller S, DeRisi JL, Delwart E, Arias CF, Chiu CY. 2012. Discovery of a novel polyomavirus in acute diarrheal samples from children. PLoS One 7:e49449.

71. Buck CB, Phan GQ, Raiji MT, Murphy PM, McDermott DH, McBride AA. 2012. Complete genome sequence of a tenth human polyomavirus. J Virol 86:10887.

72. Lim ES, Reyes A, Antonio M, Saha D, Ikumapayi UN, Adeyemi M, Stine OC, Skelton R, Brennan DC, Mkakosya RS, Manary MJ, Gordon JI, Wang D. 2013. Discovery of STL polyomavirus, a polyomavirus of ancestral recombinant origin that encodes a unique T antigen by alternative splicing. Virology 436:295–303.

73. Korup S, Rietscher J, Calvignac-Spencer S, Trusch F, Hofmann J, Moens U, Sauer I, Voigt S, Schmuck R, Ehlers B. 2013. Identification of a novel human polyomavirus in organs of the gastrointestinal tract. PLoS One 8:e58021.

74. Mishra N, Pereira M, Rhodes RH, An P, Pipas JM, Jain K, Kapoor A, Briese T, Faust PL, Lipkin WI. 2014. Identification of a Novel Polyomavirus in a Pancreatic Transplant Recipient With Retinal Blindness and Vasculitic Myopathy. J Infect Dis.

75. Gheit T, Dutta S, Oliver J, Robitaille A, Hampras S, Combes JD, McKay-Chopin S, Le Calvez-Kelm F, Fenske N, Cherpelis B, Giuliano AR, Franceschi S, McKay J, Rollison DE, Tommasino M. 2017. Isolation and characterization of a novel putative human polyomavirus. Virology.

76. Prado JCM, Monezi TA, Amorim AT, Lino V, Paladino A, Boccardo E. 2018. Human polyomaviruses and cancer: An overview. Clinics.

77. Johne R, Buck CB, Allander T, Atwood WJ, Garcea RL, Imperiale MJ, Major EO, Ramqvist T, Norkin LC. 2011. Taxonomical developments in the family Polyomaviridae. Arch Virol.

78. Calvignac-Spencer S, Feltkamp MCW, Daugherty MD, Moens U, Ramqvist T, Johne R, Ehlers B. 2016. A taxonomy update for the family Polyomaviridae. Arch Virol.

79. Buck CB, Van Doorslaer K, Peretti A, Geoghegan EM, Tisza MJ, An P, Katz JP, Pipas JM, McBride AA, Camus AC, McDermott AJ, Dill JA, Delwart E, Ng TFF, Farkas K, Austin C, Kraberger S, Davison W, Pastrana D V., Varsani A. 2016. The Ancient Evolutionary History of Polyomaviruses. PLoS Pathog.

80. Damania B, Pipas JM. 2009. DNA tumor virusesDNA Tumor Viruses.

81. Ajiro M, Zheng ZM. 2014. Oncogenes and RNA splicing of human tumor viruses. Emerg Microbes Infect.

82. Gjoerup O, Chang Y. 2010. Update on human polyomaviruses and cancer. Adv Cancer Res 106:1–51.

83. Shuda M, Feng H, Kwun HJ, Rosen ST, Gjoerup O, Moore PS, Chang Y. 2008. T antigen mutations are a human tumor-specific signature for Merkel cell polyomavirus. Proc Natl Acad Sci U S A 105:16272–16277.

84. Zerrahn J, Knippschild U, Winkler T, Deppert W. 1993. Independent expression of the transforming amino-terminal domain of SV40 large I antigen from an alternatively spliced third SV40 early mRNA. EMBO J.

85. van der Meijden E, Kazem S, Dargel CA, van Vuren N, Hensbergen PJ, Feltkamp MCW. 2015. Characterization of T Antigens, Including Middle T and Alternative T, Expressed by the Human Polyomavirus Associated with Trichodysplasia Spinulosa. J Virol.

86. Abend JR, Joseph AE, Das D, Campbell-Cecen DB, Imperiale MJ. 2009. A truncated T antigen expressed from an alternatively spliced BK virus early mRNA. J Gen Virol.

87. Shen PS, Enderlein D, Nelson CDS, Carter WS, Kawano M, Xing L, Swenson RD, Olson NH, Baker TS, Cheng RH, Atwood WJ, Johne R, Belnap DM. 2011. The structure of avian polyomavirus reveals variably sized capsids, non-conserved inter-capsomere interactions, and a possible location of the minor capsid protein VP4. Virology.

88. Daniels R, Sadowicz D, Hebert DN. 2007. A very late viral protein triggers the lytic release of SV40. PLoS Pathog.

89. Raghava S, Giorda KM, Romano FB, Heuck AP, Hebert DN. 2013. SV40 late protein VP4 forms toroidal pores to disrupt membranes for viral release. Biochemistry.

90. Cheng J, DeCaprio JA, Fluck MM, Schaffhausen BS. 2009. Cellular transformation by Simian Virus 40 and Murine Polyoma Virus T antigens. Semin Cancer Biol.

91. Carter JJ, Daugherty MD, Qi X, Bheda-Malge A, Wipf GC, Robinson K, Roman A, Malik HS, Galloway DA. 2013. Identification of an overprinting gene in Merkel cell polyomavirus provides evolutionary insight into the birth of viral genes. Proc Natl Acad Sci U S A 110:12744–12749.

92. Saribas AS, Coric P, Hamazaspyan A, Davis W, Axman R, White MK, Abou-Gharbia M, Childers W, Condra JH, Bouaziz S, Safak M. 2016. Emerging From the Unknown: Structural and Functional Features of Agnoprotein of Polyomaviruses. J Cell Physiol.

93. Gerits N, Moens U. 2012. Agnoprotein of mammalian polyomaviruses. Virology 432:316–326.

94. Sullivan CS, Grundhoff AT, Tevethia S, Pipas JM, Ganem D. 2005. SV40-encoded microRNAs regulate viral gene expression and reduce susceptibility to cytotoxic T cells. Nature 435:682–686.

95. Seo GJ, Fink LH, O'Hara B, Atwood WJ, Sullivan CS. 2008. Evolutionarily conserved function of a viral microRNA. J Virol 82:9823–9828.

96. Seo GJ, Chen CJ, Sullivan CS. 2009. Merkel cell polyomavirus encodes a microRNA with the ability to autoregulate viral gene expression. Virology 383:183–187.

97. Sullivan CS, Sung CK, Pack CD, Grundhoff A, Lukacher AE, Benjamin TL, Ganem D. 2009. Murine Polyomavirus encodes a microRNA that cleaves early RNA transcripts but is not essential for experimental infection. Virology.

98. Eash S, Manley K, Gasparovic M, Querbes W, Atwood WJ. 2006. The human polyomaviruses. Cell Mol Life Sci.

99. Neu U, Stehle T, Atwood WJ. 2009. The Polyomaviridae: Contributions of virus structure to our understanding of virus receptors and infectious entry. Virology.

100. Dugan AS, Eash S, Atwood WJ. 2006. Update on BK virus entry and intracellular trafficking. Transpl Infect Dis.

101. Eash S, Atwood WJ. 2005. Involvement of Cytoskeletal Components in BK Virus Infectious Entry. J Virol.

102. Norkin LC, Anderson HA, Wolfrom SA, Oppenheim A. 2002. Caveolar Endocytosis of Simian Virus 40 Is Followed by Brefeldin A-Sensitive Transport to the Endoplasmic Reticulum, Where the Virus Disassembles. J Virol.

103. Ahuja D, Sáenz-Robles MT, Pipas JM. 2005. SV40 large T antigen targets multiple cellular pathways to elicit cellular transformation. Oncogene.

104. Topalis D, Andrei G, Snoeck R. 2013. The large tumor antigen: A “ Swiss Army knife” protein possessing the functions required for the polyomavirus life cycle. Antiviral Res.

105. DeCaprio JA, Garcea RL. 2013. A cornucopia of human polyomaviruses. Nat Rev Microbiol 11:264–276.

106. Bullock PA. 1997. The initiation of simian virus 40 DNA replication in vitro. Crit Rev Biochem Mol Biol.

107. Nakanishi A, Nakamura A, Liddington R, Kasamatsu H. 2006. Identification of Amino Acid Residues within Simian Virus 40 Capsid Proteins Vp1, Vp2, and Vp3 That Are Required for Their Interaction and for Viral Infection. J Virol.

108. Clever J, Dean DA, Kasamatsu H. 1993. Identification of a DNA binding domain in simian virus 40 capsid proteins Vp2 and Vp3. J Biol Chem.

109. Clayson ET, Brando L V, Compans RW. 1989. Release of simian virus 40 virions from epithelial cells is polarized and occurs without cell lysis. J Virol.

110. White MK, Gordon J, Khalili K. 2013. The Rapidly Expanding Family of Human Polyomaviruses: Recent Developments in Understanding Their Life Cycle and Role in Human Pathology. PLoS Pathog.

111. Costa C. 2012. Polyomavirus-associated nephropathy. World J Transplant.

112. Purighalla R, Shapiro R, McCauley J, Randhawa P. 1995. BK virus infection in a kidney allograft diagnosed by needle biopsy. Am J Kidney Dis.

113. Dalianis T, Hirsch HH. 2013. Human polyomaviruses in disease and cancer. Virology.

114. Hirsch HH, Drachenberg CB, Steiger J, Ramos E. 2006. Polyomavirus-associated nephropathy in renal transplantation: Critical issues of screening and management. Adv Exp Med Biol.

115. Jiang M, Abend JR, Johnson SF, Imperiale MJ. 2009. The role of polyomaviruses in human disease. Virology.

116. Tan CS, Koralnik IJ. 2010. Progressive multifocal leukoencephalopathy and other disorders caused by JC virus: clinical features and pathogenesis. Lancet Neurol.

117. Saribaş AS, Özdemir A, Lam C, Safak M. 2010. JC virus-induced progressive multifocal leukoencephalopathy. Future Virol.

118. Major EO, Amemiya K, Tornatore CS, Houff SA, Berger JR. 1992. Pathogenesis and molecular biology of progressive multifocal leukoencephalopathy, the JC virus-induced demyelinating disease of the human brain. Clin Microbiol Rev.

119. Antinori A, Ammassari A, Giancola ML, Cingolani A, Grisetti S, Murri R, Alba L, Ciancio B, Soldani F, Larussa D, Ippolito G, De Luca A. 2001. Epidemiology and prognosis of AIDS-associated progressive multifocal leukoencephalopathy in the HAART era. J Neurovirol.

120. Chang Y, Moore PS. 2012. Merkel cell carcinoma: a virus-induced human cancer. Annu Rev Pathol 7:123–144.

121. Sastre-Garau X, Peter M, Avril MF, Laude H, Couturier J, Rozenberg F, Almeida A, Boitier F, Carlotti A, Couturaud B, Dupin N. 2009. Merkel cell carcinoma of the skin: pathological and molecular evidence for a causative role of MCV in oncogenesis. J Pathol 218:48–56.

122. DeCrescenzo AJ, Philips RC, Wilkerson MG. 2016. Trichodysplasia spinulosa: A rare complication of immunosuppression. JAAD Case Reports.

123. Kazem S, van der Meijden E, Kooijman S, Rosenberg AS, Hughey LC, Browning JC, Sadler G, Busam K, Pope E, Benoit T, Fleckman P, de Vries E, Eekhof JA, Feltkamp MCW. 2012. Trichodysplasia spinulosa is characterized by active polyomavirus infection. J Clin Virol.

124. Matthews MR, Wang RC, Reddick RL, Saldivar VA, Browning JC. 2011. Viral-associated trichodysplasia spinulosa: A case with electron microscopic and molecular detection of the trichodysplasia spinulosa-associated human polyomavirus. J Cutan Pathol.

125. van der Meijden E, Kazem S, Burgers MM, Janssens R, Bavinck JNB, de Melker H, Feltkamp MC. 2011. Seroprevalence of trichodysplasia spinulosa-associated polyomavirus. Emerg Infect Dis.

126. Kazem S, van der Meijden E, Feltkamp MCW. 2013. The trichodysplasia spinulosa-associated polyomavirus: Virological background and clinical implications. APMIS.

127. Ho J, Jedrych JJ, Feng H, Natalie AA, Grandinetti L, Mirvish E, Crespo MM, Yadav D, Fasanella KE, Proksell S, Kuan SF, Pastrana D V., Buck CB, Shuda Y, Moore PS, Chang Y. 2015. Human polyomavirus 7-associated pruritic rash and viremia in transplant recipients. J Infect Dis.

128. Toptan T, Yousem SA, Ho J, Matsushima Y, Stabile LP, Fernández-Figueras MT, Bhargava R, Ryo A, Moore PS, Chang Y. 2016. Survey for human polyomaviruses in cancer. JCI Insight.

129. Poulin DL, DeCaprio JA. 2006. Is there a role for SV40 in human cancer? J Clin Oncol.

130. Giacinti C, Giordano A. 2006. RB and cell cycle progression. Oncogene.

131. Goodrich DW, Wang NP, Qian YW, Lee EYHP, Lee WH. 1991. The retinoblastoma gene product regulates progression through the G1 phase of the cell cycle. Cell.

132. Buchkovich K, Duffy LA, Harlow E. 1989. The retinoblastoma protein is phosphorylated during specific phases of the cell cycle. Cell.

133. Whyte P, Buchkovich KJ, Horowitz JM, Friend SH, Raybuck M, Weinberg RA, Harlow E. 1988. Association between an oncogene and an anti-oncogene: the adenovirus E1A proteins bind to the retinoblastoma gene product. Nature.

134. DeCaprio JA, Ludlow JW, Figge J, Shew JY, Huang CM, Lee WH, Marsilio E, Paucha E, Livingston DM. 1988. SV40 large tumor antigen forms a specific complex with the product of the retinoblastoma susceptibility gene. Cell.

135. Ewen ME, Ludlow JW, Marsilio E, DeCaprio JA, Millikan RC, Cheng SH, Paucha E, Livingston DM. 1989. An N-Terminal transformation-governing sequence of SV40 large T antigen contributes to the binding of both p110Rb and a second cellular protein, p120. Cell.

136. Zalvide J, DeCaprio JA. 1995. Role of pRb-related proteins in simian virus 40 large-T-antigen-mediated transformation. Mol Cell Biol.

137. Chen S, Paucha E. 1990. Identification of a region of simian virus 40 large T antigen required for cell transformation. J Virol.

138. Srinivasan A, McClellan AJ, Vartikar J, Marks I, Cantalupo P, Li Y, Whyte P, Rundell K, Brodsky JL, Pipas JM. 1997. The amino-terminal transforming region of simian virus 40 large T and small t antigens functions as a J domain. Mol Cell Biol 17:4761–4773.

139. Manfredi JJ, Prives C. 1994. The transforming activity of simian virus 40 large tumor antigen. BBA - Rev Cancer.

140. Lane DP, Crawford L V. 1979. T antigen is bound to a host protein in SY40-transformed cells [19]. Nature.

141. Linzer DIH, Levine AJ. 1979. Characterization of a 54K Dalton cellular SV40 tumor antigen present in SV40-transformed cells and uninfected embryonal carcinoma cells. Cell.

142. Meek DW. 2015. Regulation of the p53 response and its relationship to cancer. Biochem J.

143. Kumari R, Sen N, Das S. 2014. Tumour suppressor p53: Understanding the molecular mechanisms inherent to cancer. Curr Sci.

144. Lane DP. 1992. p53, guardian of the genome. Nature.

145. Brooks CL, Gu W. 2011. P53 regulation by ubiquitin. FEBS Lett.

146. Xu Y. 2003. Regulation of p53 responses by post-translational modifications. Cell Death Differ.

147. Kierstead TD, Tevethia MJ. 1993. Association of p53 binding and immortalization of primary C57BL/6 mouse embryo fibroblasts by using simian virus 40 T-antigen mutants bearing internal overlapping deletion mutations. J Virol.

148. Lilyestrom W, Klein MG, Zhang R, Joachimiak A, Chen XS. 2006. Crystal structure of SV40 large T-antigen bound to p53: Interplay between a viral oncoprotein and a cellular tumor suppressor. Genes Dev.

149. Lin JY, Simmons DT. 1991. The ability of large T antigen to complex with p53 is necessary for the increased life span and partial transformation of human cells by simian virus 40. J Virol.

150. Zhu JY, Abate M, Rice PW, Cole CN. 1991. The ability of simian virus 40 large T antigen to immortalize primary mouse embryo fibroblasts cosegregates with its ability to bind to p53. J Virol.

151. Bargonetti J, Reynisdottir I, Friedman PN, Prives C. 1992. Site-specific binding of wild-type p53 to cellular DNA is inhibited by SV40 T antigen and mutant p53. Genes Dev 6:1886–1898.

152. Sheppard HM, Corneillie SI, Espiritu C, Gatti A, Liu X. 1999. New Insights into the Mechanism of Inhibition of p53 by Simian Virus 40 Large T Antigen. Mol Cell Biol.

153. Technau A, Wolff A, Sauder C, Birkner N, Brandner G. 2001. p53 in SV40-transformed DNA-damaged human cells binds to its cognate sequence but fails to transactivate target genes. Int J Oncol.

154. Rushton JJ, Jiang D, Srinivasan A, Pipas JM, Robbins PD. 1997. Simian virus 40 T antigen can regulate p53-mediated transcription independent of binding p53. J Virol.

155. Jiang D, Srinivasan A, Lozano G, Robbins PD. 1993. SV40 T antigen abrogates p53-mediated transcriptional activity. Oncogene.

156. Segawa K, Minowa A, Sugasawa K, Takano T, Hanaoka F. 1993. Abrogation of p53-mediated transactivation by SV40 large T antigen. Oncogene 8:543–548.

157. Oren M, Maltzman W, Levine AJ. 1981. Post-translational regulation of the 54K cellular tumor antigen in normal and transformed cells. Mol Cell Biol.

158. Tiemann F, Deppert W. 1994. Stabilization of the tumor suppressor p53 during cellular transformation by simian virus 40: Influence of viral and cellular factors and biological consequences. J Virol.

159. Herzig M, Novatchkova M, Christofori G. 1999. An unexpected role for p53 in augmenting SV40 large T antigen-mediated tumorigenesis. Biol Chem.

160. Hermannstadter A, Ziegler C, Kuhl M, Deppert W, Tolstonog G V. 2009. Wild-Type p53 Enhances Efficiency of Simian Virus 40 Large-T-Antigen-Induced Cellular Transformation. J Virol.

161. Borger DR, DeCaprio JA. 2006. Targeting of p300/CREB Binding Protein Coactivators by Simian Virus 40 Is Mediated through p53. J Virol.

162. Goodman RH, Smolik S. 2000. CBP/p300 in cell growth, transformation, and development. Genes Dev.

163. Iyer NG, Özdag H, Caldas C. 2004. p300/CBP and cancer. Oncogene.

164. Chan HM, La Thangue NB. 2001. p300/CBP proteins: HATs for transcriptional bridges and scaffolds. J Cell Sci.

165. Lill NL, Grossman SR, Ginsberg D, DeCaprio J, Livingston DM. 1997. Binding and modulation of p53 by p300/CBP coactivators. Nature.

166. Egan C, Jelsma TN, Howe JA, Bayley ST, Ferguson B, Branton PE. 1988. Mapping of cellular protein-binding sites on the products of early-region 1A of human adenovirus type 5. Mol Cell Biol.

167. Avantaggiati ML, Carbone M, Graessmann A, Nakatani Y, Howard B, Levine AS. 1996. The SV40 large T antigen and adenovirus E1a oncoproteins interact with distinct isoforms of the transcriptional co-activator, p300. EMBO J.

168. Eckner R, Ludlow JW, Lill NL, Oldread E, Arany Z, Modjtahedi N, DeCaprio JA, Livingston DM, Morgan JA. 1996. Association of p300 and CBP with simian virus 40 large T antigen. Mol Cell Biol.

169. Lill NL, Eckner R, Livingston DM, Modjtahedi N, Tevethia MJ. 1997. p300 Family members associate with the carboxyl terminus of simian virus 40 large tumor antigen. J Virol.

170. Poulin DL, Kung AL, DeCaprio JA. 2004. p53 Targets Simian Virus 40 Large T Antigen for Acetylation by CBP. J Virol.

171. Shimazu T, Komatsu Y, Nakayama KI, Fukazawa H, Horinouchi S, Yoshida M. 2006. Regulation of SV40 large T-antigen stability by reversible acetylation. Oncogene 25:7391–7400.

172. Valls E, de la Cruz X, Martínez-Balbás MA. 2003. The SV40 T antigen modulates CBP histone acetyltransferase activity. Nucleic Acids Res.

173. Ahuja D, Rathi A V., Greer AE, Chen XS, Pipas JM. 2009. A Structure-Guided Mutational Analysis of Simian Virus 40 Large T Antigen: Identification of Surface Residues Required for Viral Replication and Transformation. J Virol.

174. Kelley WL. 1998. The J-domain family and the recruitment of chaperone power. Trends Biochem Sci.

175. Campbell KS, Mullane KP, Aksoy IA, Stubdal H, Zalvide J, Pipas JM, Silver PA, Roberts TM, Schaffhausen BS, DeCaprio JA. 1997. DnaJ/hsp40 chaperone domain of SV40 large T antigen promotes efficient viral DNA replication. Genes Dev.

176. Sullivan CS, Gilbert SP, Pipas JM. 2001. ATP-Dependent Simian Virus 40 T-Antigen-Hsc70 Complex Formation. J Virol.

177. Kim HY, Ahn BY, Cho Y. 2001. Structural basis for the inactivation of retinoblastoma tumor suppressor by SV40 large T antigen. EMBO J.

178. Sullivan CS, Cantalupo P, Pipas JM. 2000. The Molecular Chaperone Activity of Simian Virus 40 Large T Antigen Is Required To Disrupt Rb-E2F Family Complexes by an ATP-Dependent Mechanism. Mol Cell Biol.

179. Zalvide J, Stubdal H, DeCaprio JA. 1998. The J Domain of Simian Virus 40 Large T Antigen Is Required To Functionally Inactivate RB Family Proteins. Mol Cell Biol.

180. Stubdal H, Zalvide J, Campbell KS, Schweitzer C, Roberts TM, DeCaprio JA. 1997. Inactivation of pRB-related proteins p130 and p107 mediated by the J domain of simian virus 40 large T antigen. Mol Cell Biol.

181. Perera D, Tilston V, Hopwood JA, Barchi M, Boot-Handford RP, Taylor SSS. 2007. Bub1 Maintains Centromeric Cohesion by Activation of the Spindle Checkpoint. Dev Cell.

182. Cotsiki M, Lock RL, Cheng Y, Williams GL, Zhao J, Perera D, Freire R, Entwistle A, Golemis EA, Roberts TM, Jat PS, Gjoerup O V. 2004. Simian virus 40 large T antigen targets the spindle assembly checkpoint protein Bub1. Proc Natl Acad Sci U S A 101:947–952.

183. Hein J, Boichuk S, Wu J, Cheng Y, Freire R, Jat PS, Roberts TM, Gjoerup O V. 2009. Simian Virus 40 Large T Antigen Disrupts Genome Integrity and Activates a DNA Damage Response via Bub1 Binding. J Virol.

184. Sarikas A, Xu X, Field LJ, Pan ZQ. 2008. The cullin7 E3 ubiquitin ligase: A novel player in growth control. Cell Cycle.

185. Ali SH, Kasper JS, Arai T, DeCaprio JA. 2004. Cul7/p185/p193 Binding to Simian Virus 40 Large T Antigen Has a Role in Cellular Transformation. J Virol.

186. Kasper JS, Kuwabara H, Arai T, Ali SH, DeCaprio JA. 2005. Simian Virus 40 Large T Antigen's Association with the CUL7 SCF Complex Contributes to Cellular Transformation. J Virol.

187. Reiss K, Del Valle L, Lassak A, Trojanek J. 2012. Nuclear IRS-1 and cancer. J Cell Physiol.

188. Prisco M, Santini F, Baffa R, Liu M, Drakas R, Wu A, Baserga R. 2002. Nuclear translocation of insulin receptor substrate-1 by the simian virus 40 T antigen and the activated type 1 insulin-like growth factor receptor. J Biol Chem.

189. D'Ambrosio C, Keller SR, Morrione A, Lienhard GE, Baserga R, Surmacz E. 1995. Transforming potential of the insulin receptor substrate 1. Cell Growth Differ.

190. Fei ZL, D'Ambrosio C, Li S, Surmacz E, Baserga R. 1995. Association of insulin receptor substrate 1 with simian virus 40 large T antigen. Mol Cell Biol.

191. DeAngelis T, Chen J, Wu A, Prisco M, Baserga R. 2006. Transformation by the simian virus 40 T antigen is regulated by IGF-I receptor and IRS-1 signaling. Oncogene.

192. Yu Y, Alwine JC. 2008. Interaction between Simian Virus 40 Large T Antigen and Insulin Receptor Substrate 1 Is Disrupted by the K1 Mutation, Resulting in the Loss of Large T Antigen-Mediated Phosphorylation of Akt. J Virol.

193. Welcker M, Clurman BE. 2005. The SV40 large T antigen contains a decoy phosphodegron that mediates its interactions with Fbw7/hCdc4. J Biol Chem.

194. Welcker M, Clurman BE. 2008. FBW7 ubiquitin ligase: a tumour suppressor at the crossroads of cell division, growth and differentiation. Nat Rev Cancer2007/12/21. 8:83–93.

195. Janssens V, Goris J, Van Hoof C. 2005. PP2A: The expected tumor suppressor. Curr Opin Genet Dev.

196. Pallas DC, Shahrik LK, Martin BL, Jaspers S, Miller TB, Brautigan DL, Roberts TM. 1990. Polyoma small and middle T antigens and SV40 small t antigen form stable complexes with protein phosphatase 2A. Cell 60:167–176.

197. Sablina AA, Hahn WC. 2008. SV40 small T antigen and PP2A phosphatase in cell transformation. Cancer Metastasis Rev.

198. Kwun HJ, Shuda M, Camacho CJ, Gamper AM, Thant M, Chang Y, Moore PS. 2015. Restricted protein phosphatase 2A targeting by Merkel cell polyomavirus small T antigen. J Virol 89:4191–4200.

199. Yeh E, Cunningham M, Arnold H, Chasse D, Monteith T, Ivaldi G, Hahn WC, Stukenberg PT, Shenolikar S, Uchida T, Counter CM, Nevins JR, Means AR, Sears R. 2004. A signalling pathway controlling c-Myc degradation that impacts oncogenic transformation of human cells. Nat Cell Biol 6:308–318.

200. Sontag E, Sontag JM, Garcia A. 1997. Protein phosphatase 2A is a critical regulator of protein kinase C ζ signaling targeted by SV40 small t to promote cell growth and NF-κB activation. EMBO J.

201. Sontag E, Fedorov S, Kamibayashi C, Robbins D, Cobb M, Mumby M. 1993. The interaction of SV40 small tumor antigen with protein phosphatase 2A stimulates the map kinase pathway and induces cell proliferation. Cell.

202. Yuan H, Veldman T, Rundell K, Schlegel R. 2002. Simian Virus 40 Small Tumor Antigen Activates AKT and Telomerase and Induces Anchorage-Independent Growth of Human Epithelial Cells. J Virol.

203. Hahn WC, Dessain SK, Brooks MW, King JE, Elenbaas B, Sabatini DM, DeCaprio JA, Weinberg RA. 2002. Enumeration of the Simian Virus 40 Early Region Elements Necessary for Human Cell Transformation. Mol Cell Biol.

204. Mungre U, Enderle K, Turk B, Porrás A, Rundell K, Wu YQ, Mumby MC. 1994. Mutations which affect the inhibition of protein phosphatase 2A by simian virus 40 small-t antigen in vitro decrease viral transformation. J Virol.

205. Becker JC, Stang A, Decaprio JA, Cerroni L, Lebbé C, Veness M, Nghiem P. 2017. Merkel cell carcinoma. Nat Rev Dis Prim 3.

206. Drusio C, Becker JC, Schadendorf D, Ugurel S. 2019. Merkel cell carcinoma. Best Pract Onkol.

207. Jaeger T, Ring J, Andres C. 2012. Histological, immunohistological, and clinical features of merkel cell carcinoma in correlation to merkel cell polyomavirus status. J Ski Cancer 2012:983421.

208. Hodgson NC. 2005. Merkel cell carcinoma: Changing incidence trends. J Surg Oncol.

209. Agelli M, Clegg LX. 2003. Epidemiology of primary Merkel cell carcinoma in the United States. J Am Acad Dermatol 49:832–841.

210. Sihto H, Kukko H, Koljonen V, Sankila R, Bohling T, Joensuu H. 2009. Clinical factors associated with Merkel cell polyomavirus infection in Merkel cell carcinoma. J Natl Cancer Inst 101:938–945.

211. Lemos BD, Storer BE, Iyer JG, Phillips JL, Bichakjian CK, Fang LC, Johnson TM, Liegeois-Kwon NJ, Otley CC, Paulson KG, Ross MI, Yu SS, Zeitouni NC, Byrd DR, Sondak VK, Gershenwald JE, Sober AJ, Nghiem P. 2010. Pathologic nodal evaluation improves prognostic accuracy in Merkel cell carcinoma: Analysis of 5823 cases as the basis of the first consensus staging system. J Am Acad Dermatol.

212. Engels EA, Frisch M, Goedert JJ, Biggar RJ, Miller RW. 2002. Merkel cell carcinoma and HIV infection. Lancet 359:497–498.

213. Buell JF, Trofe J, Hanaway MJ, Beebe TM, Gross TG, Alloway RR, First MR, Woodle ES. 2002. Immunosuppression and Merkel cell cancer. Transpl Proc 34:1780–1781.

214. Lee S, Paulson KG, Murchison EP, Afanasiev OK, Alkan C, Leonard JH, Byrd DR, Hannon GJ, Nghiem P. 2011. Identification and validation of a novel mature microRNA encoded by the Merkel cell polyomavirus in human Merkel cell carcinomas. J Clin Virol 52:272–275.

215. Neu U, Bauer J, Stehle T. 2011. Viruses and sialic acids: Rules of engagement. Curr Opin Struct Biol.

216. Neu U, Hengel H, Blaum BS, Schowalter RM, Macejak D, Gilbert M, Wakarchuk WW, Imamura A, Ando H, Kiso M, Arnberg N, Garcea RL, Peters T, Buck CB, Stehle T. 2012. Structures of Merkel cell polyomavirus VP1 complexes define a sialic acid binding site required for infection. PLoS Pathog 8:e1002738.

217. Schowalter RM, Pastrana D V, Buck CB. 2011. Glycosaminoglycans and sialylated glycans sequentially facilitate Merkel cell polyomavirus infectious entry. PLoS Pathog 7:e1002161.

218. Spurgeon ME, Lambert PF. 2013. Merkel cell polyomavirus: a newly discovered human virus with oncogenic potential. Virology 435:118–130.

219. Feng H, Kwun HJ, Liu X, Gjoerup O, Stolz DB, Chang Y, Moore PS. 2011. Cellular and viral factors regulating Merkel cell polyomavirus replication. PLoS One 6:e22468.

220. Neumann F, Borchert S, Schmidt C, Reimer R, Hohenberg H, Fischer N, Grundhoff A. 2011. Replication, gene expression and particle production by a consensus Merkel Cell Polyomavirus (MCPyV) genome. PLoS One 6:e29112.

221. Harrison CJ, Meinke G, Kwun HJ, Rogalin H, Phelan PJ, Bullock PA, Chang Y, Moore PS, Bohm A. 2011. Asymmetric assembly of Merkel cell polyomavirus large T-antigen origin binding domains at the viral origin. J Mol Biol 409:529–542.

222. Kwun HJ, Chang Y, Moore PS. 2017. Protein-mediated viral latency is a novel mechanism for Merkel cell polyomavirus persistence. Proc Natl Acad Sci U S A.

223. Foulongne V, Kluger N, Dereure O, Mercier G, Moles JP, Guillot B, Segondy M. 2010. Merkel cell polyomavirus in cutaneous swabs. Emerg Infect Dis 16:685–687.

224. Schowalter RM, Reinhold WC, Buck CB. 2012. Entry tropism of BK and Merkel cell polyomaviruses in cell culture. PLoS One.

225. Liu W, Yang R, Payne AS, Schowalter RM, Spurgeon ME, Lambert PF, Xu X, Buck CB, You J. 2016. Identifying the Target Cells and Mechanisms of Merkel Cell Polyomavirus Infection. Cell Host Microbe.

226. Calder KB, Smoller BR. 2010. New insights into merkel cell carcinoma. Adv Anat Pathol.

227. Liu W, MacDonald M, You J. 2016. Merkel cell polyomavirus infection and Merkel cell carcinoma. Curr Opin Virol.

228. Tilling T, Moll I. 2012. Which Are the Cells of Origin in Merkel Cell Carcinoma? J Skin Cancer 2012:1–6.

229. Hausen A Zur, Rennspiess D, Winnepenninckx V, Speel EJ, Kurz AK. 2013. Early B-Cell differentiation in merkel cell carcinomas: Clues to cellular ancestry. Cancer Res.

230. Harold A, Amako Y, Hachisuka J, Bai Y, Li MY, Kubat L, Gravemeyer J, Franks J, Gibbs JR, Park HJ, Ezhkova E, Becker JC, Shuda M. 2019. Conversion of Sox2-dependent Merkel cell carcinoma to a differentiated neuron-like phenotype by T antigen inhibition. Proc Natl Acad Sci U S A.

231. Kervarrec T, Aljundi M, Appenzeller S, Samimi M, Maubec E, Cribier B, Deschamps L, Sarma B, Sarosi E-M, Berthon P, Levy A, Bousquet G, Tallet A, Touze A, Guyetant S, Schrama D, Houben R. 2019. Polyomavirus-positive Merkel cell carcinoma derived from a trichoblastoma suggests an epithelial origin of this Merkel cell carcinoma. J Invest Dermatol.

232. Sunshine JC, Jahchan NS, Sage J, Choi J. 2018. Are there multiple cells of origin of Merkel cell carcinoma? Oncogene.

233. Shuda M, Arora R, Kwun HJ, Feng H, Sarid R, Fernandez-Figueras MT, Tolstov Y, Gjoerup O, Mansukhani MM, Swerdlow SH, Chaudhary PM, Kirkwood JM, Nalesnik MA, Kant JA, Weiss LM, Moore PS, Chang Y. 2009. Human Merkel cell polyomavirus infection I. MCV T antigen expression in Merkel cell carcinoma, lymphoid tissues and lymphoid tumors. Int J Cancer 125:1243–1249.

234. Laude HC, Jonchere B, Maubec E, Carlotti A, Marinho E, Couturaud B, Peter M, Sastre-Garau X, Avril MF, Dupin N, Rozenberg F. 2010. Distinct merkel cell polyomavirus molecular features in tumour and non tumour specimens from patients with merkel cell carcinoma. PLoS Pathog 6:e1001076.

235. Houben R, Shuda M, Weinkam R, Schrama D, Feng H, Chang Y, Moore PS, Becker JC. 2010. Merkel cell polyomavirus-infected Merkel cell carcinoma cells require expression of viral T antigens. J Virol 84:7064–7072.

236. Shuda M, Chang Y, Moore PS. 2014. Merkel cell polyomavirus-positive Merkel cell carcinoma requires viral small T-antigen for cell proliferation. J Invest Dermatol 134:1479–1481.

237. Kwun HJ, Shuda M, Feng H, Camacho CJ, Moore PS, Chang Y. 2013. Merkel cell polyomavirus small T antigen controls viral replication and oncoprotein expression by targeting the cellular ubiquitin ligase SCFFbw7. Cell Host Microbe 14:125–135.

238. Shuda M, Guastafierro A, Geng X, Shuda Y, Ostrowski SM, Lukianov S, Jenkins FJ, Honda K, Maricich SM, Moore PS, Chang Y. 2015. Merkel Cell Polyomavirus Small T Antigen Induces Cancer and Embryonic Merkel Cell Proliferation in a Transgenic Mouse Model. PLoS One 10:e0142329.

239. Verhaegen ME, Mangelberger D, Harms PW, Vozheiko TD, Weick JW, Wilbert DM, Saunders TL, Ermilov AN, Bichakjian CK, Johnson TM, Imperiale MJ, Dlugosz AA. 2015. Merkel cell polyomavirus small T antigen is oncogenic in transgenic mice. J Invest Dermatol 135:1415–1424.

240. Tolstov YL, Pastrana D V, Feng H, Becker JC, Jenkins FJ, Moschos S, Chang Y, Buck CB, Moore PS. 2009. Human Merkel cell polyomavirus infection II. MCV is a common human infection that can be detected by conformational capsid epitope immunoassays. Int J Cancer 125:1250–1256.

241. Pastrana D V, Tolstov YL, Becker JC, Moore PS, Chang Y, Buck CB. 2009. Quantitation of human seroresponsiveness to Merkel cell polyomavirus. PLoS Pathog 5:e1000578.

242. Wong SQ, Waldeck K, Vergara IA, Schröder J, Madore J, Wilmott JS, Colebatch AJ, De Paoli-Iseppi R, Li J, Lupat R, Semple T, Arnau GM, Fellowes A, Leonard JH, Hruby G, Mann GJ, Thompson JF, Cullinane C, Johnston M, Shackleton M, Sandhu S, Bowtell DDL, Johnstone RW, Fox SB, McArthur GA, Papenfuss AT, Scolyer RA, Gill AJ, Hicks RJ, Tothill RW. 2015. UV-associated mutations underlie the etiology of MCV-negative Merkel cell carcinomas. Cancer Res.

243. Goh G, Walradt T, Markarov V, Blom A, Riaz N, Doumani R, Stafstrom K, Moshiri A, Yelistratova L, Levinsohn J, Chan TA, Nghiem P, Lifton RP, Choi J. 2016. Mutational landscape of MCPyV-positive and MCPyV-negative merkel cell carcinomas with implications for immunotherapy. Oncotarget.

244. Harms PW, Vats P, Verhaegen ME, Robinson DR, Wu YM, Dhanasekaran SM, Palanisamy N, Siddiqui J, Cao X, Su F, Wang R, Xiao H, Kunju LP, Mehra R, Tomlins SA, Fullen DR, Bichakjian CK, Johnson TM, Dlugosz AA, Chinnaiyan AM. 2015. The distinctive mutational spectra of polyomavirus-negative merkel cell carcinoma. Cancer Res.

245. Lill C, Schneider S, Item CB, Loewe R, Houben R, Halbauer D, Heiduschka G, Brunner M, Thurnher D. 2011. P53 mutation is a rare event in Merkel cell carcinoma of the head and neck. Eur Arch Oto-Rhino-Laryngology.

246. Scuda N, Hofmann J, Calvignac-Spencer S, Ruprecht K, Liman P, Kuhn J, Hengel H, Ehlers B. 2011. A novel human polyomavirus closely related to the african green monkey-derived lymphotropic polyomavirus. J Virol 85:4586–4590.

247. Pipas JM. 1992. Common and unique features of T antigens encoded by the polyomavirus group. J Virol 66:3979–3985.

248. Kwun HJ, Guastafierro A, Shuda M, Meinke G, Bohm A, Moore PS, Chang Y. 2009. The minimum replication origin of merkel cell polyomavirus has a unique large T-antigen loading architecture and requires small T-antigen expression for optimal replication. J Virol 83:12118–12128.

249. Nakamura T, Sato Y, Watanabe D, Ito H, Shimonohara N, Tsuji T, Nakajima N, Suzuki Y, Matsuo K, Nakagawa H, Sata T, Katano H. 2010. Nuclear localization of Merkel cell polyomavirus large T antigen in Merkel cell carcinoma. Virology 398:273–279.

250. Liu X, Hein J, Richardson SC, Basse PH, Toptan T, Moore PS, Gjoerup O V, Chang Y. 2011. Merkel cell polyomavirus large T antigen disrupts lysosome clustering by translocating human Vam6p from the cytoplasm to the nucleus. J Biol Chem 286:17079–17090.

251. An P, Saenz Robles MT, Pipas JM. 2012. Large T antigens of polyomaviruses: amazing molecular machines. Annu Rev Microbiol 66:213–236.

252. Arora R, Shuda M, Guastafierro A, Feng H, Toptan T, Tolstov Y, Normolle D, Vollmer LL, Vogt A, Domling A, Brodsky JL, Chang Y, Moore PS. 2012. Survivin is a therapeutic target in Merkel cell carcinoma. Sci Transl Med 4:133ra56.

253. Houben R, Adam C, Baeurle A, Hesbacher S, Grimm J, Angermeyer S, Henzel K, Hauser S, Elling R, Brocker EB, Gaubatz S, Becker JC, Schrama D. 2012. An intact retinoblastoma protein-binding site in Merkel cell polyomavirus large T antigen is required for promoting growth of Merkel cell carcinoma cells. Int J Cancer 130:847–856.

254. Dresang LR, Guastafierro A, Arora R, Normolle D, Chang Y, Moore PS. 2013. Response of Merkel cell polyomavirus-positive merkel cell carcinoma xenografts to a survivin inhibitor. PLoS One 8:e80543.

255. Diaz J, Wang X, Tsang SH, Jiao J, You J. 2014. Phosphorylation of large T antigen regulates merkel cell polyomavirus replication. Cancers (Basel) 6:1464–1486.

256. Pipas JM, Levine AJ. 2001. Role of T antigen interactions with p53 in tumorigenesis. Semin Cancer Biol 11:23–30.

257. Borchert S, Czech-Sioli M, Neumann F, Schmidt C, Wimmer P, Dobner T, Grundhoff A, Fischer N. 2014. High-affinity Rb binding, p53 inhibition, subcellular localization, and transformation by wild-type or tumor-derived shortened Merkel cell polyomavirus large T antigens. J Virol 88:3144–3160.

258. Cheng J, Rozenblatt-Rosen O, Paulson KG, Nghiem P, DeCaprio JA. 2013. Merkel cell polyomavirus large T antigen has growth-promoting and inhibitory activities. J Virol 87:6118–6126.

259. Fischer N, Brandner J, Fuchs F, Moll I, Grundhoff A. 2010. Detection of Merkel cell polyomavirus (MCPyV) in Merkel cell carcinoma cell lines: cell morphology and growth phenotype do not reflect presence of the virus. Int J Cancer 126:2133–2142.

260. Houben R, Angermeyer S, Haferkamp S, Aue A, Goebeler M, Schrama D, Hesbacher S. 2014. Characterization of functional domains in the Merkel cell polyoma virus Large T antigen. Int J Cancer.

261. zur Hausen H. 2008. A specific signature of Merkel cell polyomavirus persistence in human cancer cells. Proc Natl Acad Sci U S A 105:16063–16064.

262. Manos MM, Gluzman Y. 1984. Simian virus 40 large T-antigen point mutants that are defective in viral DNA replication but competent in oncogenic transformation. Mol Cell Biol 4:1125–1133.

263. Kadaja M, Sumerina A, Verst T, Ojarand M, Ustav E, Ustav M. 2007. Genomic instability of the host cell induced by the human papillomavirus replication machinery. EMBO J 26:2180–2191.

264. Li J, Wang X, Diaz J, Tsang SH, Buck CB, You J. 2013. Merkel cell polyomavirus large T antigen disrupts host genomic integrity and inhibits cellular proliferation. J Virol 87:9173–9188.

265. Shuda M, Kwun HJ, Feng H, Chang Y, Moore PS. 2011. Human Merkel cell polyomavirus small T antigen is an oncoprotein targeting the 4E-BP1 translation regulator. J Clin Invest 121:3623–3634.

266. Boyapati A, Wilson M, Yu J, Rundell K. 2003. SV40 17KT antigen complements dnaj mutations in large T antigen to restore transformation of primary human fibroblasts. Virology 315:148–158.

267. Rodriguez-Viciana P, Collins C, Fried M. 2006. Polyoma and SV40 proteins differentially regulate PP2A to activate distinct cellular signaling pathways involved in growth control. Proc Natl Acad Sci U S A 103:19290–19295.

268. Hwang JH, Jiang T, Kulkarni S, Faure N, Schaffhausen BS. 2013. Protein phosphatase 2A isoforms utilizing Abeta scaffolds regulate differentiation through control of Akt protein. J Biol Chem 288:32064–32073.

269. Andrabi S, Hwang JH, Choe JK, Roberts TM, Schaffhausen BS. 2011. Comparisons between murine polyomavirus and Simian virus 40 show significant differences in small T antigen function. J Virol 85:10649–10658.

270. Pores Fernando AT, Andrabi S, Cizmecioglu O, Zhu C, Livingston DM, Higgins JM, Schaffhausen BS, Roberts TM. 2014. Polyoma small T antigen triggers cell death via mitotic catastrophe. Oncogene.

271. Hwang JH, Pores Fernando AT, Faure N, Andrabi S, Hahn WC, Schaffhausen BS, Roberts TM. 2014. Polyomavirus small T antigen interacts with yes-associated protein to regulate cell survival and differentiation. J Virol 88:12055–12064.

272. Kwun HJ, Wendzicki JA, Shuda Y, Moore PS, Chang Y. 2017. Merkel cell polyomavirus small T antigen induces genome instability by E3 ubiquitin ligase targeting. Oncogene 36.

273. Shuda M, Velasquez C, Cheng E, Cordek DG, Kwun HJ, Chang Y, Moore PS. 2015. CDK1 substitutes for mTOR kinase to activate mitotic cap-dependent protein translation. Proc Natl Acad Sci U S A2015/04/18. 112:5875–5882.

274. Velásquez C, Cheng E, Shuda M, Lee-Oesterreich PJ, Von Strandmann LP, Gritsenko MA, Jacobs JM, Moore PS, Chang Y. 2016. Mitotic protein kinase CDK1 phosphorylation of mRNA translation regulator 4E-BP1 Ser83 may contribute to cell transformation. Proc Natl Acad Sci U S A.

275. Griffiths DA, Abdul-Sada H, Knight LM, Jackson BR, Richards K, Prescott EL, Peach AH, Blair GE, Macdonald A, Whitehouse A. 2013. Merkel cell polyomavirus small T antigen targets the NEMO adaptor protein to disrupt inflammatory signaling. J Virol 87:13853–13867.

276. Knight LM, Stakaityte G, Wood JJ, Abdul-Sada H, Griffiths DA, Howell GJ, Wheat R, Blair GE, Steven NM, Macdonald A, Blackbourn DJ, Whitehouse A. 2014. Merkel cell polyomavirus small T antigen mediates microtubule destabilisation to promote cell motility and migration. J Virol.

277. Cheng J, Park DE, Berrios C, White EA, Arora R, Yoon R, Branigan T, Xiao T, Westerling T, Federation A, Zeid R, Strober B, Swanson SK, Florens L, Bradner JE, Brown M, Howley PM, Padi M, Washburn MP, DeCaprio JA. 2017. Merkel cell polyomavirus recruits MYCL to the EP400 complex to promote oncogenesis. PLoS Pathog.

278. Park DE, Cheng J, Berrios C, Montero J, Cortés-Cros M, Ferretti S, Arora R, Tillgren ML, Gokhale PC, DeCaprio JA. 2019. Dual inhibition of MDM2 and MDM4 in virus-positive Merkel cell carcinoma enhances the p53 response. Proc Natl Acad Sci U S A.

279. Gomez BP, Wang C, Viscidi RP, Peng S, He L, Wu TC, Hung CF. 2012. Strategy for eliciting antigen-specific CD8+ T cell-mediated immune response against a cryptic CTL epitope of merkel cell polyomavirus large T antigen. Cell Biosci 2:36.

280. Gomez B, He L, Tsai YC, Wu TC, Viscidi RP, Hung CF. 2013. Creation of a Merkel cell polyomavirus small T antigen-expressing murine tumor model and a DNA vaccine targeting small T antigen. Cell Biosci 3:29.

281. Lyngaa R, Pedersen NW, Schrama D, Thrue CA, Ibrani D, Met O, Thor Straten P, Nghiem P, Becker JC, Hadrup SR. 2014. T-cell responses to oncogenic merkel cell polyomavirus proteins distinguish patients with merkel cell carcinoma from healthy donors. Clin Cancer Res 20:1768–1778.

282. Willmes C, Adam C, Alb M, Volkert L, Houben R, Becker JC, Schrama D. 2012. Type I and II IFNs inhibit Merkel cell carcinoma via modulation of the Merkel cell polyomavirus T antigens. Cancer Res 72:2120–2128.

283. Demetriou SK, Ona-Vu K, Sullivan EM, Dong TK, Hsu SW, Oh DH. 2012. Defective DNA repair and cell cycle arrest in cells expressing Merkel cell polyomavirus T antigen. Int J Cancer 131:1818–1827.

284. Kenan DJ, Mieczkowski PA, Burger-Calderon R, Singh HK, Nickeleit V. 2015. The oncogenic potential of BK-polyomavirus is linked to viral integration into the human genome. J Pathol.

285. Chen Y, Williams V, Filippova M, Filippov V, Duerksen-Hughes P. 2014. Viral carcinogenesis: Factors inducing DNA damage and virus integration. Cancers (Basel). MDPI AG.

286. Schrama D, Sarosi EM, Adam C, Ritter C, Kaemmerer U, Klopocki E, König EM, Utikal J, Becker JC, Houben R. 2019. Characterization of six Merkel cell polyomavirus-positive Merkel cell carcinoma cell lines: Integration pattern suggest that large T antigen truncating events occur before or during integration. Int J Cancer.

287. Guastafierro A, Feng H, Thant M, Kirkwood JM, Chang Y, Moore PS, Shuda M. 2013. Characterization of an early passage Merkel cell polyomavirus-positive Merkel cell carcinoma cell line, MS-1, and its growth in NOD scid gamma mice. J Virol Methods 187:6–14.

288. Velásquez C, Amako Y, Harold A, Toptan T, Chang Y, Shuda M. 2018. Characterization of a merkel cell polyomavirus-positive merkel cell carcinoma cell line CVG-1. Front Microbiol.

289. Richards KF, Guastafierro A, Shuda M, Toptan T, Moore PS, Chang Y. 2015. Merkel cell polyomavirus T antigens promote cell proliferation and inflammatory cytokine gene expression. J Gen Virol 96:3532–3544.

290. Ma W, Kong Q, Grix M, Mantyla JJ, Yang Y, Benning C, Ohlrogge JB. 2015. Deletion of a C-terminal intrinsically disordered region of WRINKLED1 affects its stability and enhances oil accumulation in Arabidopsis. Plant J.

291. Loetscher P, Pratt G, Rechsteiner M. 1991. The C terminus of mouse ornithine decarboxylase confers rapid degradation on dihydrofolate reductase: Support for the pest hypothesis. J Biol Chem.

292. Ghoda L, Phillips MA, Bass KE, Wang CC, Coffino P. 1990. Trypanosome ornithine decarboxylase is stable because it lacks sequences found in the carboxyl terminus of the mouse enzyme which target the latter for intracellualr degradation. J Biol Chem.

293. Bies J, Nazarov V, Wolff L. 1999. Identification of protein instability determinants in the carboxy-terminal region of c-Myb removed as a result of retroviral integration in murine monocytic leukemias. J Virol.

294. Li X, Zhao X, Fang Y, Jiang X, Duong T, Fan C, Huang CC, Kain SR. 1998. Generation of destabilized green fluorescent protein as a transcription reporter. J Biol Chem 273:34970–34975.

295. Koren I, Timms RT, Kula T, Xu Q, Li MZ, Elledge SJ. 2018. The Eukaryotic Proteome Is Shaped by E3 Ubiquitin Ligases Targeting C-Terminal Degrons. Cell 173:1622-1635.e14.

296. Seneca NT, Saenz Robles MT, Pipas JM. 2014. Removal of a small C-terminal region of JCV and SV40 large T antigens has differential effects on transformation. Virology 468–470:47–56.

297. Madeira F, Park Y mi, Lee J, Buso N, Gur T, Madhusoodanan N, Basutkar P, Tivey ARN, Potter SC, Finn RD, Lopez R. 2019. The EMBL-EBI search and sequence analysis tools APIs in 2019. Nucleic Acids Res.

298. Zimmermann L, Stephens A, Nam SZ, Rau D, Kübler J, Lozajic M, Gabler F, Söding J, Lupas AN, Alva V. 2018. A Completely Reimplemented MPI Bioinformatics Toolkit with a New HHpred Server at its Core. J Mol Biol.

299. Kelley LA, Mezulis S, Yates CM, Wass MN, Sternberg MJE. 2015. The Phyre2 web portal for protein modeling, prediction and analysis. Nat Protoc.

300. Erales J, Coffino P. 2014. Ubiquitin-independent proteasomal degradation. Biochim Biophys Acta2013/05/21. 1843:216–221.

301. Bhaskara RM, Srinivasan N. 2011. Stability of domain structures in multi-domain proteins. Sci Rep.

302. Meinke G, Phelan PJ, Harrison CJ, Bullock PA. 2013. Analysis of the costructure of the simian virus 40 T-antigen origin binding domain with site I reveals a correlation between GAGGC spacing and spiral assembly. J Virol 87:2923–2934.

303. Meinke G, Phelan P, Moine S, Bochkareva E, Bochkarev A, Bullock PA, Bohm A. 2007. The crystal structure of the SV40 T-antigen origin binding domain in complex with DNA. PLoS Biol.

304. Chang YP, Xu M, Machado ACD, Yu XJ, Rohs R, Chen XS. 2013. Mechanism of Origin DNA Recognition and Assembly of an Initiator-Helicase Complex by SV40 Large Tumor Antigen. Cell Rep.

305. Gai D, Wang D, Li SX, Chen XS. 2016. The structure of SV40 large T hexameric helicase in complex with AT-rich origin DNA. Elife.

306. Fang NN, Chan GT, Zhu M, Comyn SA, Persaud A, Deshaies RJ, Rotin D, Gsponer J, Mayor T. 2014. Rsp5/Nedd4 is the main ubiquitin ligase that targets cytosolic misfolded proteins following heat stress. Nat Cell Biol.

307. Rosenbaum JC, Fredrickson EK, Oeser ML, Garrett-Engele CM, Locke MN, Richardson LA, Nelson ZW, Hetrick ED, Milac TI, Gottschling DE, Gardner RG. 2011. Disorder targets misorder in nuclear quality control degradation: A disordered ubiquitin ligase directly recognizes its misfolded substrates. Mol Cell.

308. Murata S, Minami Y, Minami M, Chiba T, Tanaka K. 2001. CHIP is a chaperone-dependent E3 ligase that ubiquitylates unfolded protein. EMBO Rep.

309. Davey NE. 2019. The functional importance of structure in unstructured protein regions. Curr Opin Struct Biol.

310. Schad E, Fichó E, Pancsa R, Simon I, Dosztányi Z, Mészáros B. 2018. DIBS: A repository of disordered binding sites mediating interactions with ordered proteins. Bioinformatics.

311. Van Roey K, Uyar B, Weatheritt RJ, Dinkel H, Seiler M, Budd A, Gibson TJ, Davey NE. 2014. Short linear motifs: Ubiquitous and functionally diverse protein interaction modules directing cell regulation. Chem Rev.

312. Uversky VN, Roman A, Oldfield CJ, Dunker AK. 2006. Protein intrinsic disorder and human papillomaviruses: Increased amount of disorder in E6 and E7 oncoproteins from high risk HPVs. J Proteome Res.

313. Nicolau-Junior N, Giuliatti S. 2013. Modeling and molecular dynamics of the intrinsically disordered e7 proteins from high- and low-risk types of human papillomavirus. J Mol Model.

314. Tamarozzi ER, Giuliatti S. 2018. Understanding the role of intrinsic disorder of viral proteins in the oncogenicity of different types of HPV. Int J Mol Sci.

315. Li J, Diaz J, Wang X, Tsang SH, You J. 2015. Phosphorylation of Merkel Cell Polyomavirus Large Tumor Antigen at Serine 816 by ATM Kinase Induces Apoptosis in Host Cells. J Biol Chem.

316. Varshavsky A. 2019. N-degron and C-degron pathways of protein degradation. Proc Natl Acad Sci U S A.

317. Mészáros B, Kumar M, Gibson TJ, Uyar B, Dosztányi Z. 2017. Degrons in cancer. Sci Signal.

318. Holt LJ. 2012. Regulatory modules: Coupling protein stability to phopshoregulation during cell division. FEBS Lett.

319. Skowyra D, Craig KL, Tyers M, Elledge SJ, Harper JW. 1997. F-box proteins are receptors that recruit phosphorylated substrates to the SCF ubiquitin-ligase complex. Cell.

320. Feldman RMR, Correll CC, Kaplan KB, Deshaies RJ. 1997. A complex of Cdc4p, Skp1p, and Cdc53p/cullin catalyzes ubiquitination of the phosphorylated CDK inhibitor Sic1p. Cell.

321. Abed M, Abed M, Heuberger J, Novak R, Zohar Y, Beltran Lopez AP, Trausch-Azar JS, Ilagan MXG, Benhamou D, Dittmar G, Kopan R, Birchmeier W, Schwartz AL, Orian A. 2016. RNF4-Dependent Oncogene Activation by Protein Stabilization. Cell Rep.

322. White MK, Safak M, Khalili K. 2009. Regulation of Gene Expression in Primate Polyomaviruses. J Virol.

323. Itahana K, Dimri G, Campisi J. 2001. Regulation of cellular senescence by p53. Eur J Biochem.

324. Sato Y, Tsurumi T. 2013. Genome guardian p53 and viral infections. Rev Med Virol.

325. Carson DA, Lois A. 1995. Cancer progression and p53. Lancet.

326. Crawford L V., Lane DP, Denhardt DT, Harlow EE, Nicklin PM, Osborn K, Pim DC. 1979. Characterization of the complex between SV40 large T antigen and the 53K host protein in transformed mouse cells. Symp Quant Biol.

327. Li D, Zhao R, Lilyestrom W, Gai D, Zhang R, DeCaprio JA, Fanning E, Jochimiak A, Szakonyi G, Chen XS. 2003. Structure of the replicative helicase of the oncoprotein SV40 large tumour antigen. Nature.

328. Tan TH, Wallis J, Levine AJ. 1986. Identification of the p53 protein domain involved in the formation of the simian virus 40 large T-antigen-p53 protein complex. J Virol 59:574–583.

329. Li B, Fields S. 1993. Identification of mutations in p53 that affect its binding to SV40 large T antigen by using the yeast two-hybrid system. FASEB J 7:957–963.

330. Peden KWC, Srinivasan A, Vartikar J V., Pipas JM. 1998. Effects of mutations within the SV40 large T antigen ATPase/p53 binding domain on viral replication and transformation. Virus Genes.

331. Houben R, Dreher C, Angermeyer S, Borst A, Utikal J, Haferkamp S, Peitsch WK, Schrama D, Hesbacher S. 2013. Mechanisms of p53 restriction in merkel cell carcinoma cells are independent of the merkel cell polyoma virus T antigens. J Invest Dermatol.

332. Sihto H, Kukko H, Koljonen V, Sankila R, Böhling T, Joensuu H. 2011. Merkel cell polyomavirus infection, large T antigen, retinoblastoma protein and outcome in Merkel cell carcinoma. Clin Cancer Res.

333. Rodig SJ, Cheng J, Wardzala J, DoRosario A, Scanlon JJ, Laga AC, Martinez-Fernandez A, Barletta JA, Bellizzi AM, Sadasivam S, Holloway DT, Cooper DJ, Kupper TS, Wang LC, DeCaprio JA. 2012. Improved detection suggests all Merkel cell carcinomas harbor Merkel polyomavirus. J Clin Invest 122:4645–4653.

334. Tsang SH, Wang X, Li J, Buck CB, You J. 2014. Host DNA damage response factors localize to merkel cell polyomavirus DNA replication sites to support efficient viral DNA replication. J Virol 88:3285–3297.

335. Wang X, Li J, Schowalter RM, Jiao J, Buck CB, You J. 2012. Bromodomain protein Brd4 plays a key role in Merkel cell polyomavirus DNA replication. PLoS Pathog 8:e1003021.

336. Dahl J, You J, Benjamin TL. 2005. Induction and Utilization of an ATM Signaling Pathway by Polyomavirus. J Virol.

337. Sowd GA, Li NY, Fanning E. 2013. ATM and ATR Activities Maintain Replication Fork Integrity during SV40 Chromatin Replication. PLoS Pathog.

338. Wobbe CR, Dean F, Weissbach L, Hurwitz J. 1985. In vitro replication of duplex circular DNA containing the simian virus 40 DNA origin site. Proc Natl Acad Sci U S A.

339. Yu J, Wang Z, Kinzler KW, Vogelstein B, Zhang L. 2003. PUMA mediates the apoptotic response to p53 in colorectal cancer cells. Proc Natl Acad Sci U S A.

340. Chen W, Hahn WC. 2003. SV40 early region oncoproteins and human cell transformation. Histol Histopathol.

341. Peden KWC, Srinivasan A, Farber JM, Pipas JM. 1989. Mutants with changes within or near a hydrophobic region of simian virus 40 large tumor antigen are defective for binding cellular protein p53. Virology.

342. Cho S, Tian Y, Benjamin TL. 2001. Binding of p300/CBP Co-activators by Polyoma Large T Antigen. J Biol Chem.

343. Dey D, Dahl J, Cho S, Benjamin TL. 2002. Induction and Bypass of p53 during Productive Infection by Polyomavirus. J Virol.

344. Nemethova M, Wintersberger E. 1999. Polyomavirus large T antigen binds the transcriptional coactivator protein p300. J Virol.

345. Doherty J, Freund R. 1997. Polyomavirus large T antigen overcomes p53 dependent growth arrest. Oncogene.

346. Wang EH, Friedman PN, Prives C. 1989. The murine p53 protein blocks replication of SV40 DNA in vitro by inhibiting the initiation functions of SV40 large T antigen. Cell.

347. Söderberg O, Leuchowius KJ, Gullberg M, Jarvius M, Weibrecht I, Larsson LG, Landegren U. 2008. Characterizing proteins and their interactions in cells and tissues using the in situ proximity ligation assay. Methods.

348. Fischer M. 2017. Census and evaluation of p53 target genes. Oncogene.

349. Kaeser MD, Iggo RD. 2002. Chromatin immunoprecipitation analysis fails to support the latency model for regulation of p53 DNA binding activity in vivo. Proc Natl Acad Sci U S A.

350. Resnick-Silverman L, St. Clair S, Maurer M, Zhao K, Manfredi JJ. 1998. Identification of a novel class of genomic DNA-binding sites suggests a mechanism for selectivity in target gene activation by the tumor suppressor protein p53. Genes Dev.

351. Hill R, Bodzak E, Blough MD, Lee PWK. 2008. p53 binding to the p21 promoter is dependent on the nature of DNA damage. Cell Cycle.

352. Rohaly G, Chemnitz J, Dehde S, Nunez AM, Heukeshoven J, Deppert W, Dornreiter I. 2005. A novel human p53 isoform is an essential element of the ATR-intra-S phase checkpoint. Cell.

353. Ard PG, Chatterjee C, Kunjibettu S, Adside LR, Gralinski LE, McMahon SB. 2002. Transcriptional Regulation of the mdm2 Oncogene by p53 Requires TRRAP Acetyltransferase Complexes. Mol Cell Biol.

354. Lee DH, Kim C, Zhang L, Lee YJ. 2008. Role of p53, PUMA, and Bax in wogonin-induced apoptosis in human cancer cells. Biochem Pharmacol.

355. Tacar O, Sriamornsak P, Dass CR. 2013. Doxorubicin: An update on anticancer molecular action, toxicity and novel drug delivery systems. J Pharm Pharmacol.

356. White MK, Khalili K. 2006. Interaction of retinoblastoma protein family members with large T-antigen of primate polyomaviruses. Oncogene.

357. Appella E, Anderson CW. 2001. Post-translational modifications and activation of p53 by genotoxic stresses. Eur J Biochem.

358. Grossman SR. 2001. p300/CBP/p53 interaction and regulation of the p53 response. Eur J Biochem.

359. Huibregtse JM, Scheffner M, Howley PM. 1993. Cloning and expression of the cDNA for E6-AP, a protein that mediates the interaction of the human papillomavirus E6 oncoprotein with p53. Mol Cell Biol.

360. Werness BA, Levine AJ, Howley PM. 1990. Association of human papillomavirus types 16 and 18 E6 proteins with p53. Science (80- ).

361. Scheffner M, Werness BA, Huibregtse JM, Levine AJ, Howley PM. 1990. The E6 oncoprotein encoded by human papillomavirus types 16 and 18 promotes the degradation of p53. Cell.

362. Deppert W, Steinmayer T, Richter W. 1989. Cooperation of SV40 large T antigen and the cellular protein p53 in maintenance of cell transformation. Oncogene.

363. Giaccia AJ, Kastan MB. 1998. The complexity of p53 modulation: Emerging patterns from divergent signals. Genes Dev.

364. Krumbholz A, Bininda-Emonds ORP, Wutzler P, Zell R. 2009. Phylogenetics, evolution, and medical importance of polyomaviruses. Infect Genet Evol.

365. Manos MM, Gluzman Y. 1985. Genetic and biochemical analysis of transformation-competent, replication-defective simian virus 40 large T antigen mutants. J Virol 53:120–127.

366. Busam KJ, Jungbluth AA, Rekthman N, Coit D, Pulitzer M, Bini J, Arora R, Hanson NC, Tassello JA, Frosina D, Moore P, Chang Y. 2009. Merkel cell polyomavirus expression in merkel cell carcinomas and its absence in combined tumors and pulmonary neuroendocrine carcinomas. Am J Surg Pathol 33:1378–1385.

367. Negrini S, Gorgoulis VG, Halazonetis TD. 2010. Genomic instability--an evolving hallmark of cancer. Nat Rev Mol Cell Biol 11:220–228.

368. Nigg EA. 2002. Centrosome aberrations: cause or consequence of cancer progression? Nat Rev Cancer 2:815–825.

369. Sahi H, Savola S, Sihto H, Koljonen V, Bohling T, Knuutila S. 2014. RB1 gene in Merkel cell carcinoma: hypermethylation in all tumors and concurrent heterozygous deletions in the polyomavirus-negative subgroup. APMIS 122:1157–1166.

370. Peel N. 2013. Everything in moderation: Proteolytic regulation of centrosome duplication. Worm2013/09/24. 2:e22497.

371. Ang XL, Wade Harper J. 2005. SCF-mediated protein degradation and cell cycle control. Oncogene 24:2860–2870.

372. Rajagopalan H, Jallepalli P V, Rago C, Velculescu VE, Kinzler KW, Vogelstein B, Lengauer C. 2004. Inactivation of hCDC4 can cause chromosomal instability. Nature2004/03/06. 428:77–81.

373. Silverman JS, Skaar JR, Pagano M. 2012. SCF ubiquitin ligases in the maintenance of genome stability. Trends Biochem Sci 37:66–73.

374. Korzeniewski N, Treat B, Duensing S. 2011. The HPV-16 E7 oncoprotein induces centriole multiplication through deregulation of Polo-like kinase 4 expression. Mol Cancer 10:61.

375. Holland AJ, Lan W, Niessen S, Hoover H, Cleveland DW. 2010. Polo-like kinase 4 kinase activity limits centrosome overduplication by autoregulating its own stability. J Cell Biol 188:191–198.

376. Martin-Lluesma S, Schaeffer C, Robert EI, van Breugel PC, Leupin O, Hantz O, Strubin M. 2008. Hepatitis B virus X protein affects S phase progression leading to chromosome segregation defects by binding to damaged DNA binding protein 1. Hepatology 48:1467–1476.

377. Liu B, Hong S, Tang Z, Yu H, Giam CZ. 2005. HTLV-I Tax directly binds the Cdc20-associated anaphase-promoting complex and activates it ahead of schedule. Proc Natl Acad Sci U S A 102:63–68.

378. Duensing S, Lee LY, Duensing A, Basile J, Piboonniyom S, Gonzalez S, Crum CP, Munger K. 2000. The human papillomavirus type 16 E6 and E7 oncoproteins cooperate to induce mitotic defects and genomic instability by uncoupling centrosome duplication from the cell division cycle. Proc Natl Acad Sci U S A 97:10002–10007.

379. Yun C, Cho H, Kim SJ, Lee JH, Park SY, Chan GK, Cho H. 2004. Mitotic aberration coupled with centrosome amplification is induced by hepatitis B virus X oncoprotein via the Ras-mitogen-activated protein/extracellular signal-regulated kinase-mitogen-activated protein pathway. Mol Cancer Res 2:159–169.

380. Peloponese Jr. JM, Haller K, Miyazato A, Jeang KT. 2005. Abnormal centrosome amplification in cells through the targeting of Ran-binding protein-1 by the human T cell leukemia virus type-1 Tax oncoprotein. Proc Natl Acad Sci U S A 102:18974–18979.

381. Pan H, Zhou F, Gao SJ. 2004. Kaposi's sarcoma-associated herpesvirus induction of chromosome instability in primary human endothelial cells. Cancer Res 64:4064–4068.

382. White EA, Sowa ME, Tan MJ, Jeudy S, Hayes SD, Santha S, Munger K, Harper JW, Howley PM. 2012. Systematic identification of interactions between host cell proteins and E7 oncoproteins from diverse human papillomaviruses. Proc Natl Acad Sci U S A 109:E260-7.

383. Chi YH, Jeang KT. 2007. Aneuploidy and cancer. J Cell Biochem 102:531–538.

384. Kops GJ, Weaver BA, Cleveland DW. 2005. On the road to cancer: aneuploidy and the mitotic checkpoint. Nat Rev Cancer 5:773–785.

385. Fujiwara T, Bandi M, Nitta M, Ivanova E V, Bronson RT, Pellman D. 2005. Cytokinesis failure generating tetraploids promotes tumorigenesis in p53-null cells. Nature 437:1043–1047.

386. Vitale I, Galluzzi L, Castedo M, Kroemer G. 2011. Mitotic catastrophe: a mechanism for avoiding genomic instability. Nat Rev Mol Cell Biol 12:385–392.

387. Storchova Z, Pellman D. 2004. From polyploidy to aneuploidy, genome instability and cancer. Nat Rev Mol Cell Biol2004/01/07. 5:45–54.

388. Fang X, Zhang P. 2011. Aneuploidy and tumorigenesis. Semin Cell Dev Biol 22:595–601.

389. Ganem NJ, Godinho SA, Pellman D. 2009. A mechanism linking extra centrosomes to chromosomal instability. Nature 460:278–282.

390. Miron K, Golan-Lev T, Dvir R, Ben-David E, Kerem B. 2015. Oncogenes create a unique landscape of fragile sites. Nat Commun 6:7094.

391. Iarmarcovai G, Bonassi S, Botta A, Baan RA, Orsiere T. 2008. Genetic polymorphisms and micronucleus formation: a review of the literature. Mutat Res 658:215–233.

392. Bonassi S, Znaor A, Ceppi M, Lando C, Chang WP, Holland N, Kirsch-Volders M, Zeiger E, Ban S, Barale R, Bigatti MP, Bolognesi C, Cebulska-Wasilewska A, Fabianova E, Fucic A, Hagmar L, Joksic G, Martelli A, Migliore L, Mirkova E, Scarfi MR, Zijno A, Norppa H, Fenech M. 2007. An increased micronucleus frequency in peripheral blood lymphocytes predicts the risk of cancer in humans. Carcinogenesis 28:625–631.

393. Witt KL, Livanos E, Kissling GE, Torous DK, Caspary W, Tice RR, Recio L. 2008. Comparison of flow cytometry- and microscopy-based methods for measuring micronucleated reticulocyte frequencies in rodents treated with nongenotoxic and genotoxic chemicals. Mutat Res 649:101–113.

394. Nakayama KI, Nakayama K. 2006. Ubiquitin ligases: cell-cycle control and cancer. Nat Rev Cancer 6:369–381.

395. Crusio KM, King B, Reavie LB, Aifantis I. 2010. The ubiquitous nature of cancer: the role of the SCF(Fbw7) complex in development and transformation. Oncogene 29:4865–4873.

396. Li M, Fang X, Wei Z, York JP, Zhang P. 2009. Loss of spindle assembly checkpoint-mediated inhibition of Cdc20 promotes tumorigenesis in mice. J Cell Biol 185:983–994.

397. Cizmecioglu O, Krause A, Bahtz R, Ehret L, Malek N, Hoffmann I. 2012. Plk2 regulates centriole duplication through phosphorylation-mediated degradation of Fbxw7 (human Cdc4). J Cell Sci2012/03/09. 125:981–992.

398. Duensing A, Chin A, Wang L, Kuan SF, Duensing S. 2008. Analysis of centrosome overduplication in correlation to cell division errors in high-risk human papillomavirus (HPV)-associated anal neoplasms. Virology 372:157–164.

399. Lau AW, Fukushima H, Wei W. 2012. The Fbw7 and betaTRCP E3 ubiquitin ligases and their roles in tumorigenesis. Front Biosci (Landmark Ed) 17:2197–2212.

400. Guderian G, Westendorf J, Uldschmid A, Nigg EA. 2010. Plk4 trans-autophosphorylation regulates centriole number by controlling betaTrCP-mediated degradation. J Cell Sci 123:2163–2169.

401. Duensing S, Munger K. 2002. Human papillomaviruses and centrosome duplication errors: modeling the origins of genomic instability. Oncogene2002/09/06. 21:6241–6248.

402. Desmaze C, Soria JC, Freulet-Marriere MA, Mathieu N, Sabatier L. 2003. Telomere-driven genomic instability in cancer cells. Cancer Lett 194:173–182.

403. Alwine JC, Reed SI, Ferguson J, Stark GR. 1975. Properties of T antigens induced by wild-type SV40 and tsA mutants in lytic infection. Cell.

404. Robb JA, Tegtmeyer P, Ishikawa A, Ozer HL. 1974. Antigenic phenotypes and complementation groups of temperature sensitive mutants of simian virus 40. J Virol.

405. Paulin D, Cuzin F. 1975. Polyoma virus T antigen. I. Synthesis of modified heat labile T antigen in cells transformed with the ts a mutant. J Virol.

406. Henning W, Rohaly G, Kolzau T, Knippschild U, Maacke H, Deppert W. 1997. MDM2 is a target of simian virus 40 in cellular transformation and during lytic infection. J Virol.

407. Lowe SW, Earl Ruley H. 1993. Stabilization of the p53 tumor suppressor is induced by adeno virus 5 E1A and accompanies apoptosis. Genes Dev.

408. Hanahan D, Weinberg RA. 2011. Hallmarks of cancer: The next generation. Cell.